Order Number 8906938

Digestion theory and applications to deposit feeders

Penry, Deborah Lynn, Ph.D.

University of Washington, 1988

Digestion Theory and Applications to Deposit Feeders

by

Deborah Lynn Penry

A dissertation submitted in partial fulfillment
of the requirements for the degree of

Doctor of Philosophy

University of Washington
1988

Approved by 
(Chairperson of Supervisory Committee)

Program Authorized
to Offer Degree School of Oceanography

Date 25 July 1988

Doctoral Dissertation

In presenting the dissertation in partial fulfillment of the requirements for the Doctoral degree at the University of Washington, I agree that the Library shall make its copies freely available for inspection. I further agree that extensive copying of this dissertation is allowable only for scholarly purposes, consistent with "fair use" as prescribed in the U.S. Copyright Law. Requests for copying or reproduction of this dissertation may be referred to University Microfilms, 300 North Zeeb Road, Ann Arbor, Michigan 48106, to whom the author has granted "the right to reproduce and sell (a) copies of the manuscript in microform and/or (b) printed copies of the manuscript made from microform."

Signature Deborah L. Penry

Date 25 July 1988

University of Washington

Abstract

DIGESTION THEORY AND APPLICATIONS TO DEPOSIT FEEDERS

By Deborah Lynn Penry

Chairman of Supervisory Committee: Professor Peter A. Jumars

School of Oceanography

A general theory of digestion can be derived from principles of chemical reactor theory, and three ideal reactor models, the batch reactor, plug-flow reactor (PFR), and continuous-flow, stirred-tank reactor (CSTR), are the basic components of models of animals' guts. These models express the extent to which an animal digests ingested food as a function of food parameters, digestive reaction kinetics, and gut throughput time. If digestive reaction kinetics are specified, the best gut-reactor in which to carry out the given reactions can be determined. Two basic predictions result. If digestive reactions follow Michaelis-Menten enzyme kinetics, an animal's gut should operate as a PFR, and if an animal's digestive strategy incorporates fermentation of refractory organics, its gut should operate (except for very long throughput times) as a CSTR-PFR series (foregut fermenters) or a PFR-CSTR (hindgut fermenters).

Michaelis-Menten kinetics are postulated as the general case for digestive reactions in deposit feeders. It is predicted, and observed, that many deposit feeders have simple, tubular guts that operate as PFRs, but experimental tests reveal necessary model modifications. The modified PFR model represents an extreme case of segregated flow: flow through most of the gut is characterized by the absence of axial and radial mixing of sediment. Deposit feeders with simple, tubular guts are small in size and predominate in environments with fine-grained sediments of relatively low permeability. Ontogenetic changes in gut architecture suggest that digestion may be diffusion-limited in many of these species.

Terebellimorph polychaetes are exceptions to the PFR model. Their guts must be modeled as CSTR-PFR series with a ventral bypass stream that shunts particles from the CSTR through the PFR for rapid

elimination from the gut. Post-ingestion sorting may remove relatively indigestible particles and thus increase the proportion of gut volume available for processing higher-quality particles.

Gut architecture varies with diet quality. Carnivorous polychaetes have less gut volume per unit of body volume than do deposit feeders, and deep-sea deposit feeders tend to have longer guts than closely-related, shallow-water species. As individuals within a deposit-feeding species increase in size, throughput time and thus extent of digestion should increase.

Table of Contents

List of Figures

List of Tables

Acknowledgements

I am deeply indebted to Drs. Peter A. Jumars and Arthur R. M. Nowell for providing the many opportunities and intellectual challenges that have made my graduate studies so exciting and rewarding. I thank the members of my Supervisory Committee, Drs. Jumars, Nowell, John I. Hedges and Barbara B. Krieger, for their guidance and encouragement throughout the course of these studies. Their comments and suggestions have helped me clarify ideas and improve this dissertation.

The suggestion by Drs. Sarah A. Woodin and David Wethey that I use a video digitizer to analyze gut drawings contributed directly to the breadth and success of the polychaete gut survey in Chapter IV. I thank Dr. Woodin the loan of her Cahn microbalance, and I thank Dr. Wethey for his help in debugging computer programs. I thank Dr. A. O. D. Willows for the use of the facilities and resources of Friday Harbor Laboratories so that I could perform experiments necessary to test the theory I developed.

I thank Liko Self for his help both in the lab and in the field. Numerous discussions with Liko Self and my office mates, Brian Dade, Doug Miller and Tish Yager, about subjects scientific and not, have been useful and enjoyable and have helped me to maintain my sanity.

I was supported in part during my graduate studies by a Graduate Opportunities Research Assistantship from the University of Washington and a Graduate Fellowship from the National Science Foundation. I thank Mr. and Mrs. E. Porter Whitson for their generosity in establishing the Whitson Scholarship. It provided support to allow me to complete this dissertation.

I thank Don Weston for his insight as a scientist, his diligence as a lab assistant, and his love and support as my husband.

INTRODUCTION

Sediment processing by marine deposit feeders can affect the physical, chemical and biological structure of benthic environments. Advances in deposit-feeder ecology have resulted from theoretical and modeling approaches (e.g., Taghon et al. 1978; Taghon 1981; Miller et al. 1984) that focus on food availability and acquisition. One approach, optimal foraging theory for deposit feeders (Taghon et al. 1978; Taghon 1981), allows examination of foraging strategies under the premise that deposit feeders maximize net rates of energy and nutrient gain. Foraging is, however, only one determinant of net gain. It is also necessary to consider digestion. Sediment-processing rates may be constrained by deposit feeders' digestive capabilities as well as food availability and foraging activities.

I use principles of chemical reactor analysis and design to develop a theoretical framework for digestion that is analogous to optimal foraging theory. I model animal guts as chemical reactors (Chapters I and II). I then use two approaches to validate these gut-reactor models and to demonstrate their utility. The first approach involves direct, experimental tests of the models for two deposit feeders, Parastichopus californicus, a holothuroid, and Amphicteis scaphobranchiata, an ampharetid polychaete (Chapter III). The second approach can be considered the inverse of the first. I use gut-reactor models to infer gut kinematics from gut architectures and to examine hypotheses about inter-relationships among food resources, foraging strategies and digestive constraints (Chapter IV).

Digestion theory and gut-reactor models are based on the premise that modeling digestion is a problem in chemical engineering. Application of chemical reactor theory identifies the important variables necessary to describe compactly the process of digestion and provides biologically meaningful, mathematical relationships among the variables. Given an expression for digestive reaction rate, the extent to which ingested food is digested is a function of gut-reactor type,

concentration of a limiting or otherwise important food component, gut volume, and gut holding or throughput time. Given functional relationships among digestive variables, gut-reactor configurations and digestive strategies that maximize an animal's net rate of gain of energy and nutrients are identified. Two basic predictions result. If digestive reaction kinetics are described by a Michaelis-Menten model, an animal's gut should function as a plug-flow reactor (PFR). If an animal ferments refractory materials (autocatalytic digestive reaction kinetics) its gut should operate as a continuous-flow, stirred-tank reactor (CSTR)-PFR series or a PFR-CSTR series.

Chapters I and II develop optimal digestion theory and review existing literature to test these basic predictions. Digestive processes in deposit feeders and mammalian herbivores are further examined in the context of gut-reactor models and hypotheses are generated about digestive constraints in these two groups. I suggest, for example, that digestion may be diffusion limited in deposit feeders that ingest fine-grained, relatively less permeable sediments (i.e., digestion may be limited by diffusion of digestive enzymes into, or digestive products out, of ingested sediment). Results of experimental tests (Chapter III) and applications (Chapter IV) of gut-reactor models lend support to this hypothesis. Chapters I and II have been published in revised forms in BioScience (Penry and Jumars 1986) and The American Naturalist (Penry and Jumars 1987).

Testing gut-reactor models requires description of patterns of material movement within animals' guts (Chapter III). Deposit feeders are good subjects for initial tests because most of the material they ingest is inert mineral grains, and thus, changes in volume of material in a deposit feeder's gut during digestion are negligible. Quantitative tracer experiments confirm the plug-flow model for the holothuroid, Parastichopus californicus, and suggest that the plug-flow model, with some modifications, can be generalized to all deposit feeders with simple, tubular guts. Deviations from plug flow observed in the gut of the ampharetid polychaete, Amphicteis scaphobranchiata, require that its gut, and presumably the guts of other terebellimorph

polychaetes, be modeled as a CSTR (mixing reactor) - PFR series. Consideration of potential roles of an anterior mixing chamber in digestive processes of this group of deposit feeders provides additional insight into digestive constraints in all deposit feeders. Experimental tests of gut-reactor models show that the models are more than just ideal engineering constructs -- they describe patterns of sediment movement within the guts of deposit feeders.

Validation of gut-reactor models provides the basis for inferences of gut kinematics and digestive constraints from characteristics of gut architectures (Chapter IV). I analyze and group deposit-feeding polychaetes on the basis of similarities in gut architecture. Since my goal is to model their guts in terms of reactor components, I use an "engineering" approach in this comparative survey. I describe guts in terms of anatomically-distinct compartments and describe differences among individuals and species in basic engineering terms, e.g. ratios of body volume to gut volume, total gut aspect ratios, and relative volumes and aspect ratios of gut compartments. These data are then used to suggest digestive constraints and examine hypotheses about inter-relationships among food quality, foraging strategies, and digestive strategies. For example, ontogenetic changes in total gut aspect ratios in deposit feeders that ingest relatively immpermeable sediments support the hypothesis that digestion may be diffusion limited in these species.

In sum this dissertation demonstrates how digestion theory and gut-reactor models can provide the context for experimentation and inference. I focus on deposit feeders because their roles in sedimentary processes are of interest to oceanographers, but the approach I have taken can be generalized to studies of digestive strategies in any group of animals.

Chapter I. Chemical reactor analysis and optimal digestion

INTRODUCTION

Foraging and digestion are two stages of a single process that determines an animal's net rate of energy and nutrient gain. According to the principles of dynamic programming, a method for formulating and solving optimization problems (Bellman 1957), the entire process is optimized only if digestion follows an optimal path constrained by the food items actually ingested. An animal feeding on a variety of foods should thus exhibit the flexibility to optimize digestion with respect to that range of food types. Conversely, the net rate of gain to an animal lacking the flexibility to alter its digestive tactics will be maximized over a restricted set of food types, making it a dietary specialist.

To test these general predictions and to formulate more specific ones, we must identify the operating variables for each stage. Many foraging theories exist (e.g., Charnov 1976; Orians and Pearson 1979; Pyke 1984; Schoener 1971), but there are only rudiments of an optimal digestion theory (Milton 1981; Sibly 1981; Taghon 1981; Troyer 1984). Without such a theory, studies of digestive systems (e.g. gut anatomy, histology, or enzymology) tend to be static, piecemeal, and most often nonpredictive. To date, for example, conspicuously few predictions and data exist on patterns and rates of material throughput.

Modeling the digestive process is a problem in chemical engineering. Given a chemical reaction and physical and economic constraints, a chemical engineer designs a reactor and an operating strategy that maximize the yield or rate of yield of desired reaction products (Carberry 1976). Similarly, given the chemical reactions and the physical and energetic constraints of digestion, we try to discover how various gut configurations and digestive tactics may maximize an animal's net rate of energy and nutrient gain. The first step is descriptive: We must describe animal guts in terms of chemical reactor components and then use principles of reactor design to identify variables that characterize digestive strategies.

CHEMICAL REACTOR DESIGN

There are three general classes of reactors: batch reactors, steady-state flow reactors, and semibatch or unsteady-state flow reactors which combine characteristics of the first two types (Levenspiel 1972). The batch reactor, as its name implies, processes reactants in discrete batches. All reactants are loaded into the reactor and allowed to react; the resulting products are then removed. Composition of material within the reactor changes over time. In contrast, a steady-state flow reactor maintains constant flow of reactants into and products out of the reaction vessel. Composition at any point within the reactor is unchanged over time. Any reactor that cannot be classified as one of the first two types is a semibatch, or unsteady-state flow, reactor. Its operation may involve any or all of the following: intermittent flow of reactants into, or products out of, the reactor, and composition or volume changes of the material within the reactor.

Animals eating discrete meals can be classified as batch reactors and those that eat more or less continuously as steady-state flow reactors. Semibatch reactors may more realistically represent gut kinematics of animals that feed at irregular intervals, but these reactors are comparatively difficult to model (Levenspiel 1972). Understanding of the gut kinematics of animals that approximate the easily-modeled batch and steady-state flow reactors provides the basis for future consideration of semi-batch or unsteady-state flow guts.

Three ideal, theoretical models -- the batch reactor and two steady-state flow reactors (the plug-flow reactor and the continuous-flow, stirred-tank reactor) form the basis of all chemical reactor design. These ideal reactor models differ principally in how reactants meet to react in the reaction vessel, and for any given reaction, one of these three reactors usually represents the best method of processing the necessary reactants. Industrial reactors are often designed so that their flow and mixing patterns approach these

ideals (Levenspiel 1972).

In contrast with many industrial situations, temperature is approximately constant in an animal's gut, so we need consider only conservation of mass in our development of reactor models for guts. For a given reaction-rate equation, reaction extent and operating conditions in the reactor can be obtained by solving the appropriate mass balance equation. Comparing the detailed solutions for different reactor types enables us to identify the best reactor design for given reactions, for example, digestive reactions of specified kinetics (Penry and Jumars 1987).

To identify their respective operating variables, we here introduce the basic considerations in formulation of each ideal reactor model, including the reactor-specific mass balance equations (notation after Levenspiel 1972). Since our intent is, at this point to provide the descriptive basis for future theoretical and experimental analyses, digression soley for the purpose of deriving these equations is unwarranted. The interested reader is referred to chemical engineering texts (Levenspiel 1972; J. Smith 1981) for the derivations. Examining these equations and the assumptions on which the derivations are based emphasizes the homology between animal guts and chemical reactors.

Batch Reactors

In a batch reactor all reactants are initially loaded, then mixed thoroughly and allowed to react; the resulting product mixture is then completely removed. Changes occur only with respect to time; properties are assumed to be spatially uniform within the reactor. Since material neither enters nor leaves the reactor during reaction (input = output = 0), the mass balance consists of only two terms summing to zero: disappearance of reactant A by reaction and accumulation of reactant A in the reactor. The amount of A that disappears by reaction is a function of reaction rate ($-r_A$, in units of moles volume^{-1} time^{-1}), volume of reactants in the reactor (V), and the reactor holding time over which the reaction occurs (t). The amount of A that accumulates in the reactor is a function of the amount of A

initially added (N_{A0}), and the fraction of A not converted to products ($1 - X_A$), where (X_A) is the fraction of A converted to products. The time required to achieve a conversion (X_{Af}) in a batch reactor is

$$t = N_{A0} \int_0^{X_{Af}} \frac{dX_A}{(-r_A)\, V}$$

If we assume that each time an animal feeds it ingests enough food to fill the space available in its gut, then the reacting volume, as measured by the volume of food initially ingested, equals reactor volume. But in contrast to the ideal batch reactor, the volume of the reacting mixture in an animal's gut decreases with increasing reaction time as products are removed through absorption. The ideal batch reactor model can be modified to describe this flow of products from the gut. In this initial exposition, however, we choose to neglect volume variations resulting from absorption of digestive products -- a simplification that proves reasonable for animals such as deposit feeders and other detritivores, herbivores, and folivores with diets that normally include large quantities of inert or refractory materials like sediment grains, cellulose and lignin. If the reacting volume does not vary significantly, V may be removed from under the integral. (N_{A0}/V) is the initial concentration of A (C_{A0}), and the performance equation becomes

$$t = C_{A0} \int_0^{X_{Af}} \frac{dX_A}{(-r_A)}$$

This equation can be solved for the holding time t required to achieve a desired level of conversion X_{Af} of reactants to products ($-r_A$ and C_{A0} specified) or for the reactor volume V required to achieve a given rate of production ($-r_A$, C_{A0}, t, and X_{Af} specified).

Examining the reactor performance equation indicates that, for a given reaction rate expression, holding, or digestion, time is the important operating variable for animals with batch-reactor guts. We define an optimal operating strategy for any gut as the one which maximizes net rate of energy or nutrient production from ingested

foods. In determining an optimal operating strategy for a batch-reactor gut under a given set of conditions, we must consider constraints on holding time, adding, for example time between meals, when the gut may be idle. When we predict optimal operating policies for batch-reactor guts (X_{Af} specified), the quantity minimized should be the total time needed for a complete gut-reactor operating cycle -- foraging, ingestion, digestion, and egestion. A particular quantity (e.g., holding time or gut volume) is "minimized" or "maximized" both in the context of an optimization problem and in the broader, evolutionary context of individual fitness (e.g., Townsend and Calow 1981).

Since digestive reactions are, in general, first order reactions or zero order reactions shifting to first order as reactant concentrations decrease, the extent to which ingested food materials are digested is completely determined by holding, or digestion, time. For maximum production rate, gut volume should be maximized so more food (C_{A0} constant) can be processed in the same holding time. However, the effectiveness with which enzymes and food particles can be brought into contact decreases as gut volume and volume of material processed in each batch increase, resulting in a decrease in the amount of food converted per batch and placing upper bounds on gut volume. This decrease in effective contact among reactants may result both from a decrease in the effectiveness with which enzymes and food material can mix and, since enzymes are introduced from the gut wall, from a decrease in the gut surface-to-volume ratio.

Animals that can be modeled as having batch-reactor guts include hydras, hydroids, jellyfish, sea anemones, and corals (Cnidaria), comb jellies (Ctenophora), brittle stars and starfish (Echinodermata), and some glycerid polychaetes (Annelida) that regurgitate their wastes (Ockelmann and Vahl 1970).

Plug-Flow Reactors

The plug-flow reactor (PFR) is characterized by continuous flow of material through the reaction vessel. The flow pattern is orderly:

material parcels enter and exit the reactor in the same sequence. Material is perfectly mixed radially, but mixing or diffusion along the flow path is negligible. Residence time in the reactor is identical for all parcels -- the necessary condition for plug flow (Levenspiel 1972). Under steady-state operation, changes occur only with respect to axial position within the reactor, and the mass balance is made over a differential volume element (dV). The resulting equations relate reaction rate ($-r_A$), reaction extent (X_A), reactor volume (V), and input rate of reactant A (F_{A0}, where $F_{A0} = C_{A0} \times v_0$, the product of initial concentration of A and volumetric flow rate)

$$\frac{V}{F_{A0}} = \int_0^{X_{Af}} \frac{dX_A}{-r_A} \qquad \text{or}$$

$$\tau = \frac{V}{v_0} = C_{A0} \int_0^{X_{Af}} \frac{dX_A}{-r_A}$$

The ratio of reactor volume (V) to volumetric flow rate (v_0) is the time (τ, "space-time") required to process one reactor volume of material, or in biological terms, the ratio of gut volume to throughput rate is throughput time, the time required to process one gut volume of food. To maximize their energy and nutrient production rates, animals with PFR guts should process food so as to minimize throughput time required to achieve any given conversion ($-r_A$, C_{A0} specified). Gut volume and throughput rate are the important operating variables.

Many animals have guts that approximate plug-flow reactors. Examples include geese, corophiid amphipods (Crustacea), and deposit-feeding polychaetes (Annelida) with simple tubular guts.

Continuous-flow, stirred-tank reactors

The design of the continuous-flow, stirred tank reactor (CSTR) incorporates both constant flow of material through the reactor and complete mixing within it. At steady state, the composition of material is both uniform throughout the reactor and invariant over

time. Input of reactant A is a function of input rate (F_{A0}) and output of A is thus a function of input rate and the fraction of A that is not converted to products ($1-X_A$). The amount of A that disappears by reaction is a function of reaction rate ($-r_A$) and reactor volume (V). The mass balance equations become

$$F_{A0}\ (X_A) = (-r_A)\ V \quad \text{or}$$

$$\tau = \frac{V}{v_0} = \frac{C_{A0}(X_A)}{-r_A}$$

To maximize their energy or nutrient production rates, animals with CSTR guts should, like animals with PFR guts, process food so as to minimize the throughput time required to achieve any given conversion ($-r_A$, C_{A0} specified). Again, gut volume and throughput rate are the important operating variables.

We know of no animal that has a gut that can be modeled entirely as a CSTR. There are many animals, however, in which a portion of the gut operates as a CSTR, and the entire gut can be modeled as a series of reactors -- a common arrangement in chemical process design. A ruminant gut, for example, can be represented quite simply as CSTR followed in series by a PFR.

APPLYING OF REACTOR THEORY AND MODELS TO DIGESTION

Principles of chemical reactor design can be used to analyze the kinematics of digestion, and the three ideal reactors can serve, singly or in series, as models for animal guts. Reactor-specific mass balance equations can then be used, without any initial modifications, to predict the performance of gut reactor models with respect to digestive reactions.

Numerous empirical models have been developed to describe rates of digesta throughput and gut evacuation (e.g., Brandt and Thacker 1958, Grovum and Williams 1977, Mills et al. 1984). Rate descriptions

resulting from such empirical models hold only for the specific sets of conditions prevailing when the data were collected. They cannot predict, as reactor models can, changes that should occur in digesta throughput rates with changes in, for example, food concentration or ingestion rate.

Among empirical approaches, the compartmental method of kinetic analysis (e.g., Brandt and Thacker 1958, Hughes and Matis 1984) has become very popular, and a two-compartment model is somewhat successful in describing the cumulative output of feces in large herbivores. Previous interpretations of observed defecation patterns traced with, for example, soluble markers, dyed or radioisotopically labeled plant material, or metal oxides suggest that the ruminant digestive system functions as a sequential, irreversible, two-compartment flow process with complete mixing in each compartment (Figure 1a) and exponential loss of material from each compartment (Ellis et al. 1979; Figures 1b,c,d). This model is very close to our model derived from chemical reactor theory, but there are important differences.

We propose that the ruminant gut be modeled as two reactors in series, a continuous-flow, stirred-tank reactor (the rumen) followed by a plug-flow reactor (the remainder of the gut; Figure 2a), a model that exactly accounts for observed tracer residence time distributions. The residence time distribution for a CSTR/PFR series is an exponential function resulting from CSTR mixing characteristics. If a tracer were introduced at the beginning of the reactor series (ingestion) and its output from the reactor series (defecation) were monitored, the results would match the exponential output curve so often observed for ruminants (Figure 2b). The CSTR/PFR series model also explains the residence-time distributions observed when tracers are introduced at different points along the ruminant's gut, whereas the compartmental model does not. The residence-time distribution for a single, ideal CSTR is an exponential function (Figure 2c), but the residence time distribution for a single, ideal PFR is a step function (Figure 2d).

Balch (1950) fed stained hay to cows and also injected stained hay

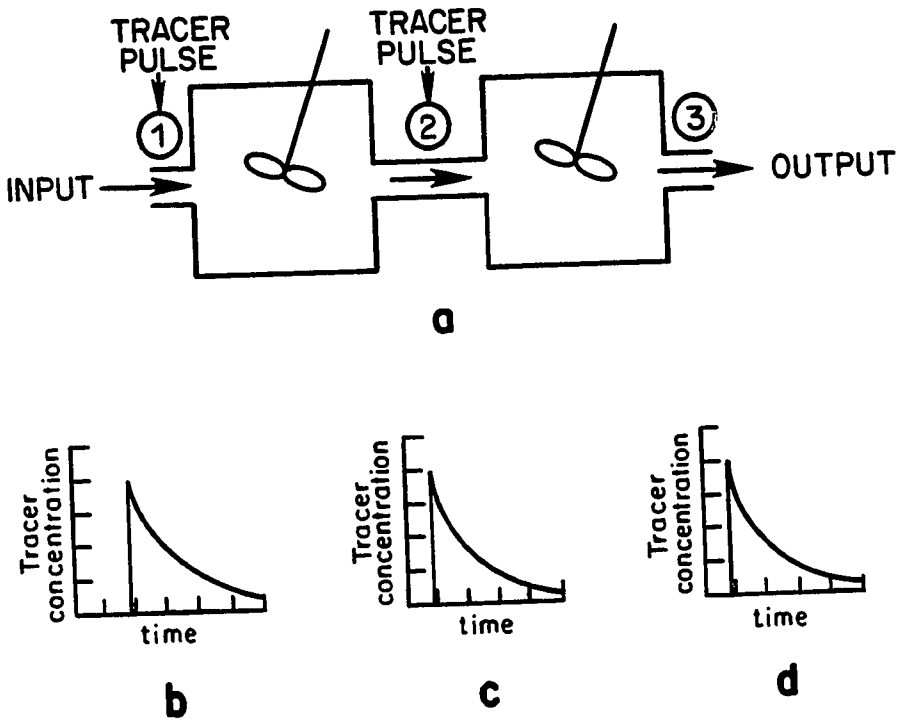

Figure I-1. (a) Empirical compartmental model for a ruminant gut. Tracer residence time distributions that result when tracer is (b) introduced at 1, measured at 3; (c) introduced at 1, measured at 2; (d) introduced at 2, measured at 3.

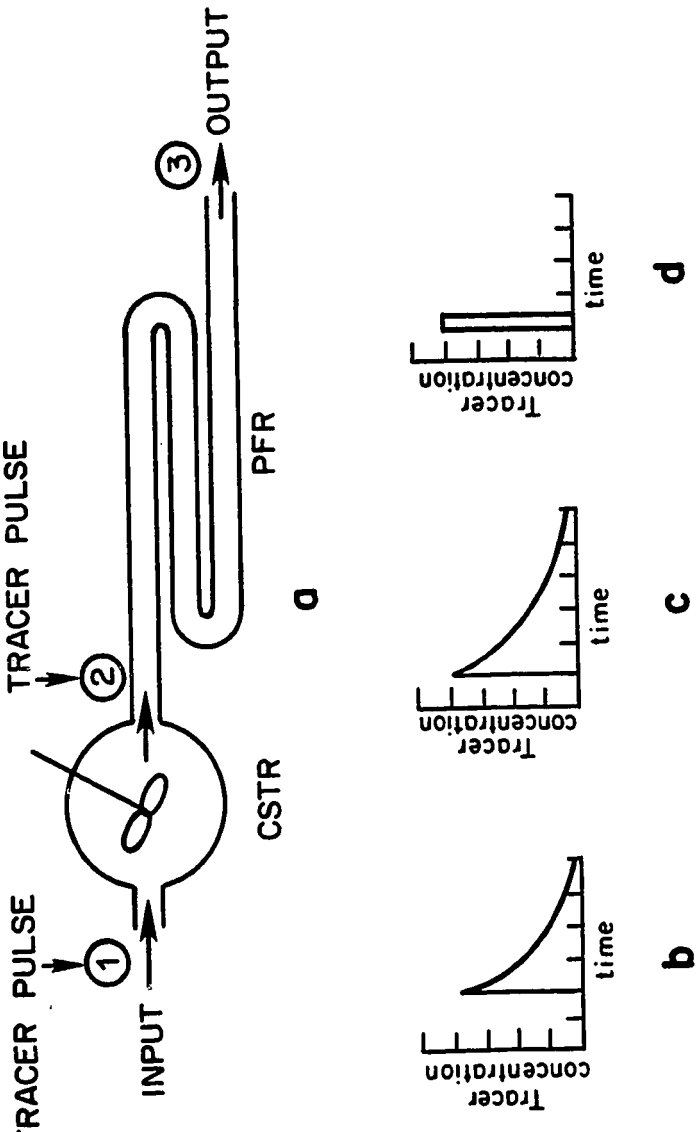

Figure I-2. (a) Theoretical reactor model for a ruminant gut. Tracer residence-time distributions that result when tracer is (b) introduced at 1, measured at 3; (c) introduced at 1, measured at 2; (d) introduced at 2, measured at 3.

into the abomasum of fistulated individuals. The observed tracer residence-time distributions confirm our hypothesis that the rumen operates as a CSTR(stained particles present close to the reticulo-omasum orifice from the beginning of the meal) and that the rest of the gut approximates a PFR (tracer excretion from the abomasum occurring over a very short time period, indicating that mixing in posterior gut segments is slight). With this better empirical fit and its predictive ability, the CSTR/PFR model offers excellent prospects for improved understanding of ruminant digestive systems.

Guts can be modeled variously as batch reactors, plug-flow reactors, and CSTR/PFR reactor series, but one basic set of operating variables exists. Given an expression for the rate of digestive reactions -- the appropriate choice of which depends on gut chemistry -- the extent to which ingested food is digested and converted to usable products depends on concentration of a limiting, or otherwise important, component of the material ingested; volume of material ingested and/or volume of the gut; and holding or throughput time of material in the gut.

The importance of quantifying each operating variable in these reactor models to determine an animal's production rate of energy and nutrients from food materials under diverse conditions seems obvious after the equations are written, but the entire set of variables has rarely been measured. For example, values for digestibility (X_{Af}) of specific diets or for energy or nutrient assimilation are frequently presented without reference to the concentrations of important food components, throughput rates, or throughput times. Not only do operating variables remain unquantified, but those variables that are considered are often quantified with inappropriate measurements. For example, it is not valid to measure gut passage or "clearance" time under starvation ($v_0 = 0$) for animals that normally feed continuously if these measures are intended to apply to normal conditions.

Having identified the operating variables for digestion, we can also more closely examine our initial predictions relating digestive

strategies and diet breadth. Flexibility in digestive strategies can now be more specifically described as the ability of an animal to vary gut volume, throughput rate, or throughput time of food material as the composition of its diet changes. Although appropriate data are extremely limited, there is evidence that certain animals are able to use a variety of diets because they can vary V, v_0, or γ in response to a change in concentration of a food component. The most striking examples are among gallinaceous birds such as grouse, quail, ptarmigan whose intestinal length (a component of V) varies seasonally with changes in diet. Birds eating poorer diets have longer intestines (Leopold 1953, Moss 1974). Laboratory studies have shown that starlings (Al-Joborae 1980) and Japanese quail (Savory and Gentle 1976) with longer guts are able to process more food per day than conspecifics with shorter guts while maintaining the same digestive efficiency (X_{Af}).

Other evidence suggests that animals unable to alter their digestive strategies must consume fairly constant diets. In a comparative study of food choice and digestive strategies in howler (Alouatta palliata) and spider monkeys (Ateles geoffroyi) Milton (1981) found that howler monkeys, with their larger hindguts and longer throughput times can ferment plant material more efficiently than spider monkeys and thus maximize energy and nutrient gains on a diet consisting primarily of leaves. Spider monkeys, with smaller hindguts and shorter throughput times, can process more food per unit time and thus specialize on a diet of fruit too low in protein to support howlers. Milton concluded that each species is committed, by physiological and morphological adaptations, to a particular digestive strategy and diet.

On evolutionary scales, ruminants (foregut fermentation, CSTR/PFR gut) outcompete horses (hindgut fermentation, PFR/CSTR gut) when food is scarce because ruminants can extract greater amounts of energy (greater X_{Af}) from limited amounts of food. When food of high nutrient concentration is abundant, horses outcompete ruminants because horses can obtain energy faster by processing large amounts of food more

quickly than ruminants can. Neither can adopt the digestive strategy of the other (Janis 1976).

The digestive strategies open to an animal in turn place constraints on its foraging strategies; any consideration of optimal strategies for maximizing energy gains should therefore include the role of digestion as well as foraging. Sibly (1981) recognized this need, arguing on intuitive grounds what the form of a digestive performance curve must be (plotted as retention time versus net energy gain per gram of ingested food). His digestion curve (Figure 3a) bears a remarkable resemblance to the profit curve for a batch reactor derived by Aris (1965), but again, some important differences exist that demonstrate the value of reactor theory.

The steps in batch operation of an industrial reactor or animal gut can be arranged in series and are repeated in each complete cycle of operation. For any animal batch processing food, these steps are: (1) foraging time, T_f; (2) ingestion time, T_i; and (3) digestion time, T_d. In some cases, a fourth step -- time spent in activities other than foraging, ingestion and digestion -- might be included. The time invested in one step results in a gain or loss of some limiting dietary component (e.g., energy), which is independent of gains or losses in every other step (except that digestive gains and losses are concurrent). Optimal holding time, t^*, of a batch of food material is the time that maximizes net rate of gain of the important component.

From this reactor analysis of digestion, two things become apparent that are not obvious from Sibly's argument. First, optimal holding time increases with increasing T_f, time between meals (Figure 3b) as, analogously, optimal foraging time in a prey patch increases with increasing travel time between patches (e.g., Figure 1 in Cowie 1977). Second, gain from digestion reaches a plateau, but costs of maintaining and operating a gut never cease. There must, therefore, be a holding time beyond which net loss occurs.

In contrast to both Sibly's model and our batch-processing model,

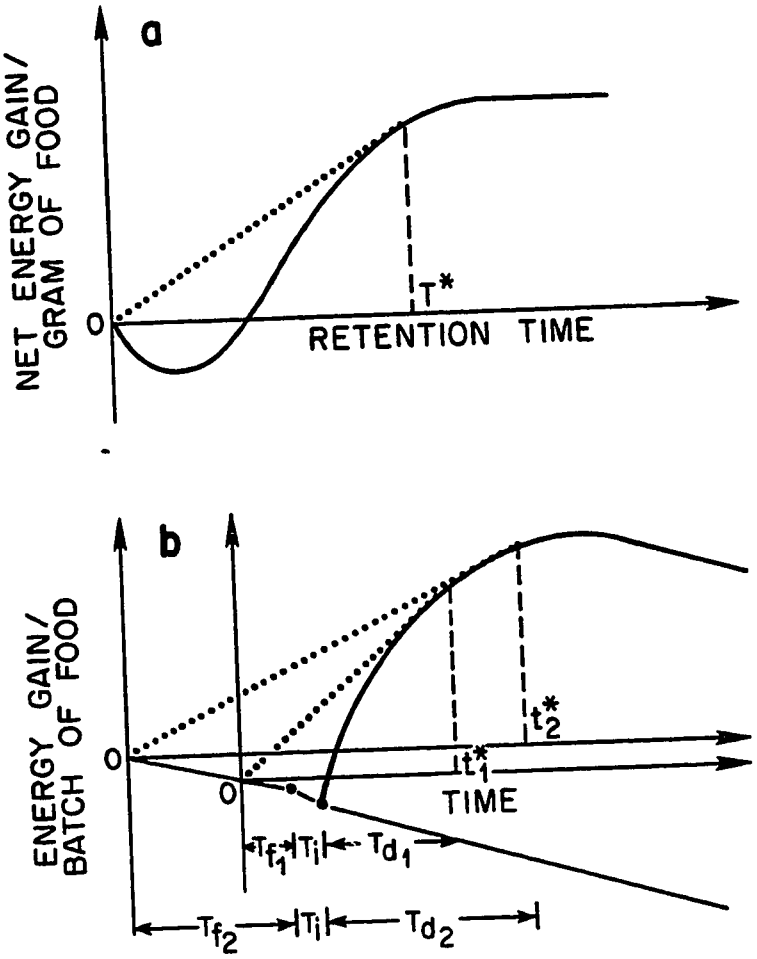

Figure I-3. (a) Digestive performance curve proposed by Sibly (1981). Optimal digestion time (T^*) maximizes net rate of gain of energy per gram of ingested food. (b) Digestive performance curve for a batch process given as gain or loss (per batch) of any limiting dietary component. Increasing time spent foraging ($T_{f_1} \rightarrow T_{f_2}$) increases optimal batch holding time ($t^*_1 \rightarrow t^*_2$).

gains and losses must all be considered simultaneously for an animal that feeds continuously. Some aspects of the steady-state performance of continuous-flow guts can be represented graphically (Figure 4), but a graphical solution for optimal mean gut residence time is convoluted at best. Net digestive gain (Figure 4a) is a function of throughput time, the cost of producing enzymes, and digestive reaction kinetics. For the sake of simplicity, the latter two components are assumed to be invariant with time, but even so, this optimization exercise is more complex than it may seem initially. Throughput time is some function of throughput rate (Figure 4b), which must also be considered to determine net gain to an individual. Moreover, as throughput rate increases, the mechanical costs of moving material through the gut increase (Figure 4c; Taghon 1981). Consequently, since the relevant interdependencies are explicitly included, specific and quantitative predictions are best made using the ideal reactor performance equations rather than a graphical approach.

Applying of chemical reactor theory to characterize digestive strategies offers a powerful framework within which different tactics can be analyzed and compared. It also generates both focus and incentive for new studies in digestive anatomy, histology, and enzymology as well as feeding ecology.

Figure I-4. Digestive performance of a continuous-flow gut at steady state. In this example, energy is the limiting component. (a) The throughput time (τ) which maximizes the net rate of gain of chemical energy per volume of food ingested is given by (τ^*). However, to find net rate of gain and the true optimum for an individual, the throughput rate (v_0) (b) and the mechanical energetic costs associated with that throughput rate (c) must also be considered. These costs are in addition to basic metabolic costs (not figured) which include the cost of maintaining a gut of volume (V).

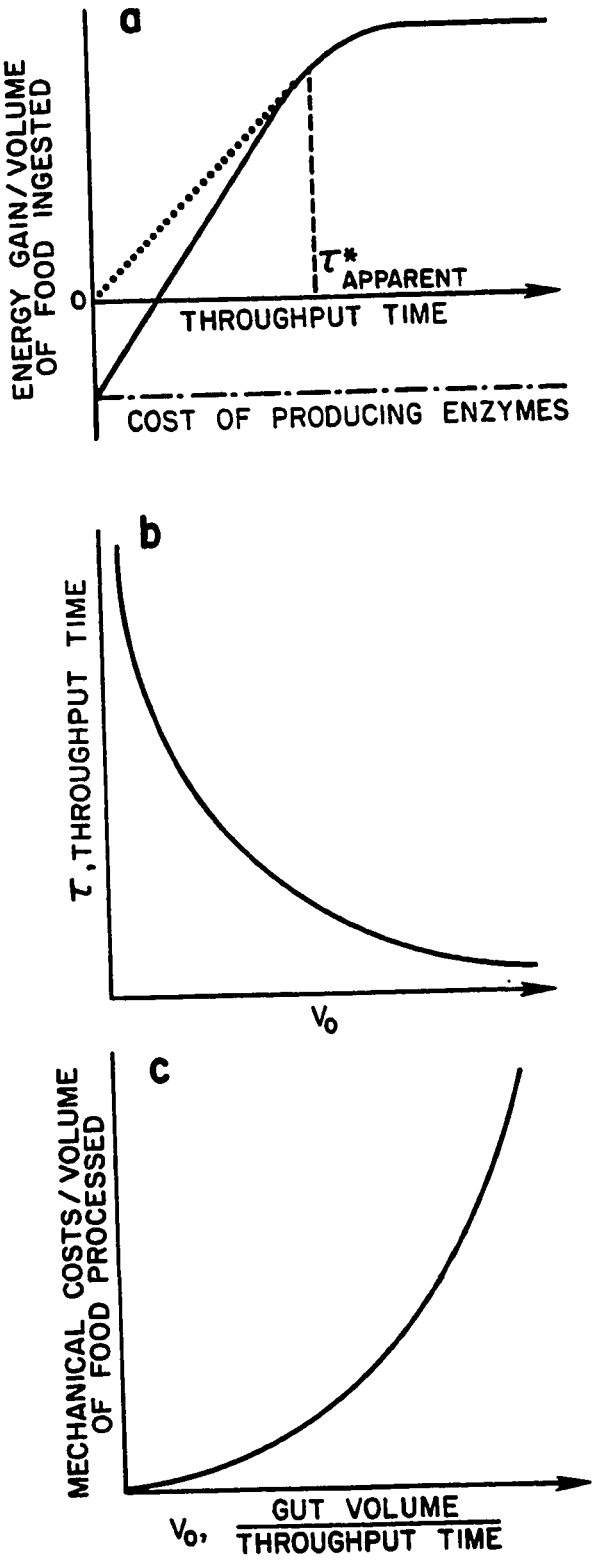
a
ENERGY GAIN/VOLUME OF FOOD INGESTED
0
$\tau^*_{APPARENT}$
THROUGHPUT TIME
COST OF PRODUCING ENZYMES
b
τ, THROUGHPUT TIME
V_0
c
MECHANICAL COSTS/VOLUME OF FOOD PROCESSED
V_0, GUT VOLUME / THROUGHPUT TIME

Chapter II. Modeling animal guts as chemical reactors

INTRODUCTION

The digestive tactics open to an animal constrain its foraging. If an animal "operates" to maximize its net rate of gain of energy or nutrients, optimality of "operating policies" must be defined with respect to both foraging and digestion. Optimality models have generally neglected digestion, although the need to parameterize it has become increasingly apparent (Milton 1981; Sibly 1981; Taghon 1981; Troyer 1984). We (Penry and Jumars 1986) suggested that principles of chemical reactor theory (from which the idea of operating policies comes) can be used to formulate optimization constraints in a general theory of digestion. In this paper we follow those principles to develop explicit models of digestion.

To design a process of chemical conversion, whether it be industrial ammonia synthesis or digestion of food materials by an animal, is to ask what type and size of reactor and what operating conditions are required to achieve a given extent of a desired reaction. The answer, the process design of a reactor, is obtained as follows:

1) Reactions of interest are identified, and models of reaction kinetics are developed from which reaction rate equations are derived.

2) With reaction kinetics specified, the ideal reactor configuration for accomplishing the given reaction is determined.

3) Operations of real reactors are compared with operations of corresponding ideal models, and deviations of real reactor performance from the ideal are analyzed.

4) There are then two options: modify the real reactor to better approximate the ideal model; or modify the model to account for deviations from ideal operations and use the modified model to achieve improved predictions of real reactor performance.

This design sequence serves as the general outline for our development. We first derive forms for digestive reaction rate equations and model guts as ideal reactors. We then compare marine deposit feeders (e.g., polychaete annelids) and mammalian foregut

(e.g., kangaroos, cows, sheep) and hindgut (e.g., horses, rabbits) fermenters with the ideal models. Deposit feeders promise to be ammenable to simple modeling (Jumars and Penry, 1988), while mammalian fermenters have the richest literature for comparison with reactor theory. Finally, since building the ideal worm or cow is not yet a viable option, we suggest generic modifications of ideal gut-reactor models to achieve improved predictions of real reactor performance.

MODEL DERIVATION

Digestive Reaction Kinetics and Rate Equations

Analysis of any chemical process begins with a theoretically or empirically derived kinetic model to provide a form for the reaction rate equation. Reactions are described as either homogeneous or heterogeneous with respect to phases (gaseous, liquid, solid): Homogeneous reactions occur in only one phase, while heterogeneous reactions involve more. General rate equations for the latter include, in addition to reaction kinetics, terms that describe mass transfer between phases.

Digestion, the process that transforms ingested food materials into assimilable components, proceeds through various enzyme-catalyzed and microbially-mediated reactions. These reactions, involving high molecular-weight proteins and other macromolecules, are intermediate between homogeneous and heterogeneous reactions, and the description chosen is the one most useful in a given situation (Levenspiel 1972). We begin by assuming digestive reactions are homogeneous with rates limited only by chemical kinetics. The basic form proposed for enzyme-catalyzed reactions is:

$$A + E \underset{k_{-1}}{\overset{k_{+1}}{\rightleftharpoons}} EA \xrightarrow{k_{+2}} P + E$$

Food component A and enzyme E combine reversibly to form complex EA which then dissociates irreversibly into product(s) P and free enzyme E. The rate equation (after Briggs and Haldane 1925) is of the form:

$$-r_A = \frac{k_{+2} C_E C_A}{\frac{k_{-1} + k_{+2}}{k_{+1}} + C_A} \quad (1)$$

where C_E and C_A are, respectively, concentrations of enzyme and of food-component A, and k_{-1}, k_{+1}, and k_{+2} are the rate constants. This equation simplifies to the more familiar Michaelis-Menten form when C_E is constant:

$$-r_A = (v_{max} C_A) / (K_m + C_A) \quad (2)$$

where $v_{max} = (k_{+2} C_E)$ and $K_m = (k_{+1} + k_{+2}) / k_{+1}$. Digestive reactions catalyzed by an animal's own enzymes will be described with this rate equation.

Digestive reactions involving microbial fermentation are autocatalytic: A reaction product (microbes) acts as a catalyst, and reaction rate is a function of concentration of both microbes and food materials. The modified Michaelis-Menten rate equation often used to describe such autocatalytic biological reactions (Bischoff 1966) is of the form:

$$-r_A = (v_{max} C_A C_M) / (K_m + C_A) \quad (3)$$

where C_M is concentration of microbes.

The basic Michaelis-Menten equation (hereafter termed the catalytic equation) and the modified form for autocatalytic, fermentation reactions (hereafter, the fermentation equation) relate digestive reaction rates to concentrations (of food substrates, enzymes and microbes). Rates of digestive reactions may also be affected, however, by changes in temperature, gut pH and gut microbial community composition. We avoid these complications by formulating reactor models for animal guts operating at steady state. In a steady-state model, temperature, gut pH and microbial community composition are assumed constant over time at any given point within the gut. The need

to insure that these steady-state assumptions are met then becomes an important consideration when designing experimental tests of model predictions.

Mass Balance

Having chosen kinetic models, the next step is to identify the ideal method for processing reactants. Our design objective in this excercise is to identify the gut (reactor) configuration and digestive (operating) strategy that maximize an animal's net rate of production of energy and nutrients from food.

We use conservation principles to predict reactor performance. Phenomena occurring in chemical reactors are reactions and transfers of mass, energy, and momentum. In contrast to many industrial situations, both temperature and pressure variations within an animal's gut generally are negligible relative to compositional changes. Reaction and mass transfer are the dominant processes, and reactor-specific equations for conservation of mass suffice. Formulation of reactor-specific equations begins with a general mass-balance expression written for any component, reactant or product, over an arbitrary element of reactor volume:

$$I = E + R + W \tag{4}$$

where I is input of component, E is output, R is disappearance by reaction and W is accumulation of in the reactor (all units in moles $time^{-1}$). Simplification of this general equation for a given reactor type yields the mass balance equation describing that reactor's performance. There are three ideal reactors differing primarily in the way reactants are processed. Although mass balance equations for each can be obtained from any chemical engineering text (e.g., Levenspiel 1972, Froment and Bischoff 1979; J. Smith 1981), we include derivations to provide the foundation for understanding gut-reactor models as well as to allow specific modifications for digestive processes. Our notation follows Levenspiel (1972).

The Batch-Reactor Performance Equation

The batch reactor (Fig. 1), as its name implies, processes reactants in discrete batches. Production periods are separated by idle periods during which the reactor is emptied of products from the previous reaction cycle, reloaded with reactants, and prepared for the next cycle. The ideal batch reactor is spatially homogeneous at any one time: Its contents are perfectly mixed, and changes in composition occur only with respect to time. Thus, the mass balance of any key component, here designated reactant A, can be written over the entire reactor volume. Since material neither enters nor leaves the batch reactor during reaction (I = E = 0), the general mass balance (Eq. 4) simplifies to two terms:

$$R = -W \tag{5}$$

where R is disappearance of A by reaction (moles $time^{-1}$) and W is accumulation of A in the reactor (moles $time^{-1}$). The amount of reactant A consumed by reaction per unit time is a function of reaction rate ($-r_A$). When ($-r_A$) is expressed on a unit-volume basis:

$$R = (-r_A)\, V \tag{6}$$

where R is amount of A reacted (moles $time^{-1}$), $-r_A$ is reaction rate (moles vol^{-1} $time^{-1}$), and V, the reacting volume. The amount of reactant A accumulated (i.e., unreacted) per unit time is:

$$W = (-N_{A0})\, (dX_A/dt) \tag{7}$$

where W is amount of A accumulated (moles $time^{-1}$), N_{A0}, the initial amount of A introduced (moles), and (dX_A/dt), the time rate-of-change of the fraction of A converted to products ($time^{-1}$). Substituting Eqs. 6 and 7 into Eq. 5,rearranging terms, and integrating the entire expression yields the performance equation (Eq. 8) for an ideal batch reactor. The holding or reaction time (t) required to achieve a given conversion (X_{Af}) of reactant A to products in a batch reactor is:

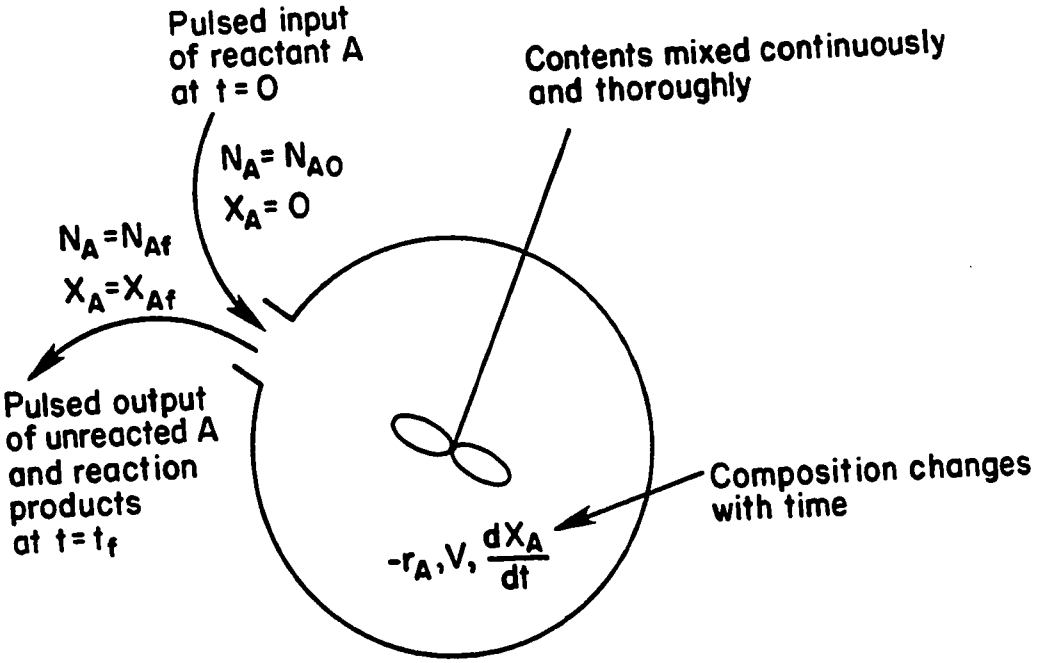

Figure II-1. The ideal batch reactor operates intermittently. Reactants are loaded at time t=0. Reaction occurs, and then the resulting reactant/product mixture is unloaded at $t=t_f$. At t=0, the amount of reactant A added to the reactor is N_{AO}; the proportion of reactant A converted to products, X_A, is zero. At $t=t_f$, the amount of A that remains unreacted and is removed from the reactor is N_{Af}; the conversion of A to products is X_{Af}. V is reactor volume, and $-r_A$ represents an equation for reaction rate.

$$t = N_{AO} \int_0^{X_{Af}} \frac{dX_A}{-r_A V} \tag{8}$$

If we assume that an animal ingests enough food to fill its gut, volume of reacting food material equals to gut volume, and V refers to total gut volume. As digestion proceeds, however, volume of food material decreases relative to gut volume as digestive products are absorbed. Such deviations from ideal batch-reactor operations can be incorporated into modified batch-reactor models, but it is reasonable to begin with consideration of the least complex case and neglect, initially, deviations from the ideal. If we assume that volume variations resulting from absorption are negligible, a justifiable assumption for some animals we discuss (e.g., deposit feeders), we can further simplify the batch-reactor performance equation. After removing reactor volume (V) from under the integral:

$$t = C_{AO} \int_0^{X_{Af}} \frac{dX_A}{-r_A} \tag{9}$$

where $C_{AO} = N_{AO}/V$, the initial concentration of reactant A. For an animal with a batch-reactor gut, Eq. 9 can be solved for the gut holding time (t) necessary to achieve a specified conversion (X_{Af}), or it can be solved for the conversion that can be achieved in a given holding time ($-r_A$, C_{AO} given in each case). Solutions to Eq. 9 (i.e., solution for t given $-r_A$, C_{AO}, X_{Af}, or solution for X_{Af} given $-r_A$, C_{AO}, t) can then be used to determine the gut volume required to achieve a specified rate of production of digestive products.

The Plug-Flow Reactor Performance Equation

The plug-flow reactor (PFR) (Fig. 2) is characterized by continuous, orderly flow of material through the (usually tubular) reaction vessel. Since perfect radial mixing is assumed, reactants are uniform in any cross-section. Axial mixing and axial diffusion rates are, by definition, negligible in comparison to axial flow rate, and material composition varies only along the flow path. The mass balance

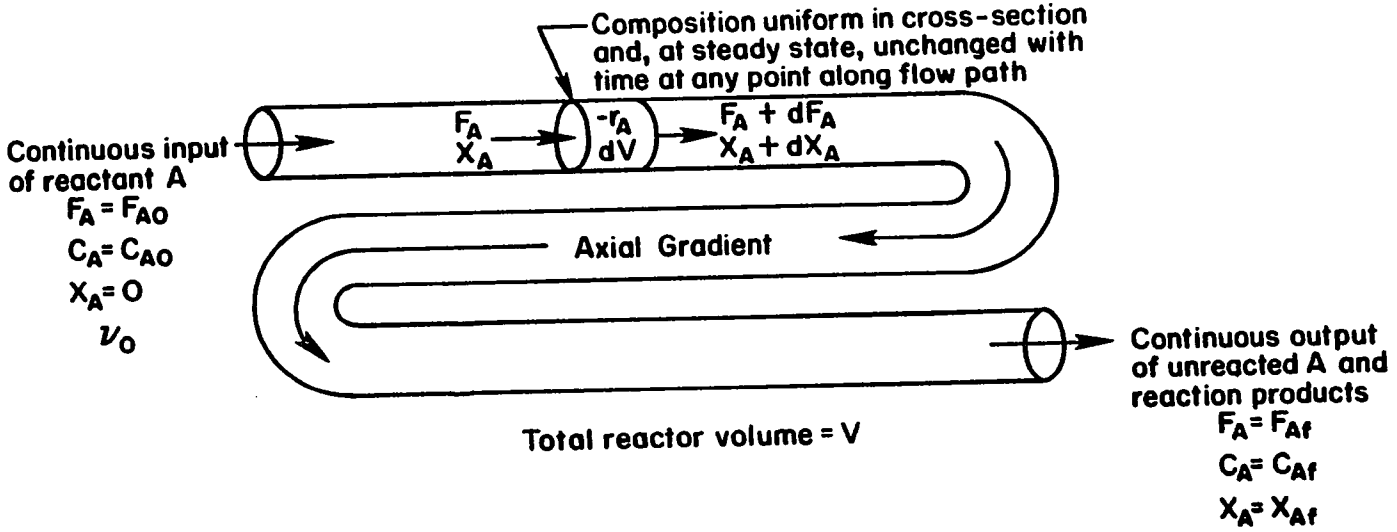

Figure II-2. The ideal plug-flow reactor operates continuously. The volume of material flowing through the reactor per unit time is the throughput rate, v_0. The input rate of reactant A is F_{A0}; initial concentration of A is C_{A0}; and the proportion of A converted to products, X_A is initially zero. The output rate of A is F_{Af}; final concentration of A is C_{Af}; and final conversion of A to products is X_{Af}. The characteristics of the ideal PFR require that a mass balance be written over a differential volume element, dV, and then integrated over the entire reactor volume, V. $-r_A$ represents an equation for reaction rate.

for a key component, reactant A, in a PFR operating at steady state must, therefore, be made over a differential volume element. Since material flows continuously through the reactor, there can be no accumulation of A within the reaction vessel (W = 0), and the general mass balance (Eq. 4) becomes:

$$I = E + R . \tag{10}$$

Input of A into volume element (dV) (Fig. 2) is:

$$I = F_A, \text{ where } F_A \text{ is the input rate of A, (moles time}^{-1}) \tag{11}$$

and output of A from dV is:

$$E = F_A + dF_A . \tag{12}$$

Amount of A consumed is a function of reaction rate, $-r_A$, (moles $\text{vol}^{-1}\text{time}^{-1}$):

$$R = -r_A \times dV . \tag{13}$$

Substituting Eqs. 11-13 into Eq. 10, $F_A = (F_A + dF_A) + (-r_A)\, dV$, and rearranging:

$$0 = dF_A + (-r_A)\, dV \tag{14}$$

The incremental change in amount of A, (dF_A), can be expressed in terms of (F_{A0}), the input rate of A, and (dX_A), the incremental change in the fraction of A converted to products:

$$dF_A = d(F_{A0}(1 - X_A)) = (-F_{A0})\, dX_A \tag{15}$$

Substituting Eq. 15 into Eq. 14, rearranging terms, and integrating the entire expression yields the ideal plug-flow reactor performance equation:

$$\frac{V}{F_{A0}} = \int_0^{X_{Af}} \frac{dX_A}{-r_A}$$

or

$$\tau = \frac{V}{v_0} = C_{A0} \int_0^{X_{AF}} \frac{dX_A}{-r_A} \qquad (16)$$

where F_{A0} is replaced by C_{A0} times v_0, initial concentration of A (moles vol^{-1}) times volumetric flow rate (vol $time^{-1}$).

Space-time, (τ, in units of time) the ratio of reactor volume (V) to volumetric flow rate (v_0), is the time required to process one reactor volume of material input. In reactor models for animal guts, is throughput time, the time in which one gut volume of food is processed. Throughput time is the ratio of gut volume (V) to throughput rate (v_0).

The Continuous-Flow, Stirred-Tank Reactor Performance Equation

The continuous-flow, stirred-tank reactor (CSTR) (Fig. 3) is characterized by continuous flow of material through, and perfect mixing of material within, the reaction vessel. Since composition of material within a CSTR operating at steady state is spatially homogeneous and constant with time, the mass balance for reactant A is written over the entire reactor volume (V). With continuous flow and perfect mixing A does not accumulate in an ideal CSTR (W = 0), and the general mass balance (Eq. 4) is:

$$I = E + R . \qquad (17)$$

Input of A is:

$$I = F_{A0} \qquad (18)$$

and output of A is:

$$E = F_{A0} (1 - X_A) \qquad (19)$$

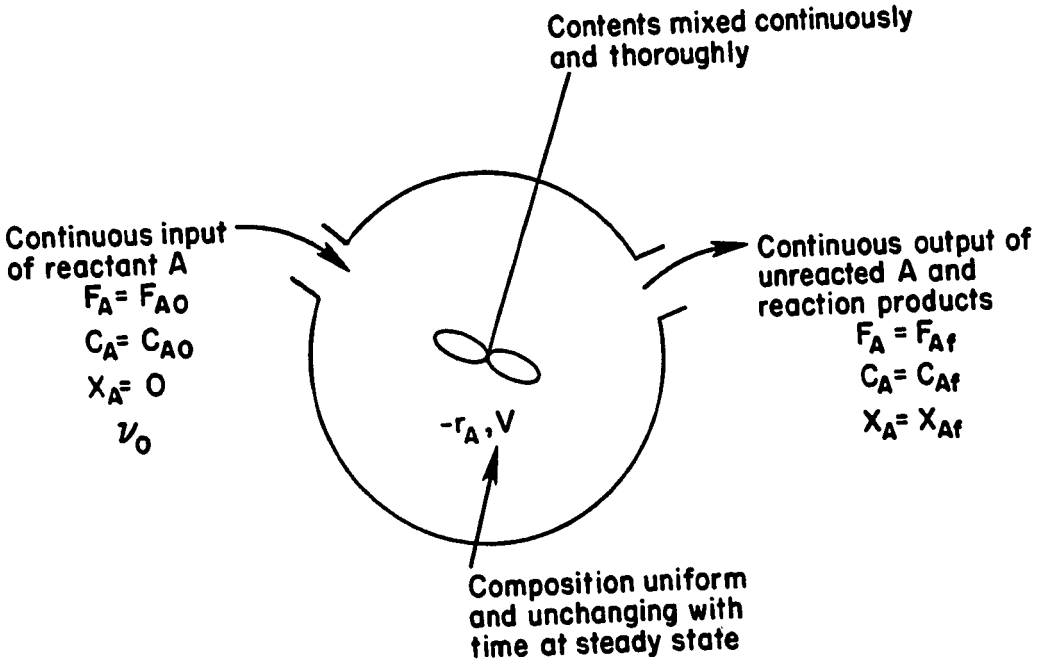

Figure II-3. The continuous-flow, stirred-tank reactor operates continuously. The volume of material flowing through the reactor per unit time is the throughput rate, v_0. The input rate of reactant A is F_{A0}; the initial concentration of A is C_{A0}; and the proportion of A converted to products, X_A, is initially zero. The output rate of A is F_{Af}; the final concentration of A is C_{Af}; and the final conversion of A to products is X_{Af}. V is reactor volume, and $-r_A$ represents an equation for reaction rate.

The amount of A that disappears by reaction is:

$$R = (-r_A)\ V \tag{20}$$

Substituting Eqs. 18-20 into Eq. 17:

$$F_{A0} = F_{A0}\ (1 - X_A) + (-r_A)\ V;$$

then, rearranging terms yields the performance equation for an ideal CSTR:

$$\frac{V}{F_{A0}} = \frac{X_A}{-r_A} \tag{21}$$

Input rate of A, F_{A0}, is C_{A0} times v_o, initial concentration of A times volumetric flow rate. The ideal CSTR performance equation (21) can therefore be expressed in terms of C_{A0} and v_0:

$$\tau = V / v_0 = (C_{A0})\ (X_A) / (-r_A) \tag{22}$$

As defined earlier, τ, is throughput time in our gut-reactor models. Throughput time for a CSTR gut, as for a PFR gut, is the ratio of gut volume (V) to volumetric throughput rate (v_0).

Throughput Time and Conversion

"Gut clearance time" is not a synonym for space-time or throughput time. It refers specifically to the time required for an animal entering starvation to evacuate its gut completely. Gut clearance time is thus throughput time measured under unsteady conditions that are both difficult to model and unnatural, especially for animals ordinarily feeding more or less continuously. Note also that neither "gut residence time" nor "gut passage time" is equivalent to throughput time or batch-reactor holding time. Residence time (θ) is the time an individual material element spends in a reactor or a gut. "Gut passage time" -- also erroneously called "gut passage rate" even when measured as time^{+1} -- is actually mean gut residence time ($\bar{\theta}$). Since mean

residence time can be precisely and unambiguously defined (e.g., J. Smith 1981), its use is preferable.

For a PFR gut in which throughput rate is constant, throughput time, residence time and mean residence time all are equal. In fact, the equation $\Theta = \bar{\Theta}$ is a necessary condition for plug flow (Levenspiel 1972). In contrast, residence times of individual material elements in a CSTR may differ, and effective description requires a residence-time distribution. Mean residence time and throughput time are equal in an ideal CSTR. Since batch reactor operation does not involve flow of material into or out of the reactor, we use holding time rather than throughput time. The characteristics of ideal batch reactor operation require that holding time, residence time and mean residence time all be equal for any given batch.

We express performance equations for all three ideal reactors (Eqs. 9, 16 and 22), in terms of conversion (X_A), the fraction of reactant A that reacts to form products. It is important to future tests of gut-reactor models that we define conversion in terms of experimentally measurable quantities. If we assume that digestion is a constant-density (mass volume^{-1}) system, conversion can be defined as:

$$X_A = 1 - C_A / C_{A0} \tag{23}$$

The boundary conditions we use are: (1) initial conversion of food material: $X_{A0} = 0$; and (2) final conversion: $X_{Af} = 1 - C_{Af} / C_{A0}$ where C_{Af} is the concentration of A in egested material, and C_{A0} is the concentration of A in ingested material. These boundary conditions are arbitrary and may be changed as appropriate. For example, ($X_{A0} = 0$) may not hold when, as in some spiders, breakdown of food materials begins before food is ingested. Equation 23 can also be used to convert reaction rate equations (Eqs. 2 and 3) from the functions of concentration (C_A) initially derived to known functions of conversion (X_A).

Ideal Reactor Designs with Respect to Digestion

As previously stated, our design objective for digestive reactions is to identify gut (reactor) configurations and digestive (operating) strategies that maximize production rate of energy and nutrients from food. In terms of design variables we have defined, our objective is to identify the gut-reactor configuration in which the maximum conversion (X_{Af}) of ingested food to assimilable products is achieved in minima of time (t or τ) and gut-reactor volume (V). Note that reaction rates ($-r_A$) are expressed as functions of conversions (X_A).

Holding time in a batch reactor and throughput time in a plug-flow reactor are compared as areas under the curve of the reciprocal of reaction rate versus conversion (C_{A0} constant). Since we have assumed that volume of reacting food material is equal to gut volume and does not change significantly during the course of reaction, the performance equations for ideal batch and plug-flow reactors are interchangeable: $t = \tau_{PFR}$ where C_{A0} is constant. For any given reaction, the time (t, τ_{PFR}) and the reactor volume required to achieve a specified final conversion are identical for the two ideal reactors (Fig. 4).

The contrast between batch and plug-flow reactors becomes one of discontinuous versus continuous operation. In the batch reactor production (reaction) periods are interrupted by discharge and idle periods, whereas the PFR is continuously productive. To compensate for intermittent operation, a larger batch-reactor volume is required to match the production-rate capabilities of the PFR. Our design objective is, therefore, better satisfied by a gut-reactor configuration that allows continuous processing of food.

The ratio of throughput time in a PFR (τ_{PFR}) to throughput time in a CSTR (τ_{CSTR}) is given graphically by the ratio of the areas designated in Figure 5. For reactions with rates that fall monotonically as reactant concentration decreases, a greater throughput time (or if throughput rate is constant, a greater reactor volume) is always required to achieve a given conversion with stirred flow than with plug flow. Since catalytic digestive reactions (Eq. 1) belong to

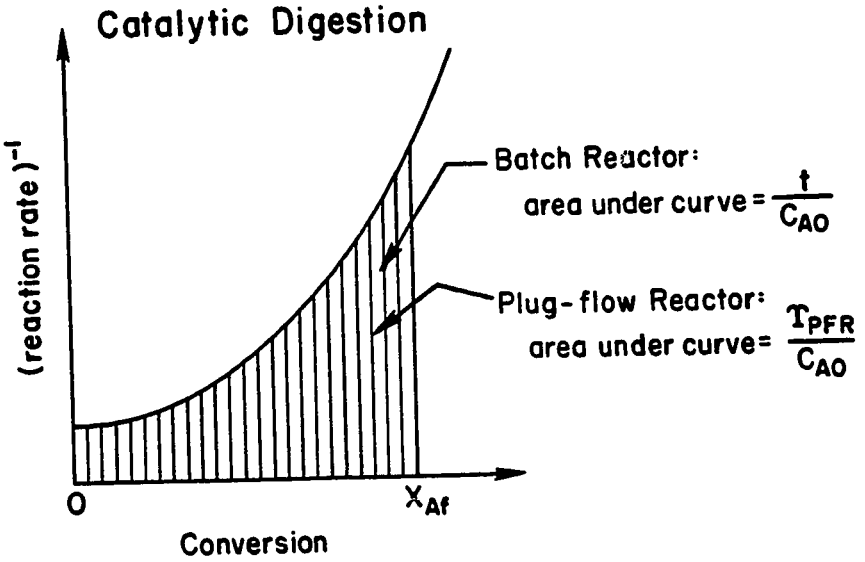

Figure II-4. Comparison of ideal batch and plug-flow reactor performances with respect to catalytic digestive reactions where reaction kinetics are given by the Michaelis-Menten enzyme model. If C_{AO}, initial concentration of reactant A, is constant, batch reactor holding time, t, and plug-flow reactor throughput time, τ_{PFR}, are identical.

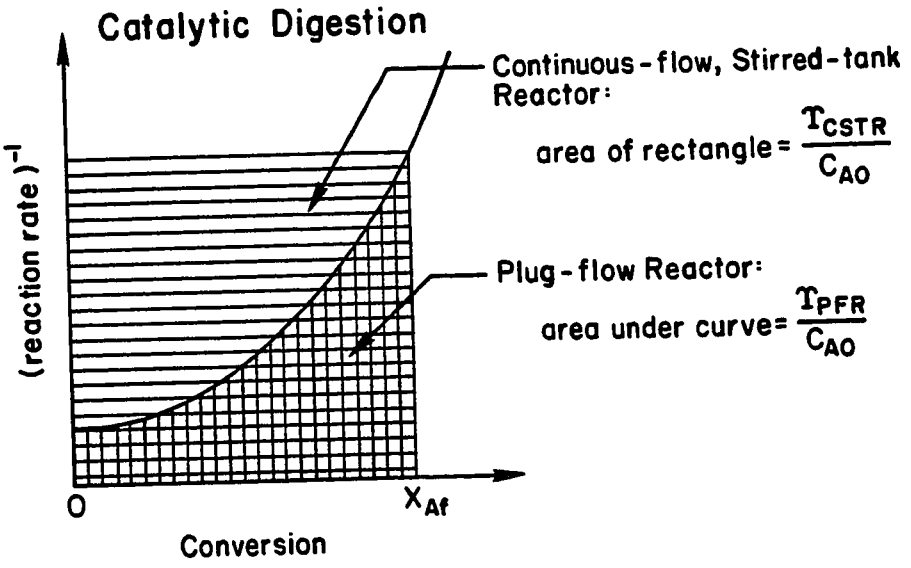

Figure II-5. Comparison of ideal plug-flow and continuous-flow, stirred-tank reactor performances with respect to catalytic digestive reactions where reaction kinetics are given by the Michaelis-Menten enzyme model. If C_{A0}, initial concentration of reactant A, is constant, the plug-flow reactor throughput time, τ_{PFR}, required to achieve any final conversion, X_{Af}, is always less than the continuous-flow, stirred-tank reactor throughput time, τ_{CSTR}, required to achieve the same conversion.

this category, our design objective for them is best satisfied by a gut that functions as an ideal PFR.

Development of the PFR model for animal guts, however, does more than confirm the obvious. It provides concrete physical and chemical reasons why animal guts should operate as PFRs. The PFR design represents the better method of accomplishing catalytic digestion because it maintains a gradient in reactant concentration, and therefore, in reaction rate, from higher values near the reactor entrance to lower values near the exit. In contrast, the high reactant concentration entering a CSTR is diluted immediately to some lower, constant level by material recirculating in the reactor.

Determination of the ideal gut-reactor configuration for autocatalytic reactions is easily solved with graphical representations of the ideal-reactor performance equations. When digestion involves microbial fermentation, these reactions are only one process component, but we first consider the simpler case in which autocatalytic reactions comprise the entire process. For autocatalysis, the curve of reciprocal reaction rate versus conversion has a characteristic minimum (Fig. 6a), the point of maximal reaction rate. As before, comparison of the ratio of throughput time in a PFR to throughput time in a CSTR is used to identify the reactor configuration that best satisfies our design objective. At low conversions of reactants to products the CSTR requires the smaller throughput time or, if throughput rate is constant, the smaller reactor volume (Fig. 6a). As conversion increases, PFR performance equals, and then surpasses, the CSTR (Fig. 6b). To maximize conversion while minimizing total throughput time or reactor volume (v_0 constant) the ideal design for a single autocatalytic reaction is to use the two reactors in series: a CSTR followed by a PFR (Fig. 6c).

We have proposed that the ruminant gut be modeled as a CSTR-PFR reactor series because observed tracer residence-time distributions are exactly explained by this model (Penry and Jumars, 1986). We now provide additional physical and chemical justifications. The primary

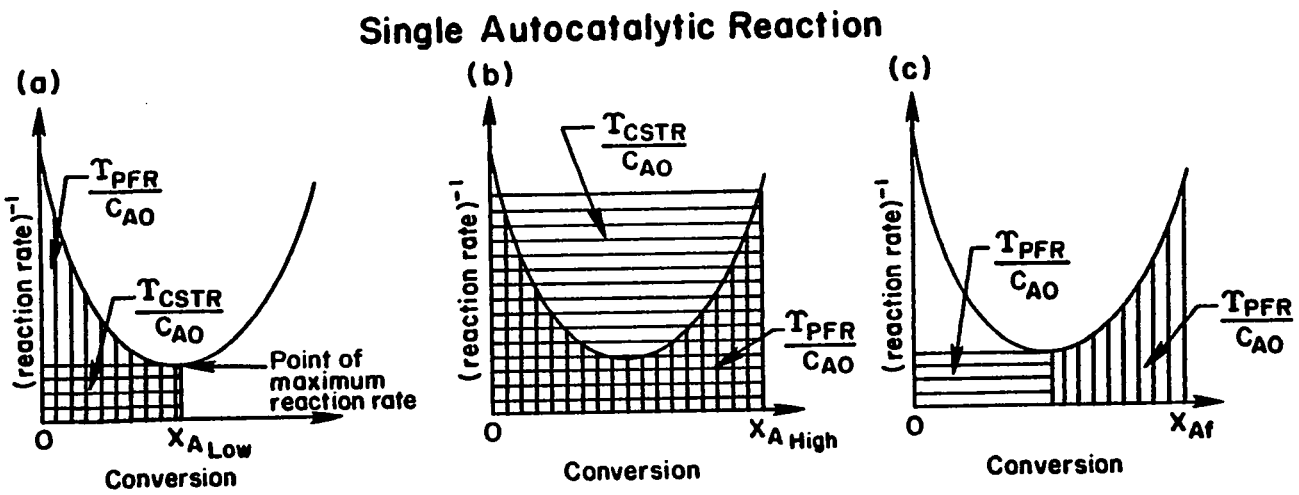

Figure II-6. Comparison of ideal plug-flow and continuous-flow, stirred-tank reactor performances with respect to any autocatalytic reaction. C_{AO}, initial concentration of reactant A, is constant among all comparisons. (a) At low conversions, the CSTR throughput time, τ_{CSTR}, is less than the PFR throughput time, τ_{PFR}. (b) At high conversions, however, CSTR throughput time exceeds PFR throughput time. (c) High conversions of reactants to products via an autocatalytic reaction can be achieved in minima of total throughput time or total reactor volume if a CSTR-PFR series is used.

fermentation site in ruminants (e.g., cows, sheep, goats, deer) is the foregut. Our discussion generalizes to other foregut fermenters as well (e.g., hippos, kangaroos, monkeys of the subfamily Colobinae).

As we have shown, fermentation rate is maximized in minimal throughput time or gut-reactor volume (v_0 constant) if the foregut (rumen or stomach) functions as a CSTR (Fig. 6a). However, in contrast to the simple case of a single, autocatalytic reaction just analyzed, acid treatment in foregut fermenters stops fermentation as material leaves the CSTR chamber. Digestion then proceeds primarily through catalysis, better accomplished in a PFR (Fig. 5). Thus, digestion in foregut fermenters involves two consecutive reaction types in a CSTR-PFR series (Fig. 7a):

fermentation reactions

1) ingested food (C_A = 0 with respect to fermentation) ⟶ fermentation products ($X_A = X_{Af}$ with respect to fermentation)

catalytic digestive reactions

2) fermentation products (X_A = 0 with respect to catalysis) ⟶ assimilable components ($X_A = X_{Af}$ with respect to catalysis)

Suppose catalytic digestive reactions precede fermentation. In this case the entire digestive process is best accomplished in a PFR-CSTR series (Fig. 7b), and we have designed a hindgut fermenter (e.g., elephants, rhinos, horses, koalas, rabbits, gallinaceous birds, monkeys of the family Indriidae, some aquatic, leaf-shredding insects, wood-boring bivalves of the subfamily Xylophagainae). Differences between the two digestive strategies are direct consequences of the order in which the reactions occur. Since the exact curves of reciprocal reaction rate versus conversion are unknown, we can not further compare foregut and hindgut fermentation strategies using the graphical approach.

Two very general predictions thus result from our simple

Figure II-7. Determination of gut-reactor configurations when digestion involves both autocatalytic, fermentation reactions and catalytic, enzyme reactions. (a) When fermetation precedes catalytic digestion, high conversions of food to useable components can be achieved in minima of throughput time and gut volume is the gut operates as a CSTR-PFR series. This gut-reactor configuration is the basic representation for any foregut fermenter. (b) When catalytic digestion precedes fermentation, the gut should operate as a PFR-CSTR series. This gut-reactor configuration is the basic representation for any hindgut fermenter.

(a) Digestive Reaction Series:

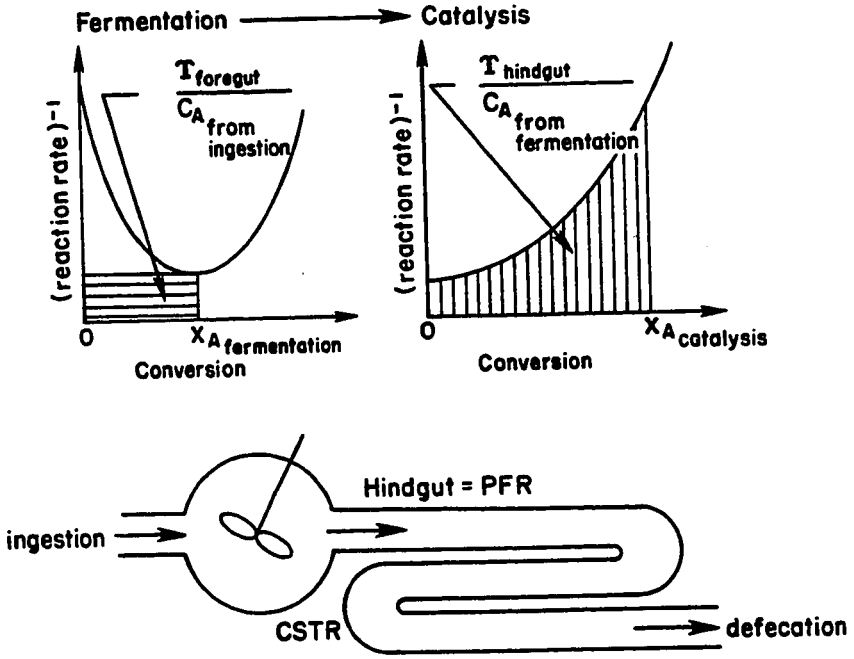

(b) Digestive Reaction Series:

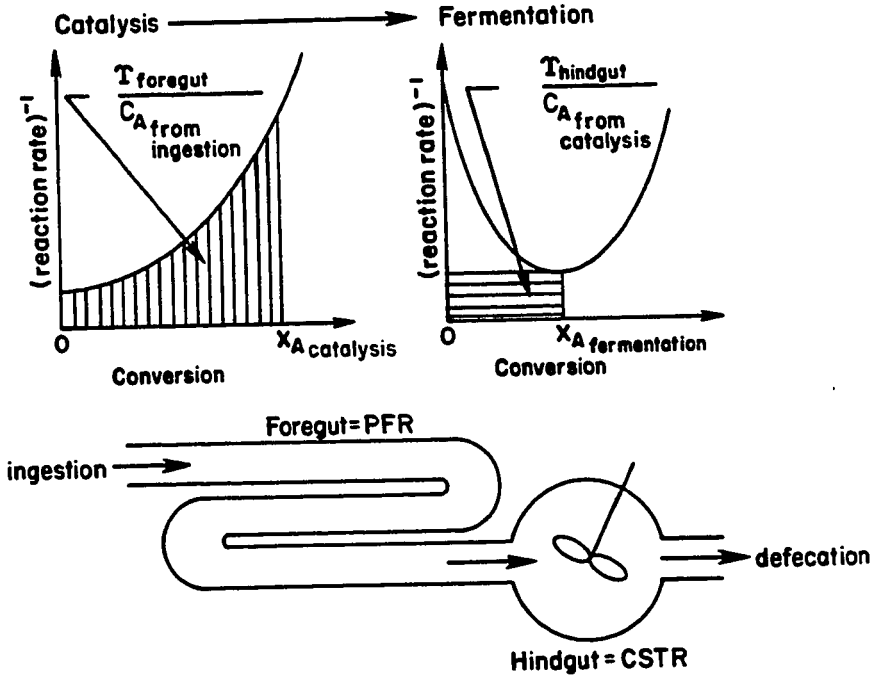

application of chemical reactor analysis to the study of digestion. Under the assumptions given, an animal's net rate of production of energy and nutrients from food via catalytic digestive reactions (Eq. 2) is maximized when its gut is an ideal PFR. If, in addition to catalytic digestive reactions, fermentation reactions (Eq. 3) are important digestive components, fermentive production rate is maximized when a portion of the gut is a CSTR.

COMPARISON WITH REAL REACTORS

It takes only a brief, qualitative review to substantiate both predictions. Tubular guts predominate among more complex, multicellular animals, and digesta flow through tubular guts can be described quite reasonably by the plug-flow model. Large chambers are important features of guts in animals using fermentation. Digesta flow through these chambers, for example through the rumen of cows (Balch 1950; Demment and Van Soest 1985; Van Soest 1982) or the caecum of rabbits (Pickard and Stevens 1972; Stevens et al. 1980), can be approximated by flow through a CSTR. Additional value of the reactor theory formalism, then, must lie in its ability to deal with more specific cases (e.g., more narrowly defined feeding or digestive guilds or more quantitative prediction) and with exceptions to our two general predictions.

Deposit Feeding

Use of chemical reactor analysis to study deposit-feeder digestion serves as a simple example of reactor model utility in generation of specific predictions for future experimentation and measurement. Of all animals, deposit feeders are most likely to conform to the assumption that volume changes are negligible during digestion; the volumetric bulk of food ingested is in mineral grains. We postulate initially that deposit-feeder digestion involves only catalytic digestive reactions and consequently predict that deposit-feeder guts should operate as ideal PFRs. Qualitative observations of tracer movements through guts of representatives of three deposit-feeding taxa have shown approximation to plug flow: Nereis succinea (a polychaete;

Cammen 1980), Corophium spp. (an amphipod; Miller 1984), and Pseudopolydora kempi japonica (a polychaete; Jumars and Self 1986). Our unpublished tracer observations add two more polychaetes, Abarenicola pacifica and Pygospio elegans, and one holothuroid, Parastichopus californicus, to this list. Axial mixing was observed to be negligible in all these species, thus fulfilling the most important assumption of the ideal plug-flow model and confirming the results of our theoretical analysis.

Deviations from plug flow have been observed, however, in guts of the ampharetid polychaetes, Amphicteis scaphobranchiata and Hobsonia florida. Qualitative tracer observations in conjunction with gut dissections (Jumars and Self 1986; D. L. Penry pers. obs.) indicate that anterior mixing occurs in these ampharetid guts and presumably in anatomically similar terebellimorphs (e.g., Dales 1955; Dales and Pell 1970). Tracer results and gut morphology are consistent with a CSTR-PFR series. In addition to already discussed disadvantages of a CSTR compared to a PFR in catalytic digestion, a CSTR incurs the energetic costs of mechanical mixing.

Under what environmental conditions is a CSTR-PFR gut necessary or advantageous for survival? Deposit feeders having guts with mixing chambers tend to be large or to ingest fine sediments of low permeability (P. A. Jumars pers. obs.). Diffusion rate of digestive enzymes to food particles may limit reaction rate in the absence of mixing. Under these conditions the advantages of a gut with a mixing chamber may outweigh the twin disadvantages of greater energy requirement for mixing and reduction in effective reactant concentration through dilution with previously ingested and partially digested material. A less likely alternative, mentioned because of its relevance to ruminants and mammalian caecal fermenters, is that mixing is the byproduct of a gut-sorting mechanism that selectively retains some particles for further digestion. Sorting within the gut has been seen in Hobsonia florida (Self and Jumars 1978). Nor can we presently discount the possibility that fermentation occurs in the CSTR, but it seems unlikely to be nutritionally important at the shorter throughput

times observed (Taghon and Jumars 1984).

The hypothesis that diffusion of digestive enzymes constrains deposit-feeder digestion suggests specific couplings of body size with foraging and digestive strategies. Relatively large deposit feeders with mixing guts may ingest and process sediments of relatively low permeability. Deposit feeders with plug-flow guts, however, may be limited to relatively small sizes and gut diameters or to ingesting and processing sediments of relatively higher permeability. Relatively small deposit feeders with plug-flow guts dominate sites of organic enrichment (Pearson and Rosenberg 1978) and the food-poor abyss (Jumars and Gallagher 1982). Food of low permeability -- poorly sorted, organic-rich muds in the former case and nearly pure clays (Hessler and Jumars 1974) in the latter -- is characteristic of these seemingly disparate environments. Selective abilities of some deposit feeders may insure permeability of digesta, while field distributions of those with limited selective abilities may be constrained by sediment permeability.

The relationship between sedimentary parameters and the distribution of Arenicola marina (Polychaeta, Arenicolidae) can be re-interpreted in light of this last hypothesis. Longbottom (1970) sampled ten sites differing in sediment type, sediment organic content and A. marina density. Median grain size and organic content were inversely correlated. Although organic content was highest in the finest sediments, adult A. marina were not found below median grain sizes of 80 um; only juveniles were. Longbottom suggests that the distributional pattern results from the inability of adult A. marina, but not of juveniles, to maintain burrows in fine sediments. We suggest instead that digestive constraints may be responsible.

From its anatomical and functional similarities to Abarenicola pacifica (Arenicolidae), a species we have studied, we infer that particle mixing in A. marina's gut is insignificant. Although finer sediments are generally higher in organic content than coarser sediments, they are also generally lower in permeability. Because

juveniles have small gut diameters, diffusion of digestive enzymes through sediments probably is not limiting. Juveniles may, however, reach a size at which diffusion of enzymes into gut contents (or digestive products out) becomes limiting, resulting in a net loss of energy or nutrients. Since A. marina is a relatively non-selective feeder (Fauchald and Jumars 1979), it similarly may be excluded from areas of poorly sorted sediments irrespective of median grain size. Data to test these hypotheses do not exist yet have potentially broad application. Studies of functional morphology and kinematics of deposit feeders' guts with reference to gut-reactor models, feeding strategies, and distributional patterns are needed.

A review of gross gut morphologies of deposit-feeding taxa yields a second apparent exception to the general plug-flow model for deposit feeders. Asteroids and ophiuroids (Echinodermata) include reportedly deposit-feeding representatives which appear to have batch-reactor guts. The simple, sac-like guts have but one major opening: Material is both ingested and egested through the mouth. Shick et al. (1981) indicate that at least one deposit-feeding asteroid, Ctenodiscus crispatus (Gonopectinidae), does operate as a batch reactor (although the egestion behavior observed conceivably could have been a response by C. crispatus to the physical disturbance of collection).

Industrial batch reactors are used when their construction and maintenance costs are low or when high conversions are more important than large production rates (i.e., when reactant supply is limiting). Bona fide deposit feeders, however, exploit a very dilute food resource and must, therefore, process large quantities of sediment per unit time. What characteristics and adaptations may enable these deposit-feeding asteroids to utilize a batch-processing rather than continuous-flow digestive strategy?

In addition to low maintenance requirements (inferred from respiratory requirements), Ctenodiscus crispatus has a very distensible stomach which may enable it to process large volumes of sediment (Shick et al. 1981). The Porcellanasteridae, taxonomically-related,

abyssal deposit-feeding asteroids, also have large, undivided, sac-like guts that, when filled with sediment, cause their disks to be greatly expanded (Madsen 1961). Assuming adequate mixing (as the batch reactor formulation does), the large gut volume and, therefore, the increased amount of sediment processed per batch may result in net production rates comparable to those achieved by a deposit feeder with a smaller, but continuous-flow, gut.

Ophiuroids do not seem to have comparably distensible guts; their disks are generally smaller and more rigid than asteroids'. They do, however, have adaptations that may minimize their energy requirements. The low metabolic rates of deposit-feeding ophiuroids (Buchanan 1964) indicate that rates at which they need to obtain energy are also low, and their simple, sac-like guts are probably energetically inexpensive to maintain. Metabolic rates are especially low in the reactor-theory relevant terms of body and gut volume, since much of the body volume is made up of metabolically inactive calcium carbonate. These low energy requirements may make batch processing a viable alternative, but the relatively limited amounts of food-poor material that can be processed per unit time still cast doubts upon the success of a purely deposit-feeding strategy.

It is possible that ophiuroids, although possessing blind guts, are able to ingest and egest material continuously, operating as CSTRs. Ophiuroids' guts may be functionally similiar to the guts of scyphozoan medusae; the latter continuously ingest and egest small particles along separate ciliary tracts, but process large particles in batches (Larson 1976). A second possibility is that "deposit-feeding" ophiuroids are very selective, searching for and ingesting food particles of the highest quality available. Oreaster reticulatus, an asteroid classified as a deposit feeder, is known to use a selective foraging strategy, concentrating on the food-rich layer at the sediment surface (Scheibling 1981) and perhaps avoiding the need to process large sediment volumes.

"Deposit-feeding" ophiuroids, thus, most probably use a mixture of

foraging modes: deposit-feeding, scavenging, and predation. This flexible, opportunistic strategy would enable an ophiuroid to minimize time between meals (by deposit feeding the gut rarely being idle), and provide some intake while searching for food particles of higher quality. Several deep-sea ophiuroid species are adept at localizing and ingesting carrion (C. Smith 1985), and in the laboratory we have observed active predation by Ophiura sarsi, a member of a genus generally considered to be deposit-feeders and scavengers (Tyler 1980). Based on intuition, Madsen (1961) similarly has suggested that porcellanasterid asteroids are scavengers and facultative predators as well as deposit feeders. We suspect that animals that prove to be bona fide deposit feeders with small, batch-reactor guts will be highly motile, selecting only the best food patches.

Existing information on foraging and digestion in deposit-feeding asteroids and ophiuroids is very limited and often inconclusive. Feeding habits are most often inferred from gut contents or lack thereof, and researchers studying feeding habits of polychaetes point out how misleading gut-contents data can be (Fauchald and Jumars 1979; Ockelmann and Vahl 1978). Direct observations of foraging modes are needed to evaluate our hypotheses. Patterns of movement of material into, within, and out of their guts must be assessed to find out whether they operate more nearly as batch reactors or CSTRs. Determination of conversion and holding time as they relate to food type and concentration are needed to answer questions raised as a result of this very simple reactor analysis.

Although not a focus in this brief analysis, microbially-mediated, autocatalytic digestive reactions may also be utilized by deposit feeders. These digestive reactions could be particularly important in deep-sea environments where rates of organic input are relatively low and organic material tends to be refractory. It is possible that deep-sea, deposit-feeding bivalves which retain fecal pellets in enlarged hindguts and xenophyophores and komokiaceans (Protozoa) which amass fecal pellets (stercomata) are fermenting and deriving further nutrition from organic material remaining in the fecal pellets (Allen

1979; Allen and Sanders 1966; Tendal 1979). Deep-sea, deposit-feeding elasipod holothuroids (Echinodermata) have large, sediment-filled, hindgut caeca which similarly may be sites of fermentation.

Fore- and Hindgut Fermenters

When they are primary components of a digestive strategy, fermentation reactions are linked in series with -- and may either precede or follow -- catalytic digestive reactions. Under the assumptions given, an animal's net production of energy and nutrients from food via this reaction series is maximized in a gut that operates as a series of two reactors, the CSTR and the PFR. Reaction sequence determines reactor sequence: When fermentation precedes catalytic digestion an animal's gut should operate as a CSTR-PFR reactor series; when fermentation succeeds catalytic digestion an animal's gut should operate as a PFR-CSTR reactor series. These gut-reactor configurations correspond to foregut fermenters (stomach or rumen as the primary fermentation site) and hindgut fermenters (colon or caecum as the primary fermentation site), respectively.

Gut-reactor models are more successful than previous compartmental models in describing digesta flow patterns (Penry and Jumars 1986). In further contrast to compartmental-model parameters of unknown biological significance, gut-reactor operating variables represent biologically important determinants of digestion. Gut architecture, gut capacity, intake level, diet composition, digesta passage rate and digestion rate are all factors experimentally identified as affecting digestibility of plant material (Parra 1978) and are all represented as operating variables in our gut-reactor models. The extent to which ingested plant material is converted to usable products (X_{Af}) is a function of gut-reactor configuration (batch reactor, PFR, CSTR, or some series), gut volume (V), throughput rate (v_0), initial concentration of some important or limiting component of ingested plant material (C_{A0}), throughput time (τ), and digestive reaction rate ($-r_A$, catalytic or autocatalytic kinetics). Using reactor theory to analyze digestion we have not only derived the important variables, but have provided, via the reactor-performance equations, biologically

meaningful, mathematical descriptions of the necessary relationships among them.

The relationship between digestive conversion, gut volume and throughput rate, quite apparent in numerous studies of digestion in herbivores and folivores, is now made explicit by the performance equations. Under the assumptions given for digestive reactions, the extent of digestive conversion is completely determined by, and increases with, throughput time. Since throughput time is the ratio of gut volume to volumetric throughput rate, conversion increases as gut volume increases relative to throughput rate, or as throughput rate decreases relative to gut volume. Extent of fiber (refractory plant material) digestion by herbivores and folivores generally increases with body size (Parra 1978). The gut-reactor performance equations allow us to assert that this pattern exists primarily because gut volume increases relative to throughput rate as body size increases, supporting in part empirical arguments by Demment and Van Soest (1985). Conversely, when gut volume is held constant, as in inter- or intraspecific comparisons of animals of similar body size (e.g., Grovum and Williams 1977), fiber conversion, as predicted, varies inversely with throughput rate.

The relative advantages and disadvantages of foregut versus hindgut fermentation have been much discussed, but reactor analysis of digestion reveals limitations in these discussions. They have focused on fermentation to the exclusion of catalytic digestion. According to the principles of dynamic programming (Bellman 1957), an entire process is optimal only when each stage functions optimally with respect to the preceding stage. Foregut fermenters ferment ingested materials, and then digest catalytically the fermentation digesta. Thus, in foregut fermenters fermentation should be optimized with respect to ingested material, and catalytic digestion should be optimized with respect to fermentation products and residue. In contrast, hindgut fermenters digest ingested material catalytically and then ferment the residue. Understanding the differences between these two digestive strategies requires that the roles of fermentation and catalytic digestion be

analyzed in the context of the stage in which they occur.

Within this dynamic programming framework we can explain, from a reaction-engineering standpoint, observations (summarized by Parra 1978) that throughput rates are smaller in foregut fermenters than in similarly-sized hindgut fermenters. Until otherwise stated, we assume that digestive reaction kinetics and diet composition are similar for foregut and hindgut fermenters of similar size. Apparent rates of fermentation are generally slower than apparent rates of catalytic digestion. Thus, optimization of fermentation, the first digestive stage in foregut fermenters, requires relatively long throughput times (larger V/v_0) while optimization of catalytic digestion, the first digestive stage in hindgut fermenters, requires shorter throughput times. Foregut fermenters are predicted--and observed--to have larger foregut volumes (V), and smaller throughput rates (v_0) than do hindgut fermenters of similar body size.

Throughput rate, determined by optimization of the first digestive stage, must remain constant along a continuous-flow gut, becoming a constraint on the second stage. Given the relatively small throughput rates of foregut fermenters, optimization of the second, catalytic stage requires relatively small hindgut volumes, smaller than the foregut volume required for fermentation. More importantly, if catalytic digestive reaction kinetics are similar in foregut and hindgut fermenters, the proportion of total gut volume foregut fermenters require for catalytic digestion is, as a result of their smaller throughput rates, relatively smaller than the proportion required by hindgut fermenters of similar size. Although differences are not dramatic in the limited data, the proportion of gut devoted to catalytic digestion is smaller in foregut fermenters than in hindgut fermenters (Table 3, Parra 1978).

During the course of evolution foregut fermenters are expected to trend toward minimizing the proportion of total gut volume required for catalytic digestion in order to maximize the proportion available for fermentation, constrained by throughput rates that are sufficient to

meet energy and nutrient requirements. When optimal apportionment of total gut volume is achieved, further increases in the extent of fermentive conversion of ingested materials can only be achieved with modifications of the fermentive capabilities of the microbial community, or with development of mechanisms that increase the mean residence times of selected digesta particles in the fermentation chamber.

Contrary to the arguments of Demment and Van Soest (1985), selective retention mechanisms like those observed in ruminants may not have been prerequisites for the success of larger foregut fermenters. Instead, these mechanisms may have been secondary adaptations to increase the efficiency with which foregut fermenters could exploit diets relatively high in refractory materials. From the earlier reactor analysis (Fig. 6b), we can predict that at the largest body sizes, longest throughput times, and highest conversion efficiencies, foregut fermentation may be accomplished efficiently in a PFR without an obviously modified fermentation chamber. The conspicuous absence of ruminants from the ranks of the largest foregut fermenters (Demment and Van Soest 1985, Fig. 3) is consistent with this prediction, and the implications for dinosaur herbivory should be noted.

Given that the proportion of total gut volume required by hindgut fermenters for catalytic digestion is larger than that required by similarly-sized foregut fermenters and that total gut volume is limited by body size, the proportion available to hindgut fermenters for fermentation is necessarily smaller than that available to foregut fermenters. Since there are no demonstrable differences in the fermentive capabilities of foregut and hindgut fermenters' microbial communities (Parra 1978), hindgut fermenters should, as a result of their shorter throughput times (i.e., smaller fermentation volumes and larger throughput rates), exhibit lower conversions of refractory materials than do foregut fermenters of similar size. As predicted, fiber digestion efficiency is generally lower in hindgut fermenters, and differences become much less apparent as body size increases (Parra 1978).

In competition with foregut fermenters over evolutionary time, hindgut fermenters appear to have found refuges at either end of the body-size spectrum. With one notable exception, large fermenters are hindgut fermenters. At body sizes larger than 600-1200Kg (Demment and Van Soest 1985) gut volume is sufficiently large and, thus, throughput times sufficiently long, for efficient exploitation of diets high in refractory materials regardless of fermentation strategy. The higher throughput rates of large hindgut fermenters and corresponding ability to process larger quantities of food per unit time may have provided a competitive advantage over large foregut fermenters (Janis 1976). Further, our analysis suggests that foregut fermentation is inherently a specialist strategy; whether or not food materials are labile to catalytic digestion, they are first broken down microbially. When food quality is high or variable, hindgut fermenters would appear to have the advantage. Whales, the notable exception in size, are foregut fermenters (Herwig et al. 1984). Too little is known of their food availability, gut kinetics, digestive reactions and metabolic costs to place them in perspective with terrestrial mammals.

Small fermenters are also hindgut fermenters, or perhaps more accurately, "foregut digesters." Smaller animals, with smaller absolute nutrient and energy requirements, are better able to obtain sufficient quantities of relatively high-"quality" foods (i.e., high in concentrations of enzymatically-digestible materials, low in refractory materials requiring fermentation) and minimize their energetic dependence on fermentation of refractory materials. Some fermentation products (methane, hydrogen gas and heat) are not utilized by the host animal, and fermentation of labile food materials can represent a net loss compared to catalytic digestion. Since net energy yield is maximized by catalytically digesting foods of relatively high quality, foregut fermentation is disadvantageous at small (< 10 Kg) body sizes (Parra 1978). For small animals fermentation may be most important as a source of limiting vitamins and other nutrients (Hornicke and Björnhag 1980).

To compensate for the reduced throughput times associated both with small size and foregut digestion, small hindgut fermenters have developed tactics to increase effective throughput times, and therefore, the utilization of fermentation products. Reactant recycling for further reaction, a common tactic in the chemical industry, exists among animals as coprophagy and caecotrophy. Coprophagy is simply recycling of digesta through reingestion of feces. Caecotrophy, a refinement that increases the overall efficiency of the recycling process, is more complex, involving separation in the gut of more readily fermented materials from less readily fermented materials. The latter bypass the fermentation chamber and are defecated, and only the relatively more "valuable" components are fermented and then recycled.

In the rabbit, which exhibits caecotrophy, (Hornicke and Bjornhag 1980; Pehrson 1983) separation of relatively more labile components from refractory components occurs before digesta enters the caecum. Refractory components bypass the caecum and are defecated as hard pellets. Labile components are fermented in the caecum, defecated as soft pellets (caecotrophes) and recycled for further fermentation in the mucus-wrapped pellet, followed by catalytic digestion. Recycling of the more "valuable" components allows small hindgut fermenters to achieve food conversions that would otherwise require larger gut volumes or smaller throughput rates.

Large hindgut fermenters typically do not recycle. How and to what extent are these animals able to utilize fermentation products? Catalytic digestion of fermentation intermediates and microbes might succeed fermentation as a third stage in digestion, but such mechanisms may not be necessary. Large throughput times may allow fermentation to proceed almost to completion. Large hindgut fermenters, with their low size-specific metabolic requirements, thus may utilize easily absorbed fermentation end-products like energy-rich volatile fatty acids (VFA). Recovery of food energy tied up in microbial biomass may not repay its additional costs. Unfortunately, little is known about fermentation in large hindgut fermenters because results of studies in foregut

fermenters have been assumed to apply. It is obvious from reactor theory that there may be very significant differences, so hindgut fermenters deserve special scrutiny.

MODIFICATIONS OF IDEAL GUT-REACTOR MODELS

Many foreseeable modfications need not be derived anew, having been enountered in chemical engineering applications. They involve either reaction modifications (e.g., modified enzyme kinetics, mass transport limitations, heterogeneous catalysis) or modifications of the ideal-model assumptions (e.g., variable digesta volume or gut volume, nonideal patterns of digesta mixing and flow).

We began with the simplest known enzyme kinetics, a catalytic Michaelis-Menten model, and simplest food characterization, concentration of a single component. Enzyme induction and poisoning, as well as competition for substrates, are likely complications. Mathematically, modified digestive reaction kinetics (e.g., Lehninger 1970) are readily incorporated in an ideal gut-reactor solution, but semantically, there are problems. "Engineering" digestive reactions helps highlight these problems by forcing strict definition of loosely defined concepts like food quality.

Quality ultimately reflects net gain of energy or of some limiting nutrient from a particular food. It is thus a composite of a number of different factors including concentration of some important or limiting component, susceptibility to degradation by an animal's enzymes or microbes, costs of producing those enzymes or maintaining those microbes, and costs of producing new body tissues from the breakdown products of the particular food. For simplicity we have equated food quality with concentration (C_{A0}), but its role in reactor models extends to considerations of enzyme activity and microbial community activity (both of which can differ with time in the same animal) and to mass-transfer constraints (which can differ with food of the same chemical, but different phase, composition). Food quality thus depends on the enzyme and microbe complements and nutritional state of the

digester as well as on various inherent food properties. Hay is useless to a carnivore. Given the need to characterize digestive reactions accurately, an intuitive sense of what is meant by food quality will no longer suffice; measurement of its component parameters becomes necessary.

Our initial simplifying assumption that digestive reactions are homogeneous can be relaxed, incorporating modifications due to the transport of: (1) enzymes from secretory sites to the bulk fluid; (2) enzymes from the bulk fluid to food particles; (3) enzymes into food-particle pores; (4) products out of pores; (5) products from particles to the bulk fluid; and (6) products from the bulk fluid to absorption sites. For example, microbes responsible for cellulose degradation attach to particles of plant material and attack the cell walls, eroding the substratum beneath their attachment points. Microcolonies occupy pits that develop (Fig. 14, Costerton et al. 1985). Thus, overall rate of cellulose degradation may be limited by rate of initial microbial attachment or by rate of diffusion of nutrients into, and metabolites out of, pits containing growing microcolonies. Cellulose degradation and digestive reactions in general fall, along with most industrial chemical processes, into the category of heterogeneous catalysis. Derivations of rate equations for heterogeneous catalysis have been considered in detail (e.g., Carberry 1976; Froment and Bischoff 1979; Smith 1981).

Subtidal marine invertebrates and mammals are perhaps uniquely immune from temperature variations resulting from digestive processes or from environmental changes. We thus assumed that reaction and mass transfer are the dominant processes in guts, allowing us to describe performances of gut-reactor models solely with the reactor-specific equations derived from mass-balance considerations. Reptilian utilization of environmental heat in digestion, however, is obvious. If in digestion, as in the chemical industry, adding or removing heat is a major design consideration, it can be treated via equations for heat conservation (Levenspiel 1972; Froment and Bischoff 1979; Smith 1981).

Another simplifying assumption in our gut-reactor models is that digesta volume is constant and equal to reactor volume. With the exception of deposit feeders, such volume changes are likely to be important in most animals. They may, for example, provide another important difference between foregut and hindgut fermentation of refractory materials. In foregut fermenters, fiber volume is reduced before material undergoes catalytic digestion in the PFR portion of the gut, while, in hindgut fermenters, fiber occupies space and impedes diffusion in the PFR portion of the gut. Volume changes may be treated as changes in reacting material density or as an additional advective term representing absorption. In either case the mass-balance approach of reactor design can be used to formulate the solution (e.g., Levenspiel 1972, Hershey 1973). Most commercial reactors have neither secretory nor absorptive walls, but mass transfer and radial diffusion constraints (e.g., Aller 1980; Smith 1981) can be added to the reactor-theory formalism. Similarly, modifying the steady-state assumptions is conceptually easy but mathematically difficult (Levenspiel 1972).

We assumed digesta mixing and flow patterns identical to ideal reactor models. If deviations from the ideal occur, gut models based on reactor theory are modified more easily (e.g., Bailey and Ollis 197/; Smith 1981) than are less mechanistic, compartmental models. Such modifications may be necessary, for example, to treat size-selective particle retention in the rumen. The basic PFR-CSTR reactor model for hindgut fermenters also is easily modified to incorporate digesta separation and recycling (e.g., Levenspiel 1972; Carberry 1976). Subsequent analyses based on this modified gut-reactor model are sure to include consideration of such chemical engineering concepts as the "optimal recycle ratio" for small hindgut fermenters (i.e., the ratio of recycled to unrecycled material that results in greatest net rate of product formation).

The validity of ideal plug flow and the PFR gut model will be questioned by anyone who has observed peristalsis. Cells of

longitudinal mixing clearly do result (Macagno and Christensen 1980). A tubular gut with mixing cells might then be modeled as a series of CSTRs. Linking CSTRs in series reduces both the total mixed-flow volume required to achieve a given conversion (X_{Af}) and the dilution effect of a single, large CSTR. As the number of CSTRs in series increases, in fact, overall reactor-system behavior rapidly approaches that of plug flow (Levenspiel 1972). Counterintuitively, then, no modification of the ideal PFR model may be required for a tubular gut with mixing cells.

From the PFR model it immediately is apparent that radial elaboration of the mucosal, absorptive surface and lengthening the gut are not (as claimed by Karasov and Diamond 1985) equivalent tactics. A radial increase in absorptive surface area increases uptake of digestive products at any point along the gut. Lengthening the gut increases surface area, but more importantly, increases total gut volume as well. With all else constant, the resulting increase in throughput time increases the extent to which ingested materials are converted to digestive products. Elaboration of surface area thus affects only extent of absorption while lengthening the gut affects both extent of absorption and extent of reaction.

It is obvious that any number of gut-reactor model modifications are possible. Experiments will indicate where necessary modifications lie. Citing Prater's principle of "optimum sloppiness," Carberry (1976) provides some timely advice with respect to the ultimate goals and value of model development. Many processes, industrial or biological, are the interactions of complex arrays of phenomena, often poorly understood. A completely fundamental model may thus be unattainable, but iteration between theory and observation most efficiently will determine acceptable imprecision and inaccuracy.

We deliberately have focused on the homologies between analysis of chemical reactors and analysis of digestion. It is useful to consider how this borrowed modeling tool may need to be modified outside the context of commercial reactor design. We have touched on some possible

changes for treating real animals, but it is worth noting some generic problems for future efforts in tailoring reactor theory for predictions of feeding optimization.

At this point cost functions remain implicit. In the chemical industry most costs are relatively easy to quantify. However, digestive costs appear difficult to parameterize and measure (Penry and Jumars 1986), as have been foraging costs. Our design objective of maximizing production rate in minima of volume and time implicitly assumes that digestive costs (e.g., energy and nutrients required to maintain digestive tissues and energy to propel digesta) are monotonically increasing functions of reactor volume and time. Based on analogy with commercial reactor costs, these constraints are reasonable, but digestive costs need to be measured and made explict. That there may be significant costs associated with maintaining a gut is suggested by the evolutionary reduction or loss of guts by some multicellular animals (e.g., pogonophorans, Cavanaugh et al. 1981; Southward and Southward 1968; and some bivalves, Reid and Bernard 1980). Like gut maintenance costs, the costs of moving digesta of varying mechanical properties and at varying flow rates are essentially unknown.

Based on fitness arguments (Townsend and Hughes 1981) net rate of assimilation of energy or limiting nutrient into those tissues that either enhance individual survival or produce offspring should be maximized. The relative costs of foraging, digestion, absorption and production of new tissues will be important in determining an animal's energy or material acquisition strategy. The latter two steps appear, in some cases, to be far more expensive than foraging or digestion (Kiørboe et al. 1985). This cost balance suggests that when food is unlimited and inexpensively obtained an animal may eat a lot, digest it relatively well, but assimilate products less efficiently. Some terrestrial isopods use such a strategy when food is abundant, but increase assimilation efficiency when food becomes limiting (Hubbell et al. 1965; Wieser 1978).

Our analysis indicates that batch processing is an undesirable digestive strategy and conflicts with the obvious success of animals like ctenophores, jellyfish, hydras, anemones, starfish, brittlestars, some glycerid polychaetes and many protozoans that do indeed use such a strategy. What characteristics and adaptations do these animals possess that may enable them to utilize a batch-processing rather than continuous-flow strategy, or which of our explicit or implicit assumptions are invalid with respect to these animals? Various, though certainly not all, representatives of groups using batch-processing strategies have low metabolic requirements (e.g., Buchanan 1964) and expend relatively little energy in foraging. Many have large bodies (reactors) composed of tissues with little metabolic support costs (mostly water or calcium carbonate). Anemones, hydras, and those glycerid polychaetes that maintain burrow complexes (Ockelmann and Vahl 1970) are essentially sessile. Batch-processing animals generally are carnivorous or specialize on labile foods (high C_{A0}, high $X_A(t)$). Low energy requirements of sit-and-wait predation (Hughes 1980) and relatively high growth efficiencies (e.g., Ockelmann and Vahl 1970) are probably significant adaptations making batch processing a viable strategy.

Our conclusion that batch processing is an undesirable digestive strategy is partly a consequence of assuming unlimited food supply. The implicit assumption of constant food availability is best met in deposit feeders and large herbivores, animals feeding on food of low quality and consequently high abundance. Continuous-flow guts may be disadvantageous under low food supply. As throughput rate decreases, for example, the PFR assumption of insignificant axial diffusion breaks down. Predicting aspects of batch-reactor performance when food supply varies is reasonably straightforward (Penry and Jumars 1986), but predicting non-steady-state PFR or CSTR performance is not. We are presently unable to compare digestive strategies across reactor types under all food supply conditions. We suspect that batch reactors may be comparatively flexible under varying food supply. If, as evidence indicates (Kiørboe et al. 1985), digestion requires relatively little investment, gut contents digested batchwise may be quickly ejected and

replaced when better items become available. Continuous-flow guts, especially those with spatially segregated secretory and absorptive sites, have more complex timing constraints.

We have inferred that animals with one gut opening are likely to be batch processors, although exceptions already are known (Larson 1976). The converse inference should not be drawn: A gut with two openings need not necessarily operate as a continuous-flow reactor. Batch processing may thus be much more frequent than our cursory overview suggests. Some carnivores, for example, some snakes and large cats as well as anemones, slowly digest and efficiently assimilate a single, high-quality item. A large item may prevent the mixing assumed in the batch-reactor formulation, but steep product gradients over small spatial distances between a constricting gut wall and the food item preclude a need for it. Mathematical models of varying-volume reactors are available (basic treatments in Carberry 1976; Levenspiel 1972) and have been used for processes outside industrial design (B. B. Krieger, pers. comm.).

Batch processing is especially likely in time minimizers constrained to widely separated feeding intervals. The similarity in predictions of optimal foraging behavior for time minimizers and energy maximizers is often noted, but consideration of digestion immediately draws an important distinction (e.g., by exercising Fig. 3b of Penry and Jumars 1986). By the end of a foraging period time minimizers should fill their guts with items that will maximize returns integrated over the entire non-foraging period rather than items with initially rapid but unsustained returns. Continuously-feeding energy maximizers with flexibility to alter gut throughput times should, in contrast, never reject an item providing higher-than-average short-term rate of gain.

The engineering approach of process design applied to feeding emphasizes the interdependence of foraging and digestion. Foraging theory suggests what foods will be available at reasonable energetic expense. Digestion theory, in turn, provides process constraints that

must be incorporated into foraging models. Digestive fermentation, for example, should be included as an initial constraint in optimal foraging models for herbivores. Foraging models for "generalist" herbivores (e.g., Westoby 1974; Owen-Smith and Novellie 1982) should be adapted for specific consideration of fore- versus hindgut fermenters. Theory coupling foraging and digestion must yield a better understanding of energy and nutrient acquisition by animals than can either body of theory alone.

SUMMARY

Chemical reactor theory recognizes three ideal reactor types: batch reactors which are filled with reactants, continously stirred during reaction, and then emptied of products after a given reaction period; plug-flow reactors (PFRs) in which reactants continuously enter and products continuously exit with no mixing along the flow path; and continuous-flow, stirred-tank reactors (CSTRs) in which reactants continuously enter and products continuously leave a stirred vessel. Performance equations for these reactors, together with kinetic models for simple enzymatic catalysis and microbially-mediated (autocatalytic) digestive fermentation reveal necessary functional relationships among initial concentration of limiting food component, gut volume, throughput time or gut holding time, and digestive reaction kinetics. We use these models to suggest optimization constraints for digestion, analogous to those of optimal foraging theory.

Two general predictions are possible. To sustain the greatest digestive production rate in minima of throughput time and gut volume, an animal dependent upon its own digestive enzymes should function as a PFR. Animals fermenting refractory materials should combine a CSTR and PFR in series at all but the slowest throughput rates, when a PFR will suffice.

We make specific predictions for deposit feeders because they digest little of the ingested volume, greatly simplifying digestive performance equations and making them ideal subjects for initial tests

of our parameterization. The majority conform to the prediction of PFR guts, but there also are deposit feeders apparently using CSTR-PFR series (terebellimorph polychaetes) and batch processing (asteroids and ophiuroids). We suggest that the former may use the CSTR to overcome digestive rate constraints imposed by diffusion limitations, while the latter may use a variety of foraging modes to obtain the highest quality foods available.

We also apply reactor theory to mammalian fermenters because empirical feeding information is extensive. Specifically we compare expected dynamics of foregut versus hindgut fermentation. Foregut fermenters should optimize fermentation with respect to ingested foods and optimize subsequent catalytic digestion with respect to fermentation products. In contrast, hindgut fermenters should optimize foregut catalytic digestion and then optimize fermentation of the residue. According to principles of dynamic programming, the first digestive stage in each case sets the pace of digesta throughput -- consequently slower in foregut fermenters than hindgut fermenters of similar size. Hindgut fermentation is seen to be competitive, especially for small animals, when food quality is high or variable or when body size is large and throughput rate set in the foregut is slow enough for hindgut fermentation to yield high conversion. Coprophagy and caecotrophy, tactics used by small hindgut fermenters to increase throughput time and utilization of fermentation digesta, are easily understood in terms of industrial "recycle reactor" equivalents. A great advantage in deriving digestion models from reactor theory is that many foreseeable modifications (e.g., explicit incorporation of volume changes during digestion or coprophagy) to ideal models have analogs in diverse industrial reactor configurations already modeled and tested.

Chapter III. Tests of gut-reactor models for deposit feeders: Descriptions of patterns of sediment movement within the guts of *Parastichopus californicus* (Echinodermata: Holothuroidea) and *Amphicteis scaphobranchiata* (Annelida: Polychaeta).

INTRODUCTION

Deposit feeders ingest large volumes of sediment and digest associated organic components. Much attention has been given to determining how they successfully exploit this nutritionally dilute food resource, the volumetric bulk of which is mineral grains. Much research has focused on understanding the processes of foraging and ingestion, i.e., the patterns of selection and rates of ingestiom of particles under various food resource conditions (e.g., Cammen 1980; Taghon 1982; Whitlach and Weinberg 1982; Lopez and Cheng 1983; Miller 1984; Taghon and Jumars 1984; Juniper 1986; Self and Jumars 1988). The process of digestion has received less attention although it is at least as important (Calow 1975, Taghon 1981, Penry and Jumars 1986, 1987). Where optimal foraging theory (Taghon et al. 1978) has provided a context for and impetus behind many foraging and ingestion studies, chemical reactor theory can do the same for digestion (Penry and Jumars 1986, 1987). Just as description of patterns of particle selection was a first step in application of optimal foraging theory to deposit feeders, description of patterns of particle movement through deposit feeders' guts must be a first step in application of reactor theory.

Description of patterns of material flow within deposit feeders' guts is a prerequisite to development of models of guts in terms of chemical reactor components. A reactor model, once developed and confirmed, can be used to predict digestive capabilites and suggest digestive constraints. The advantage of reactor model development is *a priori* identification of important digestive variables that must be measured or controlled in tests of model validity as well as in tests of model predictions.

Penry and Jumars (1987) theorized that deposit feeders should have plug-flow guts (i.e., no axial mixing, individual particle residence times exactly equal to the mean residence time). Observations from a number of species qualitatively support this prediction, but the degrees to which the conditions of ideal plug flow are met are unknown. Deviations from plug flow (i.e., evidence of axial mixing, individual

particle residence times distributed about a mean residence time) observed in the guts of two ampharetid polychaetes, Amphicteis scaphobranchiata and Hobsonia florida (Penry unpublished observations; Self and Jumars 1978; Jumars and Self 1986), seem great enough to force rejection of the ideal plug flow model for these two species. A mixing reactor (CSTR)/ plug flow reactor series (PFR) has been proposed, instead, as a model for their guts and for the guts of other terebellimorph polychaetes (Penry and Jumars 1987). Is the greater degree of mixing that may occur in the guts of these polychaetes indeed an important feature of their digestive processes that requires special attention and explanation (i.e., the diffusion limitation hypothesis of Penry and Jumars 1987), and are deviations from ideal plug flow likely to be common among deposit feeders?

These experiments apply tracer methods in tests of the validity of the ideal plug flow model for two species for which qualitative observations exist and reactor models have been proposed -- Parastichopus californicus, a deposit-feeding holothuroid, and Amphicteis scaphobranchiata. Since it was expected that the plug flow model would be rejected for A. scaphobranchiata in favor of the CSTR/PFR model, the Amphicteis experiments were also designed to test the effects of tracer particle and bulk sediment characteristics on mixing patterns.

TRACER THEORY

Tracer methods involve techniques for labeling and observing members of a given population (e.g., a population of molecules or particles or organisms) to obtain information about the population as a whole (Sheppard 1962). Studies of system kinetics, of which these experiments are examples, use patterns and rates of movement of tracers to infer the behavior of entire systems. The goal of such studies is usually to test a theoretical model of a system or to develop an empirical one. Two reactor models, the ideal plug-flow reactor (PFR) and the ideal continuous-flow, stirred-tank reactor (CSTR), provide the theoretical framework for this study. These models represent the

endpoints in a continuum of possible mixing conditions in continuous-flow systems. A brief review of some basic principles of tracer methods and residence-time distribution theory pertinent to these experiments highlights important assumptions and provides the basis for interpretations of results (for more exhaustive treatments see Sheppard 1962, Aris 1982).

Experimental design includes selection of tracer characteristics (e.g., nonreactive or reactive, and in what concentration) and identification of an appropriate tracer input function (e.g., step, pulse, periodic). Selection of a tracer obviously depends on the system and processes being investigated, and in these experiments to describe patterns of mixing and flow within guts it is required that the tracers be particulate and conservative (i.e., not digested or altered during passage through the gut). In all experiments it is generally assumed that the tracer chosen is "perfect," i.e., that tracer components behave identically to unlabeled components. This assumption is always violated; the degree to which it is violated limits the inferences that can be drawn about the behavior of the system being studied. It is required that the tracer be present in small enough concentrations for the local mass-balance equations to be linear with respect to tracer concentration, a requirement that is satisfied if the properties of the system are not changed by the presence of tracer (Bailey and Ollis 1977).

The two simplest stimulus-response techniques for investigating the behavior of a system are a step input of tracer and a pulse input of tracer. A step input (Fig. 1a) is described by the equations: concentration $c(t) = 0$ for all times $t < t_0$, and $c(t) = C_0$ for $t > t_0$, where C_0 is initial tracer concentration. A pulse input is described by the equations: $c(t) = 0$ for $t < t_0$, $c(t) = C_0$ for $t_0 < t < \Delta t$, and $c(t) = 0$ for $t > \Delta t$, where Δt is a very short time interval. The mathematical expression of an ideal pulse is the Dirac delta function (i.e., area under pulse curve = 1, pulse width = 0). The response to an input step, $F(t)$, and the response to an input pulse, $E(t)$, are expressed in terms of C^* and t, where C^*, nondimensional concentration,

Figure III-1. Predicted unit-step response curves, $F(\bar{\theta})$, for three ideal reactors. C^* = nondimensional tracer concentration; T^* = nondimensional time. (a) Tracer input function: step up in tracer concentration at T^*_0; step down in tracer concentration at T^*_s. (b) Unit-step response curve for an ideal plug-flow reactor (PFR). Responses lag input steps by $T^* = 1$, a period equal to one reactor throughput time. (c) Unit-step response curve for an ideal continuous-flow, stirred-tank reactor (CSTR). Response to input step up described by $1 - \exp(-T^*)$. Response to input step down described by $-\exp(-T^*)$. (d) Unit-step response curve for an ideal CSTR/PFR series. Responses to input steps described by equations given in (c), but responses lag input steps by $T^* = T^*_{PFR}$, a period equal to the throughput time of the PFR portion of the series.

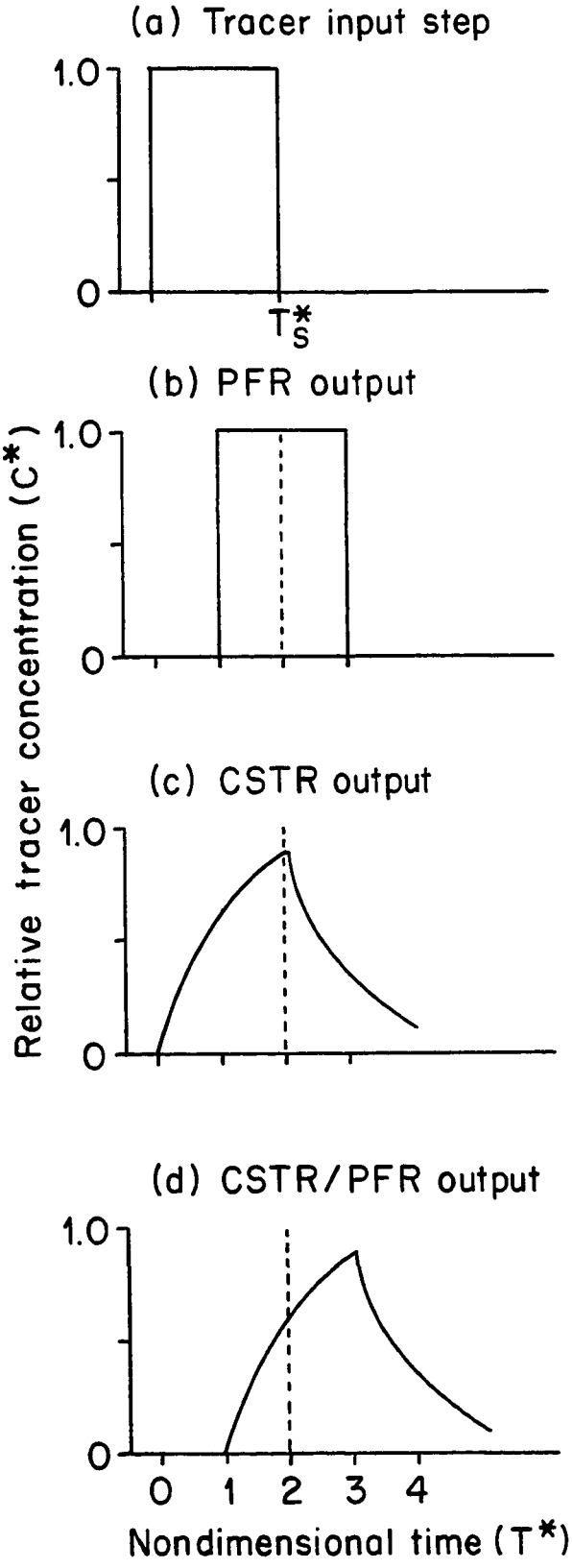
(a) Tracer input step
1.0
0
T_s^*
(b) PFR output
1.0
0
(c) CSTR output
1.0
0
Relative tracer concentration (C^*)
(d) CSTR/PFR output
1.0
0
0 1 2 3 4
Nondimensional time (T^*)

equals $c(t)/C_0$. F(t) and E(t) yield exactly the same information. The theory of linear systems states that dF/dt, the derivative of F(t) with respect to time, is equal to E(t) (Bailey and Ollis 1977). F(t) is the unit-step response function; E(t) is the corresponding residence-time distribution (RTD) function.

There is a very important difference between interpretation of a response expressed in terms of absolute amounts of tracer and a response expressed in terms of fractional amounts of tracer (i.e., tracer concentration or nondimensional tracer concentration) (Sheppard 1962). This difference seems obvious, but all too often it has not been recognized. It directly affects experimental design and interpretation of results. If no material is entering the system, any output will result in a decrease in the absolute amount of tracer, but in the absence of selective removal the concentration of tracer will remain constant. Changes in tracer concentration, in contrast, indicate dilution of tracer by unlabeled material entering the system. Rates of changes in tracer concentrations are measures of inflow rates, and reflect outflow rates only when inflow and outflow are equal (Sheppard 1962).

It is very difficult to measure inflow (i.e., ingestion), but often easy to measure outflow (i.e., egestion) in deposit feeders and other animals. For deposit feeders it is generally assumed a priori that inflow and outflow are equal, a reasonable assumption at steady state since the bulk of ingested material is mineral grains. Given this assumption, measurements of changes in tracer concentration are required to ensure that ingestion rates are nonzero, and that egestion rates do not reflect merely the rates of gut emptying (i.e., gut evacuation).

Attempts to develop empirical models for the estimation of ingestion rates from gut fullness and evacuation rates for herbivorous copepods are examples of how failure to understand these basic principles of tracer methodology has led to a mismatch of study goals and experimental design and to misinterpretation of experimental

results. A typical gut evacuation experiment involves measurement over time of the decline in the absolute amount of a fluorescent tracer, chlorophyll a and its degradation products, in the guts of nonfeeding copepods. The amounts of tracer remaining in the gut over time are measured and expressed as percentages of the initial amount of tracer present in the gut (i.e., a nondimensional expression for absolute amount of tracer, not a measure of concentration of tracer). Inflow and outflow of material are uncoupled completely, and thus, the measured rates of tracer evacuation cannot be used to infer anything about ingestion rates. The observed tracer output response (usually an exponential decay curve) represents the decline in the absolute amount of tracer in the gut as the result of the decline in amount of material in the gut, and does no more than confirm the obvious -- no material is being ingested. Tracer concentration, if it were ever to be measured in evacuation experiments, would be found to remain constant (unless pigment is digested, e.g., Conover et al. 1986) and again would do no more than confirm the obvious -- ingestion is zero.

Development of empirical models (e.g., gut fullness models for predictions of ingestion rates in herbivorous copepods) must follow the same principles as tests of theoretical models. Experimental design must include at the very least (1) conditions that permit nonzero ingestion rates, and (2) measurements of changes in tracer concentrations over time (i.e., determination of $F(t)$) in order to meet the most basic requirements for allowing inferences to be drawn from the results of tracer experiments.

If these requirements are met, a large body of theory, commonly called residence-time distribution theory (RTD theory), provides the basis for analyses and mechanistic interpretations of deviations of observed unit-step response curves and residence-time distributions from predictions (e.g., Sheppard 1962, Bailey and Ollis 1976, Carberry 1976, Smith 1981, Petho and Noble 1982). These tests of the ideal plug-flow model (PFR) and the ideal continuous-flow, stirred tank/plug-flow reactor series (CSTR/PFR) for the guts of Parastichopus californicus and Amphicteis scaphobranchiata, respectively, involve

comparisons of experimentally-determined unit-step response curves with predicted curves. Analyses are made easier if F(t) and E(t) are expressed in terms of nondimensional time, T_*, as well as nondimensional concentration, C^*, (defined above) (Carberry 1976). Nondimensional time, T^*, is obtained by dividing each observation time, t, by some reference time, usually mean residence time, $\bar{\theta}$, or throughput time, τ. The notations, $F(\bar{\theta})$ and $E(\bar{\theta})$, indicate that unit-step response curves and residence-time distributions are expressed in terms of nondimensional time with mean residence time (i.e., throughput time) as the reference time.

The ideal PFR model for a gut requires that there be no axial mixing and that residence times in the gut be equal for all particles. The unit-step response, $F(\bar{\theta})$, of an ideal PFR exactly mirrors the input function offset a period of time equal to one throughput time (τ) (Fig. 1a,b). An ideal CSTR is characterized by complete axial mixing which results in immediately detectable and gradually increasing dilution of material in the CSTR by incoming material, and thus a distribution of residence times of particles within the gut is observed. The unit-step response curve, $F(\bar{\theta})$, for a CSTR is described by the equation, $C^* = 1-\exp(-T^*)$, if the input step change in tracer concentration results in an increase in tracer concentration, and by the equation, $C^* = -\exp(-T^*)$, if the input step change results in a decrease in tracer concentration (Fig. 1c). The unit-step response curve, $F(\bar{\theta})$, for an ideal CSTR/PFR series thus resembles the curve for a single ideal CSTR offset by a period equal to the mean residence time of material within the PFR section of the series (Fig. 1d). These three predicted curves, $F(\bar{\theta})$ for the ideal PFR, CSTR, and CSTR/PFR series, provide the basis for interpretation of the results of my experiments.

METHODS

Experiments with Parastichopus californicus

Eight individuals were collected from subtidal areas around Friday Harbor, San Juan Island, WA. Seven were fed mud mixed with barium

sulfate; one very large individual was fed coarse, black basaltic sand. Both types of sediment are opaque and easily distinguished from unmodified mud or quartz sand in x-ray exposures. After feeding on x-ray opaque sediment was observed, individuals were transfered to unlabeled mud or quartz sand. A time series of x-rays of each individual (MA/KVP = 10/80, 4s exposure) was taken to examine the patterns of movement of x-ray opaque sediment through the gut. Since no attempt was made to control food concentration or mechanical properties of bulk sediment, feeding rates were not considered very meaningful and were monitored only crudely.

Experiments with Amphicteis scaphobranchiata

Two artificial sediments were prepared by culturing the marine bacterium Pseudomonas halo on glass or polystyrene beads. Cleaned glass beads (nominally 1-37 μm but elutriated to remove finest fraction, ρ = 2.42) (Ferro Corporation, Jackson, MS) or polysytrene beads (1-85 μm, ρ = 1.05) (Duke Scientific Corporation, Palo Alto, CA) were added to a rich seawater medium (10 g yeast extract and 1 g peptone per liter of 0.22-μm filtered seawater). Flasks containing medium and beads were autoclaved, cooled, inoculated with P. halo, and incubated on a shaker table at room temperature until significant bacterial growth was seen (1-7 d). Acridine orange direct counts were used to examine beads for attached bacteria. The beads in each flask were then filtered from the medium, washed with filtered seawater, and aspirated to a damp cake. The glass and polystyrene bead cakes were divided in two -- one-half of each was resuspended in filtered seawater and used immediately in the experimental pretreatments; fluorescent tracers were added to the remaining halves which were stored damp in the refrigerator overnight and resuspended in filtered seawater immediately before use in the experimental treatments.

A pair of fluorescent tracers, glass and polystyrene, was used in the experimental treatments. The fluorescent glass tracer was prepared by adding 1-37 μm glass beads to a solution of fluorescent paint in acetone (50 mg of powdered paint per ml acetone) (R-103-G chartreuse, Radiant Color, Richmond, CA). The acetone was allowed to evaporate and

the drying mass of beads was continuously mechanically disaggregated to minimize clumping. The fluorescent polystryene tracer was prepared by combining 12-20 μm and 70 μm violet beads (Particle Information Services, Inc., Kingston, WA) in 1:1 (wt:wt) proportions. The amounts of fluorescent glass and polystyrene tracers added to the bulk glass or polystyrene sediments were less than 3% of the damp weight of the bulk sediments except in the 9/87 run where the glass tracer was 9% of the weight of the polystyrene sediment.

Amphicteis scaphobranchiata were collected from Massacre Bay, Orcas Island, WA, and were maintained on natural sediment in individual plastic freezer containers in a sea table until used in the experimental runs. Two runs, 9/87 and 10/87, were performed. Eight actively-feeding individuals (numerous feeding traces visible, piles of fecal pellets present) were selected for each run and were assigned randomly both to positions within the sea table and to one of two treatments, glass or polystyrene bulk sediment. A piece of filter paper with a hole in the center to allow the worm's tube to protrude through it was placed over the sediment in each freezer container to isolate the test sediments from the natural sediment and to prevent the worms from feeding on the natural sediment. In the pretreatment phase of each run, unlabeled artificial sediment (glass or polystyrene bulk without tracers added) was pipetted onto the filter paper in each box. Enough sediment was dispensed to cover the entire feeding area of each worm to a depth of several millimeters. Worms were allowed to feed on the unlabeled sediments (12-17 h) until each individual had presumably replaced the mud in its gut entirely with unlabeled artificial sediment (at least two mud fecal pellets produced). The number of pellets produced by each worm during the pretreament was recorded, and worms were then switched from unlabeled sediments to labeled sediments, i.e., glass or polysytrene bulk with the pair of tracers added (treatment phase 1). After an individual was judged to have been able to replace its gut volume at least once with labeled sediments it was switched back to unlabeled sediments (treatment phase 2).

Worms were checked every 15 min during treatment phases 1 and 2.

Each pellet found was removed, disaggregated, aspirated on to a tared filter and rinsed thoroughly with distilled water to remove salts. When possible pellets were divided in two and the halves were preserved separately to increase the level of resolution. A. scaphobranchiata produces pellets that are more or less conical (the narrow end is the posterior end) so that pellet ends and, thus halves can be distinguished easily and reliably. Water temperature ranged from 14-16°C during the 9/87 run and from 12-15°C during the 10/87 run.

Individual pellets on tared filters were dried overnight at 50°C, cooled in a dessicator and weighed on a Cahn microbalance. Pellet weights were converted to pellet volumes using experimentally determined bulk material densities of 1.34 mg mm^{-3} for 1-37 μm glass beads and 0.66 mg mm^{-3} for 1-85 μm polystyrene beads. The numbers of each of the types of tracer particles (1-37 um fluorescent glass, 12-20 μm fluorescent polystyrene, 70 μm fluorescent polystyrene) in each pellet were counted at 100x under an epifluorescence microscope. The painted glass beads fluoresced bright yellow-green and the violet polystyrene beads fluoresced red. The two sizes of fluorescent polystyrene beads could be easily distinguished. Gray nitrocellulose filters with black grids (0.45 μm pore size, 25 mm diameter) (MicronSep, Honeoye Falls, NY) were used to reduce background fluorescence and to ensure that no area of the filter was counted more than once.

Body volumes and gut volumes were measured (see Chap. IV for description of method) for the 8 individuals used in the 10/87 run. The worms were allowed to feed for several days on natural sediment before being preserved for analysis.

RESULTS

Observed responses: Parastichopus californicus

Observations support a plug-flow model for the gut of Parastichopus californicus. Distinct interfaces between labeled and unlabeled sediment can be identified within the gut (Figs. 2-5). The

Figure III-2. Time series of x-radiographs of the gut of Parastichopus californicus, individual A. These results and the results shown in Figure 2 indicate that axial mixing does not occur in the gut. All x-radiographs are dorsal views with anterior end toward top of figure. Scale bar = 5 cm. (a) t = 0 h, the time at which individual A was switched from mud + $BaSO_4$ to unlabeled mud. (b) t = 2 h after switch. Interface between labeled and unlabeled mud indicated by arrow. (c) t = 3.5 h after switch. Interface is unchanged. (d) t = 4.5 h after switch. Interface appears in fecal coil.

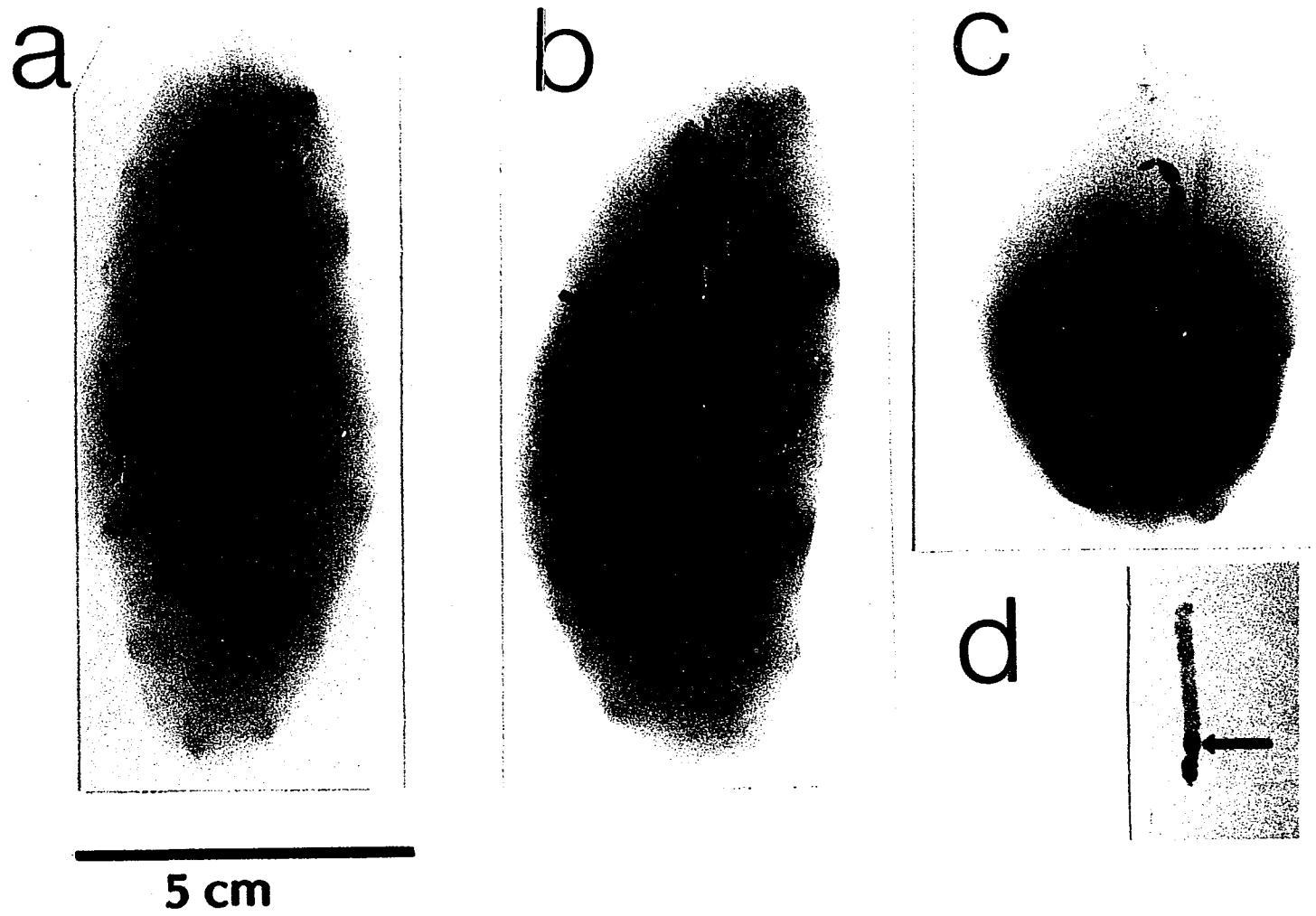
a
b
c
d
5 cm

Figure III-3. Time series of x-radiographs of the gut of Parastichopus calfornicus, individual H. All views are dorsal views with anterior ends toward top of figure. Scale bar = 5 cm. (a) t = 0 h, the time at which individual H was switched from basaltic sand to quartz sand. The series of interfaces (indicated by arrow) were formed when this individual first began feeding on basaltic sand. (b) t = 2.5 h after switch. Characteristics of interfaces unchanged. (c) t = 6 h after switch. Characteristics of interfaces unchanged, indicating that there was no axial mixing in the gut posterior to the region where the interfaces first formed.

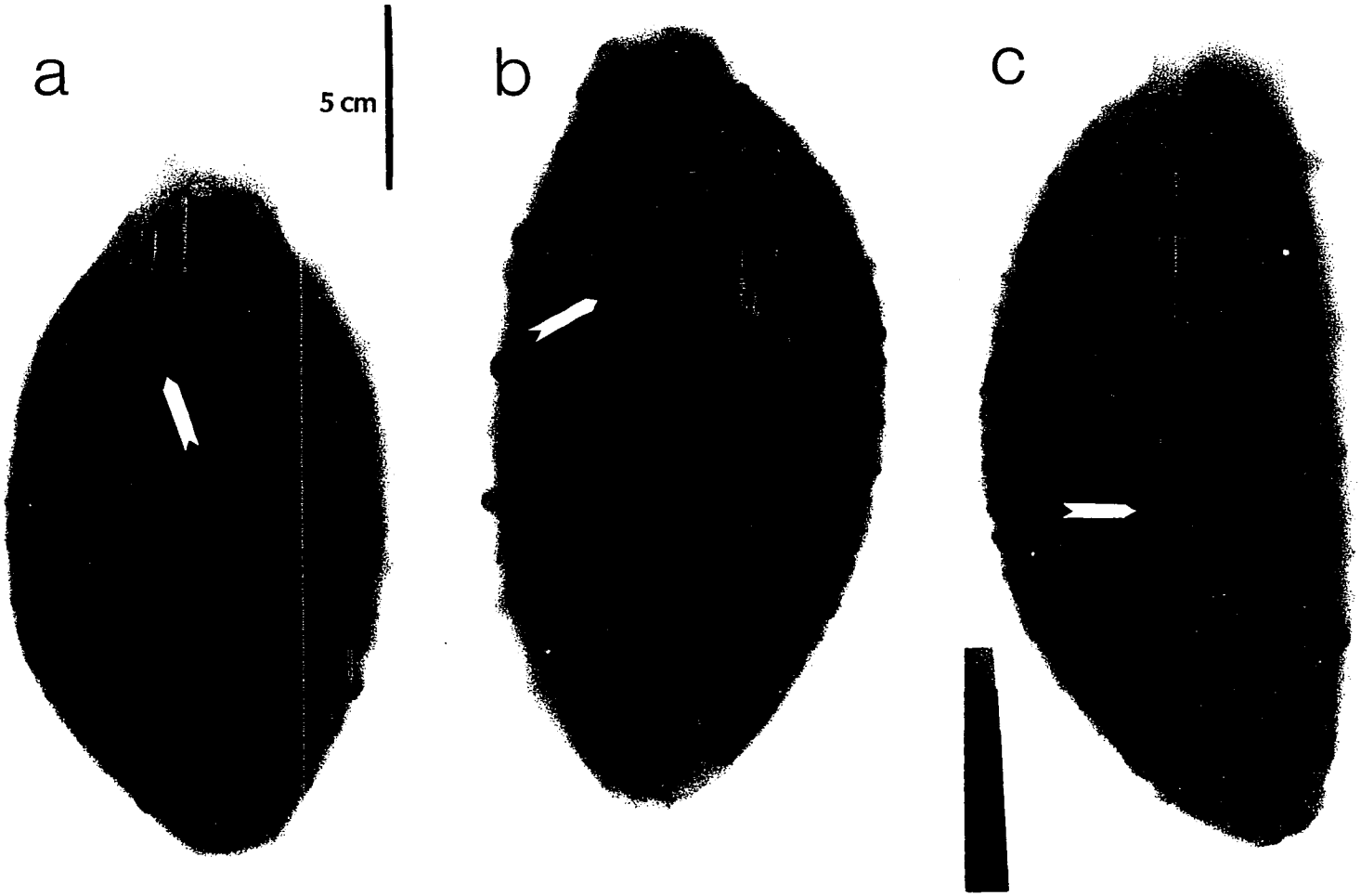
a
5 cm
b
c

Figure III-4. Time series of x-radiographs of the gut of Parastichopus californicus, individual F. All views are dorsal views with anterior ends toward top of figure. All scale bars are five cm. These results and the results in Figure 5 indicate that neither axial nor radial mixing occurs along much of the length of the gut. They also show that "boudin" structures do not represent individual mixing cells. (a) t = 9 h after individual F was switched from mud + $BaSO_4$ to unlabeled mud. Convex interface (indicated by arrow) is seen within a single "boudin" structure. (b) t = 12 h after switch. Convex interface within boudin unchanged. (c) t = 21 h after switch. Convex interface still unchanged.

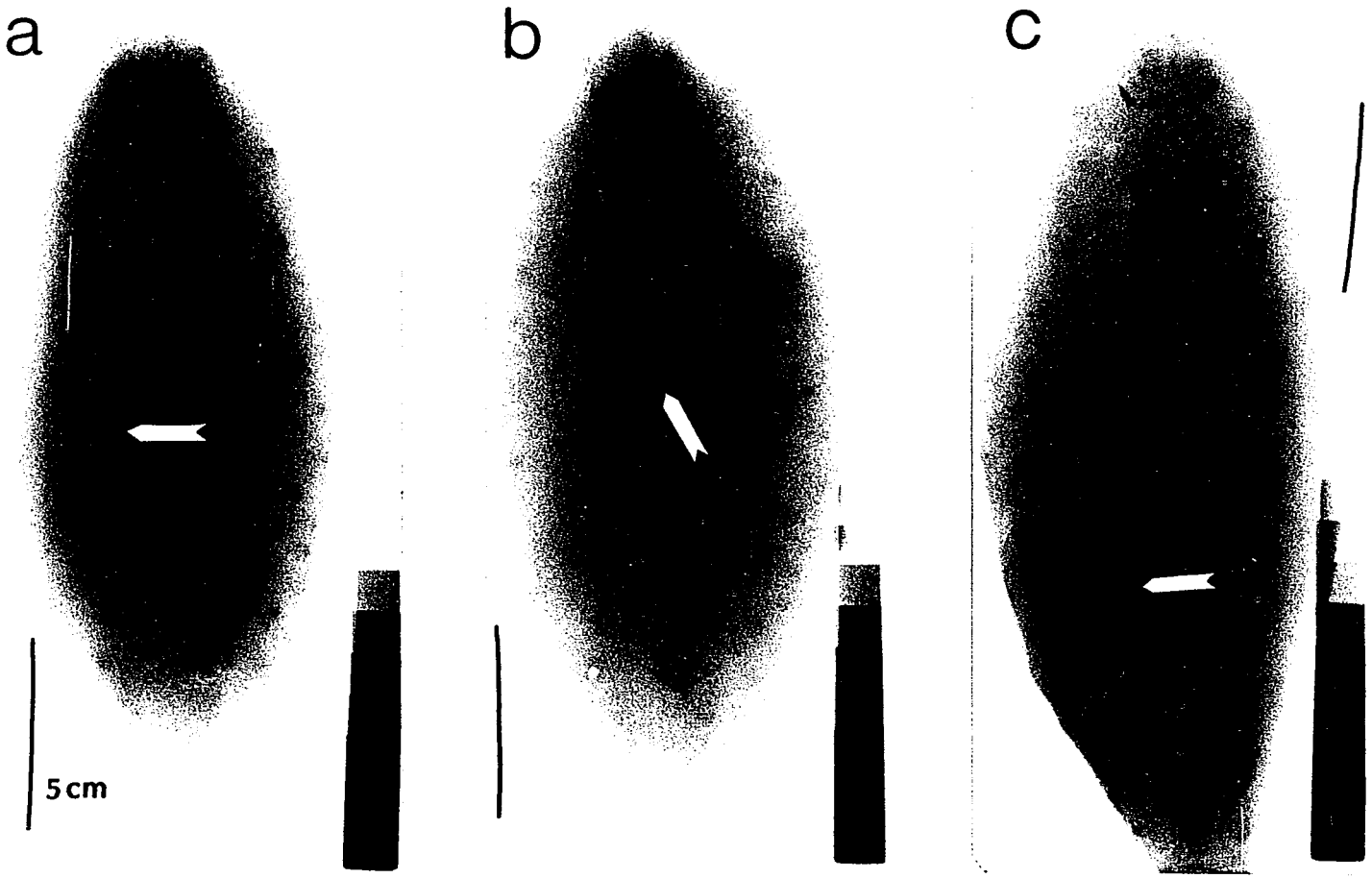
a
b
c
5cm

Figure III-5. Time series of x-radiographs of the gut of Parastichopus californicus, individual G. All views are dorsal views with anterior ends toward top of figure. Scale bar = 5 cm. (a) t = 9 h after individual G was switched from mud + $BaSO_4$ to unlabeled mud. Interface (indicated by arrow) is within a single boudin structure and is slanted with respect to axis of the gut. (b) t = 12 h after switch. Slanted interface within boudin unchanged.


a
b
5 cm

Figure III-6. Time-series of x-radiographs of the gut of Parastichopus californicus, individual D. All views are dorsal views with anterior ends toward top of figure. Scale bar = 5 cm. (a) t = 0 h. Pb = pharyngeal bulb. This exposure was made immediately after individual D was observed feeding on mud + $BaSO_4$. Sediment in anterior-most portion of the gut appears more diffuse and uncompacted than the sediment plug in the remainder of the gut. Individual D was switched to unlabeled mud immediately after this exposure was made. (b) t = 14 h. Interface between labeled and unlabeled mud (indicated by arrow) is less distinct than interfaces seen in Figures 2 - 5. Its more diffuse appearance indicates that some limited mixing must occur immediately behind the pharyngeal bulb. (c) t = 20 h. Characteristics of interface are unchanged indicating that further mixing has not occurred. (d) t = 22 h. Characteristics of interface still unchanged.

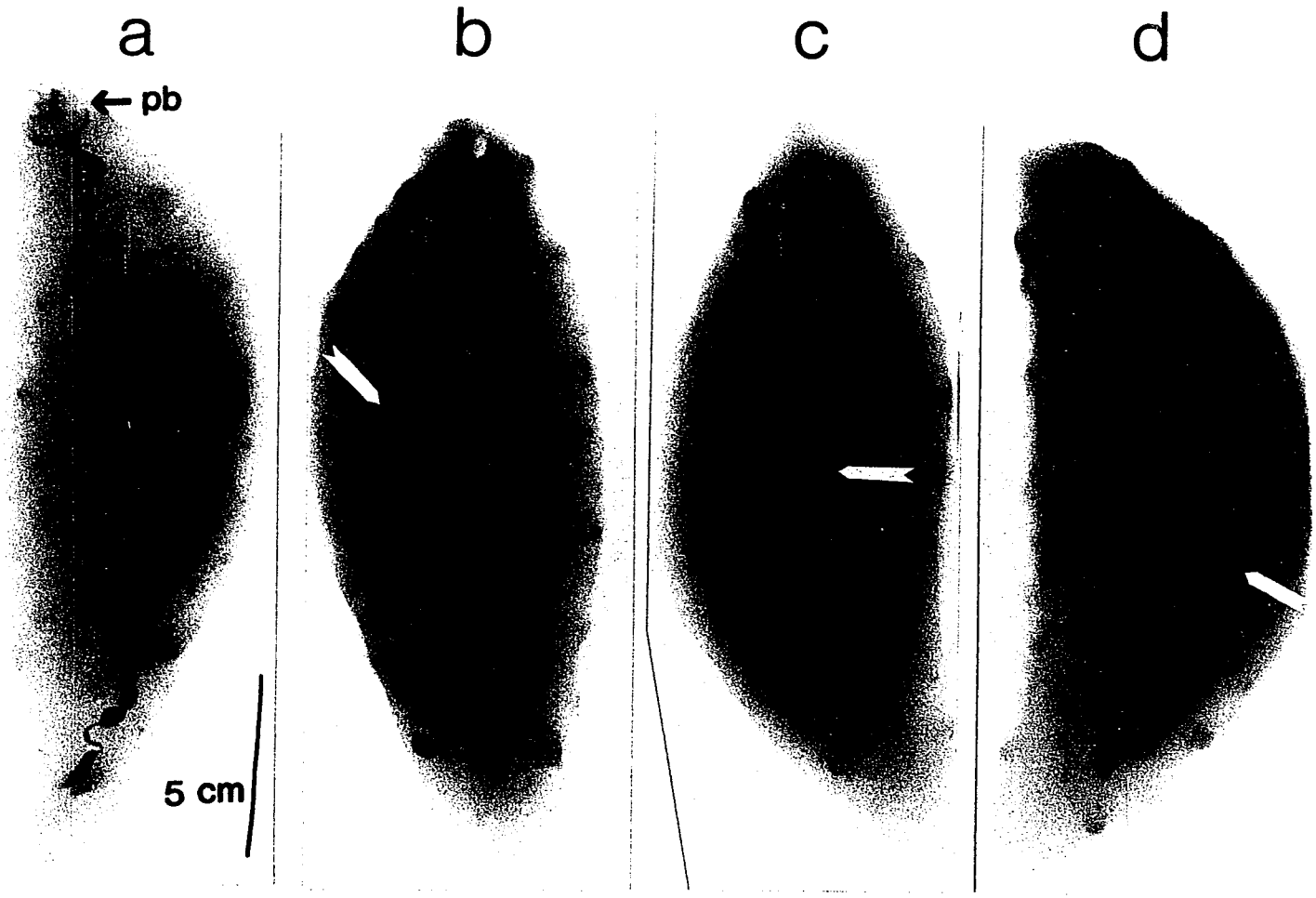
a
b
c
d
pb
5 cm

interfaces, once formed, remained unaltered as sediment moved through the gut. An x-ray exposure taken immediately after an individual was observed feeding on labeled sediment shows that the newly ingested sediment in the anteriormost section of the gut appears diffuse and uncompacted in comparison with the remainder of the sediment plug in the gut (Fig. 6a). This individual was switched to unlabeled sediment immediately after the x-ray exposure was made, and it quickly resumed feeding. The resulting interface between labeled and unlabeled sediment in its gut is less distinct than is observed in the other individuals (Figs. 2-5), but, as in the other individuals, the interface remains unchanged during passage through the rest of the gut (Fig. 6b-d). These results indicate that a limited degree of anterior mixing occurs in the gut of P. californicus. The ability to detect this mixing in a given individual depends on the timing of step changes in tracer input with respect to bouts of ingestion and patterns of sediment movement and compaction in the anteriormost section of the gut.

Observed responses: Amphicteis scaphobranchiata

Changes in numbers of tracer particles per mg of sediment in individual fecal pellets over time were used to quantify the responses of individual Amphicteis scaphobranchiata to two consecutive tracer input steps, a step up in tracer concentration at t_0 and a step down in concentration at t_s. These data, expressed in terms of nondimensional concentration, C^*, and nondimensional time, T^*, yield the observed unit-step response curves (Figs. 7-10). Since two input steps and two tracers (1-37 um fluorescent glass beads and 12-20 um fluorescent polystyrene beads) were used, four response curves were obtained for each worm. Too few 70 um fluorescent polystyrene particles were ingested to generate additional response curves for each worm from those tracer data. The reference concentrations used to calculate nondimensional concentrations are treatment- (i.e., bulk glass sediment or bulk polystyrene sediment) and date- (i.e., 9/87 or 10/87) specific. The highest concentrations of glass tracer and polystyrene tracer observed in the fecal pellets collected from worms in a given treatment on a given date were used as reference concentrations for all the worms

Figure III-7. A CSTR/PFR gut with bypass in which the CSTR is more or less empty and the PFR is more or less full at T^*_0: Predicted and observed unit-step response curves. (a) The predicted response to the step up in tracer concentration at T^*_0 resembles that of a PFR, and the response to the step down at T^*_s resembles that of a CSTR. T^*_{PFR} is the throughput time for the PFR portion of the series. Nonzero tracer concentrations between T^*_0 and T^*_{PFR} indicate bypass. Observed unit-step response curves: (b) Worm 4p, polystyrene bulk sediment treatment, 9/87 run, τ = 8 h. (c) Worm 3p, polystyrene bulk sediment treatment, 9/87 run, τ = 14 h. (d) Worm 8p, polystyrene bulk sediment treatment, 9/87 run, τ = 10 h. Tracers = fluorescent glass beads (□) and fluorescent polystyrene beads (+). Time of step up in tracer concentration: $T^* = 0$. Time of step down in tracer concentration indicated by (- - - - s). Exact orders in time of pellets labeled with (#) are unknown. Orders that give best fits to expected patterns are used; randomly-assigned orders do not change results.

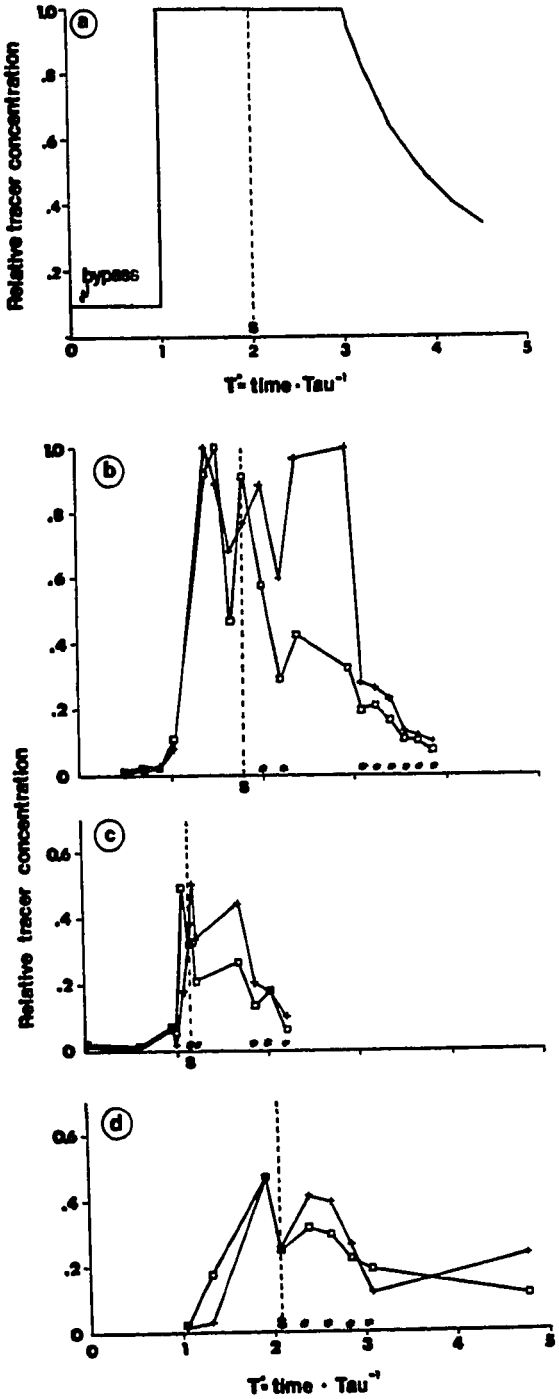
a
b
c
d
Relative tracer concentration
bypass
θ
T'= time · Tau⁻¹

Figure III-8. A CSTR/PFR gut with bypass in which the CSTR is more or less full at T^*_0 and the PFR is more or less empty: Predicted and observed unit-step response curves. (a) The predicted response resembles that for a CSTR alone. Bypass is indicated by the nonzero tracer concentration at T^*_0. Observed unit-step response curves: (b) Worm 2s, bulk glass sediment treatment, 10/87 run, τ = 11 h. (c) Worm 5s, bulk glass sediment treatment, 10/87 run, τ = 18 h. Tracers = fluorescent glass beads (□) and fluorescent polystyrene beads (+). Time of step up in tracer concentration: $T^* = 0$. Time of step down in tracer concentration indicated by (- - - - s).

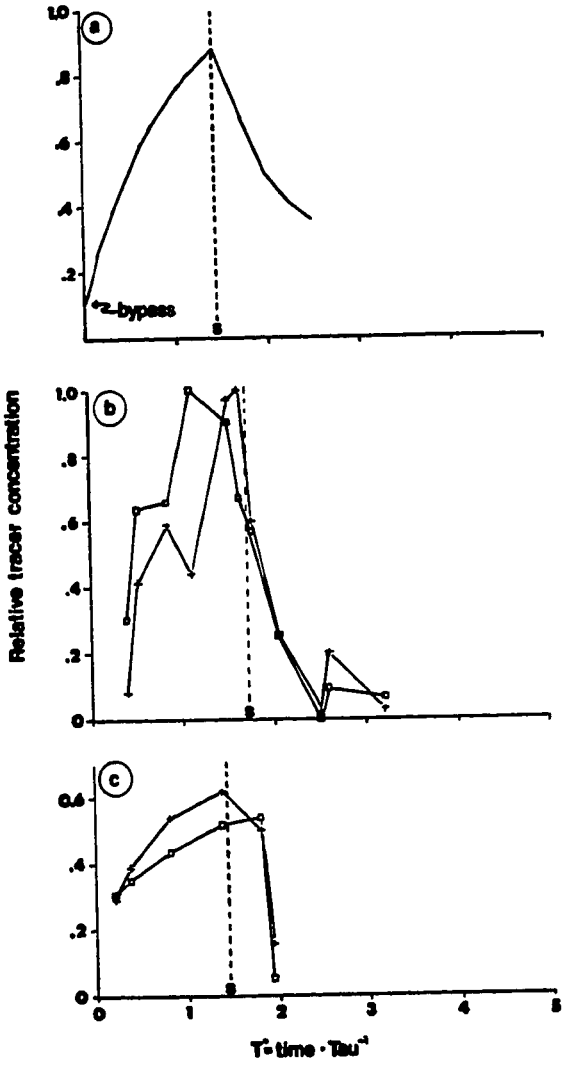
a
1.0
.8
.6
.4
.2
"z-bypass
b
Relative tracer concentration
1.0
.8
.6
.4
.2
0
c
0.6
.4
.2
0
0
1
2
3
4
5
T* time · Tau⁻¹

Figure III-9. A CSTR/PFR gut with bypass that is more or less empty at T^*_0. Observed unit-step response curves: (a) Worm 7p, polystyrene bulk sediment treatment, 10/87 run, τ = 7 h. (b) Worm 1s, glass bulk sediment treatment, 10/87 run, τ = 13 h. In each worm initially-observed tracer concentrations are essentially the highest tracer concentrations observed for that worm suggesting that sediment containing tracer passed rapidly through a more or less empty gut. Tracers = fluorescent glass beads (□) and fluorescent polystyrene beads (+). Time of step up in tracer concentration: $T^* = 0$. Time of step down in tracer concentration indicated by (- - - - s).

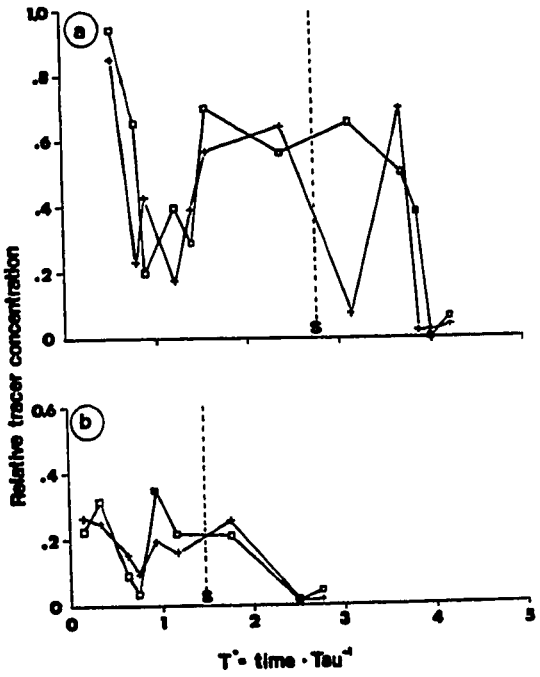
a
b
1.0
.8
.6
.4
.2
0
0.6
.4
.2
0
0
1
2
3
4
5
Relative tracer concentration
T* = time · Tau⁻¹

Figure III-10. Observed unit-step response curves for CSTR/PFR guts with bypass in which patterns of gut fullness and degrees of bypass vary. Specific curve features cannot be attributed uniquely to the effects of variations in gut fullness or to the effects of bypass, but the general characteristics of curves suggest strongly that both mechanisms were operating. (a) Worm 1s, bulk glass sediment treatment, 9/87 run, τ = 9 h. (b) Worm 2s, bulk glass sediment, 9/87 run, τ = 11 h. (c) Worm 5s, bulk glass sediment, 9/87 run, τ = 14 h. The curves for these three worms (a-c) suggest patterns of gut fullness intermediate between empty CSTR/ full PFR and full CSTR/ empty PFR, or they might reflect varying degrees of bypass, or, which is more than likely, they result from combinations of the two mechanisms. (d) Worm 8p, bulk polystyrene sediment, 10/87 run, τ = 19 h. Too few pellets were produced by this worm during the experiment to allow much inference about patterns of gut fullness and bypass. (e) Worm 4p, bulk polystyrene sediment, 10/87 run, = 7 h. This worm's gut may have been more or less empty at T^*_0, but the role of increased bypass cannot be discounted. Tracers = fluorescent glass beads (□) and fluorescent polystyrene beads (+). Time of step up in tracer concentration: $T^* = 0$. Time of step down in tracer concentration indicated by (- - - - s). Exact orders in time of pellets labeled with (#) are unknown. Orders that give best fits to expected patterns are used; randomly assigned-orders do not change results.

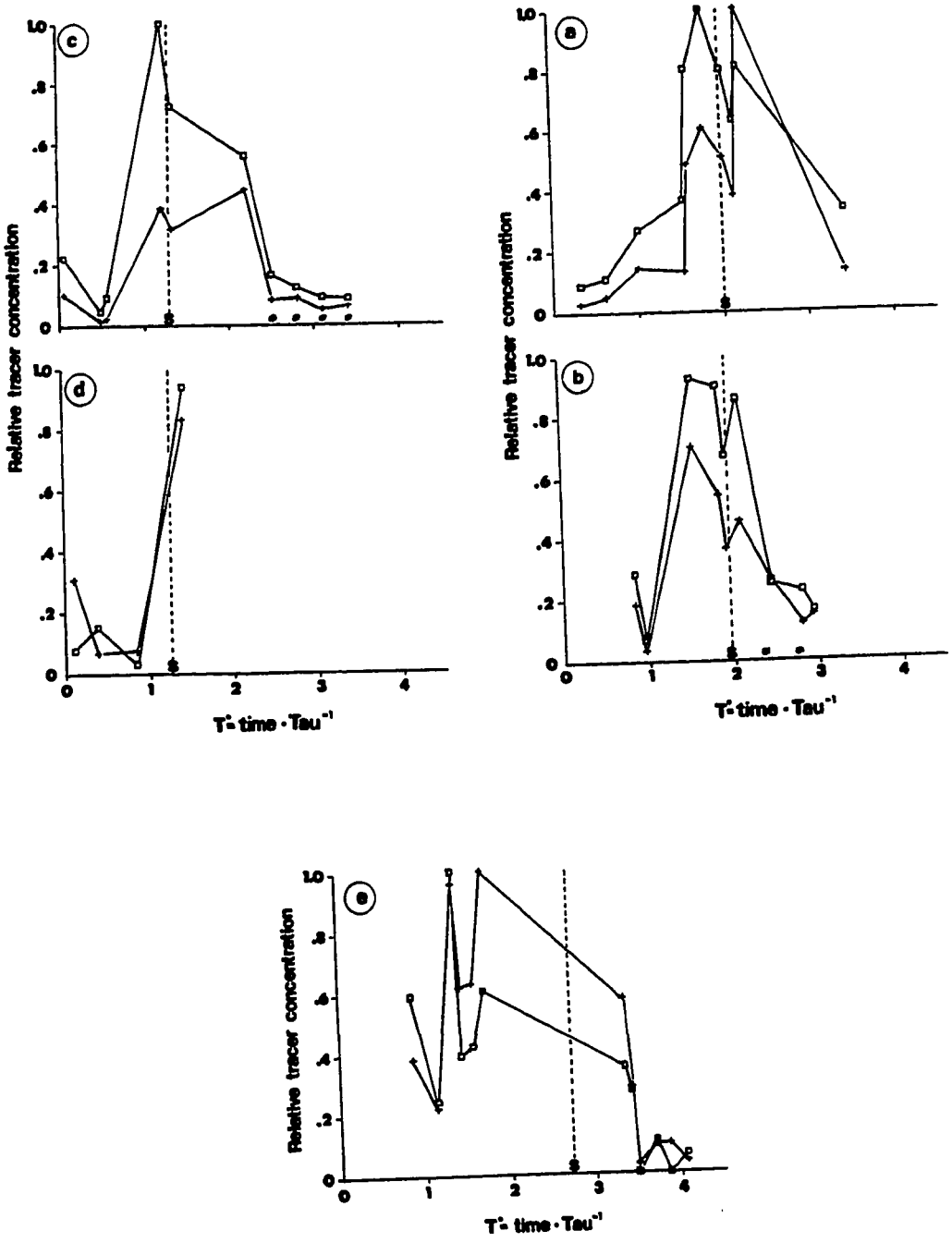
c
a
d
b
e
Relative tracer concentration
T*= time · Tau⁻¹
0
.2
.4
.6
.8
1.0
1
2
3
4

in that group (Table 1).

Individual throughput times were used as reference times in calculations of nondimensional times. Throughput time is the ratio of volume of sediment in the gut to volumetric flow rate of sediment through the gut and is equal to mean residence time of particles in the gut. Given the high variability in tracer concentrations observed in fecal pellets within individuals and the limited resolution of those observations in time (resulting from both the discontinuous method of censusing and the discontinuous output of fecal material), I decided that attempts to determine mean residence times by fitting empirical curves to the data were unwarranted. Instead, I estimated throughput times using mean pellet volumes and mean volumetric flow rates with the assumption, based on previous observations (Taghon and Jumars 1984; Penry, unpublished observations), that the volume of sediment in an individual's gut at any time was equal to three pellet volumes (Table 2). This method of estimation yielded throughput times that are reasonable when compared with observed time scales of responses to the tracer input steps (Figs. 7-10). In two cases, worms 3P and 4P in the 9/87 run, estimates of throughput times were revised upward to achieve better agreement with the observed response times.

I am able to reject the plug-flow model for the gut of Amphicteis scaphobranchiata. Even a qualitative examination of the observed response curves (Figs. 7-10) is sufficient to provide evidence that axial mixing does occur in the gut of A. scaphobranchiata. The scales on which mixing was observed in these experiments (i.e., sediment volumes on the order of 3 fecal pellets) are greater than the scales of resolution of the sampling method (i.e., sediment volumes of individual fecal pellets), and mixing, thus, is not merely the result of methodological artifacts that result from sampling, disaggregating and homogenizing individual pellets. Analyses of individual pellets divided in halves confirm that the sediment volumes affected by mixing under these experimental conditions were at least as great as the volumes of single pellets.

Table 1. Reference tracer concentrations used in calculations of C^* in generation of unit-step response curves for Amphicteis scaphobranchiata.

		Tracer concentrations (number of particles mg^{-1})	
		1-37 μm fluorescent glass beads	12-20 μm fluorescent polystyrene beads
Date	Bulk sediment		
9/87	glass beads	649	869
9/87	polystyrene beads	2242	3113
10/87	glass beads	143	1098
10/87	polystyrene beads	66	436

Table 2. Estimates of throughput times and volumes of sediment in guts for *Amphicteis scaphobranchiata*.

Date	Worm	Pellet egestion rate (# hr^{-1})	Throughput rate (mm^3 hr^{-1})	Mean pellet volume (mm^3)	Estimated volume of sediment in gut (mm^3)[a]	Throughput time (hr)[b]	Total gut volume (mm^3)	Throughput time (hr)[d]
9/87	1s	0.32	0.73	2.26	7	9	----	----
	2s	0.28	0.59	2.11	6	11	----	----
	5s	0.21	0.60	2.88	9	14	----	----
	3p	0.39	1.3	3.24	18[c]	14[c]	----	----
	4p	0.62	0.53	0.86	4[c]	8[c]	----	----
	8p	0.31	1.1	3.57	11	10	----	----
10/87	1s	0.25	0.24	0.96	3	13	23	96
	2s	0.28	0.37	1.23	4	11	13	35
	5s	0.17	0.22	1.31	4	18	17	77
	4p	0.42	0.71	1.70	5	7	17	24
	7p	0.47	1.2	2.53	8	7	28	23
	8p	0.16	0.21	1.32	4	19	14	67

[a] Volumes of sediment in guts estimated from mean pellet volumes. Sediment volume = 3 x (mean pellet volume).

[b] These throughput time estimates were obtained from estimated volumes of sediment in guts and throughput rates.
Throughput time = (volume of sediment in gut)/(throughput rate).

[c] In these two cases throughput times were estimated from unit-step response curves.
Volumes of sediment in guts then calculated from these estimates of throughput times and throughput rates.
Volume of sediment in gut = (throughput time) x (throughput rate).

[d] These estimates of throughput times are based on total gut volumes rather than estimated volumes of sediment in guts. Throughput time = (total gut volume)/(throughput rate).

Regression analyses (Nie et al. 1975) were used to compare observed unit-step response curves with predicted response curves for a mixing gut. The results suggest that a mixing model describes the patterns of sediment movement through the gut of Amphicteis scaphobranchiata observed in these experiments. The equation

$$C^* = 1 - \exp(-t/\tau) \qquad (1)$$

was used to predict responses to the step up in tracer concentrations. Equation 1 was solved for each worm at each observation time $t_0 < t < t_s$, (i.e., for each time at which a worm produced a pellet after the step up and before the step down). The equation

$$C^* = [-\exp(-(t-t_s)/\tau)]/[1 - \exp(-t_s/\tau)] \qquad (2)$$

was used to predict responses to the step down in tracer concentrations. Equation 2 was solved for each worm at each observation time $t > t_s$. The factor $[1 - \exp(-t_s/\tau)]$ normalizes each C^* predicted by equation 4 with respect to the maximum C^* predicted by equation 1 so that the two predicted response curves can be drawn as one continuous curve.

Four regressions (2 input steps x 2 tracers) were generated for each worm. Combinations of the F-test probabilities for individual regressions (Fisher's method for combining independent probabilities, Fisher 1970) are significant for ten of the twelve worms ($p < 0.05$ for 8 worms; $p < 0.10$ for 2 worms) even though less than one-half of all regressions are significant individually (Table 3).

The sequences are unknown for some of the pellets collected from worms in the 9/87 run after the step down in tracer concentrations (data points affected indicated in Figs. 7-10). These pellets are ordered in unit-step response curves and in regression analyses by decreasing tracer concentrations -- i.e., from highest to lowest concentrations of glass tracer for worms feeding on bulk glass sediment; from highest to lowest concentrations of polystyrene tracer for worms feeding on bulk polystyrene sediment. (Randomly-assigned orders do not change the results of the regression analyses).

Table 3. Results of regression ANOVAs for Amphicteis scaphobranchiata: Observed vs predicted tracer concentrations.

Date	Worm	Tracer	Input step	n	Overall F	p	χ^2	p
9/87	1s	glass	up	7	12.269	0.017		
			down	4	10.947	0.080		
		poly	up	7	8.602	0.021		
			down	4	0.982	0.426	21.730 < 0.01	
	2s	glass	up	5	8.399	0.063		
			down	5	12.254	0.039		
		poly	up	5	3.950	0.141		
			down	5	13.724	0.034	22.698 < 0.005	
	5s	glass	up	5	3.602	0.154		
			down	6	20.117	0.011		
		poly	up	5	3.277	0.168		
			down	6	3.330	0.142	20.233 < 0.01	
	3p	glass	up	7	2.421	0.180		
			down	6	5.242	0.084		
		poly	up	7	2.086	0.208		
			down	6	6.833	0.059	17.184 < 0.05	
	4p	glass	up	9	19.719	0.003		
				(6)	(6.526)	(0.063)†		
			down	11	59.201	0.000		
		poly	up	9	23.099	0.002		
				(6)	(6.006)	(0.070)†		
			down	11	10.136	0.011	48.715 < 0.001	
	8p	glass	up	4	3.969	0.185		
			down	6	6.396	0.065		
		poly	up	4	4.360	0.172		
			down	6	0.879	0.402	14.185 < 0.10	

Table 3. Results of regression ANOVAs -- continued

Date	Worm	Tracer	Input step	n	Overall F	p	χ^2	p
10/87	1s	glass	up	6	0.032	0.866		
			down	4	23.742	0.040		
		poly	up	6	4.683	0.096		
			down	4	4.791	0.160	15.077 < 0.10	
	2s	glass	up	6	4.588	0.099		
			down	6	24.340	0.008		
		poly	up	6	18.389	0.013		
			down	6	13.140	0.022	30.601 < 0.001	
	5s	glass	up	4	226.401	0.004		
			down	3	0.630	0.573		
		poly	up	4	138.208	0.007		
			down	3	2.051	0.388	23.974 < 0.005	
	4p	glass	up	6	0.011	0.921		
			down	7	22.166	0.005		
		poly	up	6	3.751	0.125		
			down	7	30.780	0.003	26.538 < 0.001	
	7p	glass	up	7	0.734	0.431		
			down	6	4.160	0.111		
		poly	up	7	0.075	0.796		
			down	6	1.562	0.280	9.082 > 0.10	
	8p	glass	up	3	0.251	0.704		
			down	2	-----	-----		
		poly	up	3	2.162	0.380		
			down	2	-----	-----	2.637 > 0.50	

† First six points ($T^* \leq 1.41$) represent initial response to input step up. ANOVA results for regressions including only these six points are given in parentheses.

The experimental treatments were designed to examine the effects on mixing within the gut of Amphicteis scaphobranchiata of two artificial sediments that were similiar as possible in particle size distributions but differed in particle excess densities. I expected degree of mixing to vary with gut throughput rate (= egestion rate = ingestion rate; units of volume time^{-1}) and mechanical properties of the bulk sediment. No unambiguous treatment effects can be identified. Throughput rates were generally lower in worms feeding on glass beads and in worms in the 10/87 run (Table 2), but there are no significant differences among the four groups (i.e., 9/87 glass, 9/87 polystyrene, 10/87 glass, 10/87 polystyrene) (Kruskal-Wallis test, $0.1 < p < 0.5$). The high degrees of variability in tracer concentrations observed within individuals and deviations from the predicted tracer response curves used in the regression analyses (i.e., the regression residuals) may indicate incomplete mixing within guts. It is more likely, however, that they reflect variations in tracer input that result from inhomogeneities in the pools of artificial sediments (e.g., incomplete mixing of tracers and bulk sediments, differential settling and segregation of particle types when bulk sediment-tracer mixtures were dispensed) and from worms' abilities to select among particles.

Throughput rates (volume time^{-1}) differed by up to a factor of six among worms in these experiments while pellet egestion rates (number of pellets time^{-1}) differed only by up to a factor of four (Table 2). There is a strong, direct correlation between mean pellet volume and throughput rate (Kendall's Tau, $p = 0.01$), but no correlation between mean pellet volume and pellet egestion rate (Kendall's Tau, $p = 0.39$)

No correlation is found between throughput rate and body volume (Kendall's Tau, $p = 0.24$) or between throughput rate and gut fullness (i.e., percent of total gut volume filled with sediment) (Kendall's Tau, $p = 0.50$) for worms in the 10/87 run. The worms in the 9/87 run could not be included in these two analyses because measurements of body volumes and total gut volumes were not made.

DISCUSSION

My results show dramatically that plug flow is more than an ideal construct with some biological relevance; it is reality among deposit feeders. It occurs within the gut of Parastichopus californicus, a large deposit-feeding holothuroid with a simple tubular gut. Deviations from plug flow are expected to be more likely to occur in large than small deposit feeders (Penry and Jumars 1987). The fact that the plug-flow model holds for a large deposit feeder like P. californicus suggests that the model also holds for smaller deposit feeders with tubular guts.

The boudin-like appearance (sensu American Geological Institute 1976) of the sediment plug within the gut of P. californicus at first suggests the presence of a series of small mixing cells driven by peristalsis (i.e., many CSTRs in series approximating a PFR), but the persistence within "boudin" structures of interfaces between sediments with and without tracer shows that they do not function as mixing cells (Figs 4 and 5). Interfaces, once formed, remain intact and unaltered as sediment is moved along the gut, indicating that axial mixing is indeed negligible posterior to the points at which they were formed. Since interfaces can be observed in the anterior region of the gut (Fig. 3a), one important feature of the plug-flow model, the absence of axial mixing, must be characteristic of flow along more or less the entire gut.

One assumption of the ideal plug-flow model, perfect radial mixing, is obviously not true in the gut of P. californicus. There is, in fact, no radial mixing. The persistence of interfaces that are concave (e.g., Fig. 3), convex (e.g., Fig. 4), or slanted with respect to the axis of the gut (e.g., Fig. 5) suggests that the absence of radial mixing parallels the absence of axial mixing and is characteristic of flow along most of the gut. "Plug flow" within a deposit feeder's gut, thus, means the total absence of mixing within the compacted sediment plug. In more rigorous engineering terms, movement of sediment through most of the volume of a deposit feeder's

gut is the extreme case of segregated flow (Levenspiel 1976).

Detection of the complete absence of axial and radial mixing throughout most of the gut requires the relatively fine scales of spatial resolution achieved with the x-ray method. If only slightly less spatial resolution were achieved in these experiments (i.e., if the entire "boudin" were the scale of spatial resolution) the slanted interfaces observed in the guts of several individuals would not have been recognized as such, and the results might have been interpreted incorrectly as evidence of cells of axial mixing.

The diffuse interface in Figure 6 indicates that some axial and radial mixing must occur just behind the pharyngeal bulb before ingested sediment is compacted into a plug in the anterior intestine (sensu Feral and Massin 1982). This anterior mixing probably acts to mix digestive enzymes into the ingested sediment. Digestive enzymes are large molecules, and rate of diffusion of enzymes into the sediment plug might otherwise limit rate of digestion (Penry and Jumars 1987). Thus, although the extent of anterior mixing in the gut of P. californicus is very limited, the fact that it does occur eliminates this one potentially important digestive constraint in an otherwise unmixed gut.

Penry and Jumars (1987) suggested that mixing of enyzmes into ingested sediment as a mechanism for overcoming diffusion limitations is likely to be important in deposit feeders that are large or feed on sediments of low permeability. It was expected that extent of mixing in the guts of such deposit feeders would be large and, thus, that their guts would need to be modeled as CSTR/PFR series. The results of these experiments with the large deposit feeder, P. californicus, suggest that the amount of mixing required may be actually very small and that a CSTR/PFR model generally may not be required. A segregated flow model with the initial condition (i.e., the condition at the reactor entrance) that digestive enzymes are perfectly mixed radially can incorporate the effects of this mixing.

These very simple tracer studies provide kinematic information that, when combined with static descriptions of gut anatomy and histology, yields a clearer understanding of digestive processes in Parastichopus californicus and other deposit feeders with unmixed guts. P. californicus is an aspidochirotid holothuroid with a very simple tubular gut that consists of a pharyngeal bulb (food gathering organ), an anterior intestine, a posterior intestine (absorptive organs that together represent most of the volume of the gut), and a rectum (organ for accumulation of feces) (Feral and Massin 1982). Anterior mixing occurs just behind the pharyngeal bulb. Its location provides the likely gut region to examine for secretion of enzymes -- something that has not yet been done in studies of aspidochirotid gut anatomy and histology.

After enzymes are mixed throughout the sediment it is compacted into a plug in the anterior intestine, and both radial and axial mixing cease. The anterior and posterior intestines are absorptive regions (Feral and Massin 1982) where radial mixing would be disadvantageous. The time it takes for a molecule to diffuse from the gut center to the wall scales as the square of the gut radius over diffusivity. Given a diffusivity within sediments of order of magnitude 10^{-5} cm^2 s (Aller 1982) and the assumption that diffusion is unhindered (i.e., sediment permeability and adsorption of molecules to sediment grains are unimportant), a small molecule could diffuse from the center of the gut to the wall in about 2 h in a Parastichopus californicus individual of the size in Figure 6 (gut radius = 0.25 cm). Throughput time in this individual was greater than 10 h under the conditions in these experiments, more than enough time for effective diffusion of digestive products to the gut wall in the absence of radial mixing. Pseudopolydora kempi japonica (Polychaeta), a much smaller deposit feeder with an unmixed gut, may have a throughput time as short as 30 min (Penry, unpublished observations), but diffusion time in its gut is estimated to be less than 2 min (gut radius = 0.03 cm).

These simple scaling arguments and calculations suggest that unhindered diffusion, the probable situation in, for example, many

deposit feeders from sandy environments, is unlikely to limit digestive absorption. Absorptive limitations imposed by hindered diffusion, however, cannot be discounted for deposit feeders that ingest relatively fine or poorly-sorted sediments (Penry and Jumars 1987). Ontogenetic changes in gut architecture, i.e., increases in ratios of gut length to diameter as individuals of a species increase in size, observed in a number of deep-sea species as well as in some nearshore and shelf species from muddy environments are in the direction predicted if diffusional constraints are operating (Chapter IV).

The boudin-like structure of the sediment plug in the gut of P. californicus may improve diffusion geometry and increase surface area for absorption. The "boudins" may also provide purchase for muscular contractions moving the sediment plug along the gut. Whatever their function, it is obvious that the mere presence of boudin structures cannot be used to infer the presence of mixing cells.

Some mixing can be incorporated reasonably and explained biologically with modifications of the ideal plug-flow model. The degrees of mixing observed in the guts of Amphicteis scaphobranchiata, however, are too great to be explained with a modified plug-flow model. A model that incorporates a specific mixing component is required, and qualitative evidence (Jumars and Self 1986, Penry, unpublished observations) suggests that an appropriate model is CSTR/PFR series with a bypass stream.

Dramatic visual evidence of the presence of a bypass stream that shunts sediment from the inlet directly to the outlet of the gut of Amphicteis scaphobranchiata (i.e., that bypasses the CSTR/PFR series) was first provided by qualitative tracer experiments in which worms were switched from natural sediment to sediment that was brightly colored by the addition of high concentrations of powdered fluorescent paint pigment (Penry, unpublished observations). The first one or two pellets produced by worms under these conditions consisted of unlabeled mud with a ventral "racing stripe" of brightly-colored mud. This racing stripe is actually a mucus-bound string of particles that lies

in a ventral groove in the fecal pellet and that is separated easily from the bulk of the pellet. A ventral bypass stream that shunts particles directly from the inlet to the outlet of the gut is the only mechanism that can account for the characteristics of the pellet racing stripe (i.e., that it is discrete from the bulk of the pellet) and the timing of its first appearance (i.e., that it appears in the first pellet produced after the step up in tracer concentration).

None of the observed response curves (Figs. 7-10) resembles very clearly the predicted curve (Fig. 1d), but they can be best explained in the context of the CSTR/PFR model. Deviations of observations from predictions result from violations of the modeling assumption that each individual's gut was full at t_0, the time of the step up in tracer concentration, and from the action of a bypass stream.

Throughput times calculated as ratios of measured total gut volume to measured volumetric feeding rate for the worms in the 10/87 run (i.e., the predicted time scales of responses to tracer steps if guts were full) are very much larger than throughput times estimated from observed time scales of responses (Table 1). The volumes of sediment in the guts of worms at t_0 in the 10/87 run had to have been less than total gut volumes to account for observed throughput times that are one-third to one-seventh of predictions. It is, thus, necessary to discard the assumption that individuals had full guts at t_0 in the 10/87 run, and reasonable to do so for individuals in the 9/87 run even though confirming data are not available.

The predicted response curves (Fig. 1) incorporate the assumptions that an individual's gut is full at the start of an experiment and that volume of sediment in the gut does not change during the experiment. If fullness of a CSTR/PFR gut varies, the shapes of response curves change. The effects of variations in gut fullness can be identified mostly readily in the CSTR/PFR response to the input step up in tracer concentration. The resulting changes in response curves depend on the location and volume of sediment within the CSTR/PFR series at t_0, the time of the tracer input step.

The predicted response curves also show evidence of a bypass stream. The qualitative effects of bypass are most easily seen in responses to the step up in tracer concentration: Bypass results in the appearance of tracer in fecal pellets, at concentrations higher than would otherwise be predicted, immediately after the step up in sediment tracer concentration occurs. The quantitative effects of bypass depend on the volumetric flow rate of the bypass stream in proportion to the volumetric flow rate through the CSTR/PFR and on patterns of gut fullness.

Since the guts of worms in these experiments were less than full three hypothetical response curves representing three different patterns of gut fullness (i.e., empty CSTR/full PFR; full CSTR/empty PFR; empty CSTR/empty PFR) must be considered in place of the single response curve predicted for a full CSTR/PFR gut. If both the CSTR and PFR contain sediment at t_0, but either (or both) is less than full, the general shape of the predicted response curve does not differ from the curve for a full gut (Fig. 1d). The effects of bypass are merely superimposed upon these curves.

1) If the PFR section of a CSTR/PFR gut contains sediment at t_0, and the CSTR section is empty, the predicted response to the step up in tracer concentration resembles that of a PFR while the response to the step down in concentration resembles that of a CSTR (Fig. 7a). Bypass is indicated by nonzero tracer concentrations in pellets produced between $T^* = t_0$ and $T^* = t_0 +$ PFR. The observed response curves for the three worms feeding on bulk polystyrene sediment on 9/87 suggest CSTR/PFR guts with bypass in which the CSTRs were more or less empty and the PFRs were more or less full at t_0 (Fig. 7b-d).

2) If the CSTR section contains sediment at t_0, and the PFR section is empty, the predicted response resembles that for a CSTR alone (Fig. 1c). Bypass of a CSTR results in a non-zero y-intercept for the response curve at $T^* = t_0$ (Fig. 8a). The observed response curves (Fig. 8b,c) for two worms feeding on bulk glass sediment in the 10/87 run seem to fit this pattern. The effects of bypass are masked by the effects of gut fullness variations in these two observed curves.

3) If the CSTR/PFR gut is empty at t_0, the first material that exits from the gut after the step up in tracer concentration (i.e., the fecal pellet produced) will contain a tracer concentration equal to C_0, and the effects of bypass will be hidden in this much larger signal. Subsequent response to the step down in tracer concentration depends on whether gut fullness increases while the individual is feeding on the sediment that contains tracer. The guts of two worms in the 10/87 run, one feeding on bulk glass sediment and on feeding on bulk polystyrene, appear to have been more or less empty a t_0 (Fig. 9a,b).

These interpretations of observed response curves are reasonable, but are by no means the only possible ones. Any number of combinations of degrees of gut fullness and degrees of bypass could yield similar curves. The observed response curves for three worms feeding on bulk glass sediment in the 9/87 run might reflect patterns and degrees of gut fullness intermediate between the empty CSTR/full PFR and full CSTR/empty PFR cases (Fig. 10a-d). They might reflect simply higher degrees of bypass. The observed response curve for one worm feeding on bulk polystyrene in the 10/87 run appears to indicate that conditions in its gut were intermediate between a full CSTR/ empty PFR and an empty gut (Fig. 10e). The role of bypass could be very important, but cannot be isolated clearly from these experiments.

The accuracy of specific interpretations is not as important as the general conclusions that can be drawn from these data. I can conclude with confidence that a PFR model is not a valid model for the gut of Amphicteis scaphobranchiata. The observed response curves also deviate significantly from the response curve predicted from the ideal CSTR/PFR model, but they can be explained within the context of the model after accounting for gut fullness and apparent bypass. Unique solutions for the relative contributions of varying gut fullness and bypass in determining the characteristics of the observed response curve of any given worm, however, cannot be obtained in these experiments.

What might be the functions of mixing and bypass in the gut of

Amphicteis scaphobranchiata? A. scaphobranchiata is a relatively large deposit feeder that lives in muddy environments, and thus one reasonable hypothesis for the function of mixing is the need to mix enzymes into ingested sediments to overcome diffusional constraints that might otherwise limit digestion in relatively less permeable sediments (Penry and Jumars 1987). The results of the experiments with Parastichopus californicus, however, suggest that the degree of mixing in the gut of A. scaphobranchiata exceeds that necessary for effective mixing of enzymes and sediments. The general CSTR/PFR arrangement of the gut of A. scaphobranchiata may indicate microbially-mediated reactions are important components of its digestive strategy, i.e., that A. scaphobranchiata is a "foregut" fermenter (cf. Penry and Jumars 1987). I would expect, however, that since deposit feeders are relatively small animals, they would be more likely to be "hindgut" fermenters than "foregut" fermenters (see Penry and Jumars 1987 for detailed discussion of comparative advantages and disadvantages of these strategies). Specific characteristics of the structure and function of the gut of A. scaphobranchiata suggest, instead, that mixing and bypass may be components of an intra-gut process of particle sorting.

Hobsonia florida, an ampharetid polychaete with a mixing gut (CSTR/PFR), sorts particles within its gut on the basis of specific gravity, apparently using its ciliated ventral gutter as a rapid bypass for particles of higher specific gravity (Self and Jumars 1978). A. scaphobranchiata, too, has a ciliated ventral gutter in its gut that functions as a bypass mechanism and, thus, possibly as a sorting mechanism. This gutter begins at the point where the foregut joins the midgut and extends the entire length of the midgut and hindgut. Both species also have tongue-like structures (termed internal caeca or blind sacs by Fauvel (1897)) in their midguts that may play roles in sorting of particles as well.

In Amphicteis scaphobranchiata this tongue (Figure 11) is attached at the anterior, ventral margin of the midgut just beneath the opening of the foregut into the midgut. It projects freely into the lumen of

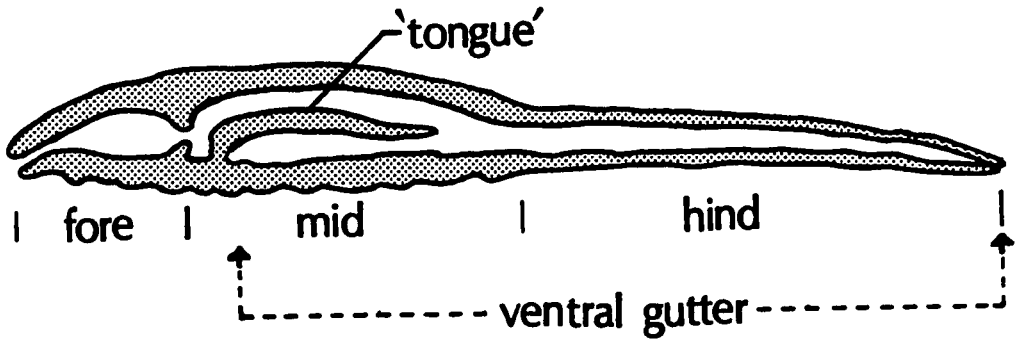

Figure III-11. Schematic of Amphicteis gut showing fore, mid (mixing) and hindgut (plug-flow) regions, location of gut "tongue" and ventral gutter: lateral view of longitudinal cross-section through body and gut (after Fauvel 1897).

the midgut and extends posteriorly for about one-half of the length of the midgut. This midgut tongue is roughly triangular in shape, broadest at the point of attachment and narrowing posteriorly, and it is folded along its entire length so that the dorsal surface is convex and the ventral surface is concave. Its surface is composed of transverse ridges and grooves.

Fauvel (1897 reports that, in Amphicteis gunneri, this tongue ("internal caecum") is formed by an invagination of the midgut wall. Its lumen opens not into the gut, but into the body cavity via a narrow pore in the ventral wall of the midgut. Its epithelium is similiar histologically to that of the anterior glandular lobes of Ampharete grubei. The tongue in Amphicteis gunneri is not ciliated, but the walls of its midgut are.

I suggest, based on gross anatomical observations, that the midgut tongue in Amphicteis scaphobranchiata may function in intragut (i.e., post-ingestion) particle sorting in a manner that is analogous to the way bivalve palps function in pre-ingestion particle sorting and regions of bivalve stomachs function in post-ingestion sorting (Barnes 1980). Sediment passing from the foregut into the midgut of A. scaphobranchiata must enter the midgut dorsally to the midgut tongue. Particles may be sorted by size and specific gravity. Smaller, less dense particles may be swept along the crests of tongue ridges and retained in the midgut for digestion. Larger, heavier particles may be swept laterally along tongue grooves to the edges of the tongue and dropped into the ventral portion of the midgut for rapid elimination via the ventral gutter. Mixing that results from muscular contractions may serve to bring particles into contact with sorting surfaces of the tongue in the midgut of A. scaphobranchiata just as mixing that results from muscular contractions and style rotation serves to bring particles into contact with sorting regions in bivalve stomachs.

If the midgut tongue and ventral gutter do function in intragut particle sorting in Amphicteis scaphobranchiata in the manner just described:

1) Sorting and mixing should occur in, at most, the anterior half of the midgut. The posterior half of the midgut might very well be a region of plug flow. My working assumption that the volume of the CSTR equals the volume of the midgut may overestimate the ratio of CSTR volume to PFR volume by at least a factor of four (see Chapter IV for pertinent gut measurements).

2) Mechanical mixing should play a role in sorting by acting to retain particles in the anterior region of the midgut in addition to its probable role in mixing digestive enzymes into the sediment. A relationship between mixing and bypass is suggested by gut anatomy of terebellid polychaetes and the trichobranchid polychaete, Terebellides stroemi. A ventral, ciliated gutter is not present in the midgut of terebellids or the trichobranchid as it is in the ampharetids Amphicteis scaphobanchiata, Amphicteis gunneri and Hobsonia florida. In terebellids and T. stroemi the gutter begins where the muscular, posterior midgut, the structure of which suggests it is a mixing chamber, joins the hindgut, and it continues the length of the hindgut (Dales 1955; Michel et al. 1984). If bypass via the ventral gutter occurs in terebellid or trichobranchid guts, it is initiated directly after mixing.

3) Most particles that exit in the bypass stream via the ventral gutter should enter the stream in the ventral, anterior region of the midgut in A. scaphobranchiata. Analyses of particle size distributions in different regions of its gut should reveal greater concentrations of larger, more dense particles in the anterior, ventral midgut and ciliated gutter.

The degrees of sorting, mixing and bypass that occur within the gut of Amphicteis scaphobranchiata should be functions of particle and bulk sediment characteristics, extent of mixing, and throughput rate. I expected that glass beads would be eliminated selectively from the gut in the bypass stream, and that a greater degree of bypass would be observed in those worms feeding on bulk glass sediments. I also expected that degree of mixing would increase with decreasing throughput rate. Unfortunately, these hypotheses cannot be tested with the data from these experiments. The test particles, the 1-37 μm

fluorescent glass beads and the 12-20 um fluorescent polystyrene beads, were present in only very small numbers relative to the bulk of particles in the artificial sediments -- a requirement in the design of a good tracer experiment that is at odds with the design of an experiment to examine particle selection or sorting. The efficiency of mechanisms for sorting particles within the gut would have had to have been perfect, or nearly so, in order to have produced a detectable effect with so few particles. The degree of mixing within the gut, patterns of gut fullness and the extent of bypass all affect the observed unit-step response curves. The effects attributable to each cannot be distinguished in any reliable, quantitative fashion.

Sorting and bypass, as Dales (1955) suggested, probably act rapidly to eliminate relatively less digestible particles from the gut. Rough calculations using the reference tracer concentrations to estimate bypass volumes from some of the tracer concentrations that were observed in fecal pellets of Amphicteis scaphobranchiata and that can be reasonably said to reflect the effects of bypass, (i.e., observed tracer concentration = some volume of sediment without tracer + some bypass volume with tracer present in concentration, C_0), indicate that bypass volume may be about five percent of the total pellet volume. Preliminary, qualitative observations suggest that this estimate is at least of the correct order of magnitude. Since particle residence times in the bypass stream are approximately one-third of the mean particle residence time in the gut, the volume of material bypassed, however, may be on the order of fifteen percent of the total volume processed by a worm in any given amount of time. Sorting and rapid bypass of relatively indigestible particles may increase significantly the volume available in the gut for processing of particles of relatively greater digestibilities, and thus, outweigh the costs associated with the processes.

Anatomical observations (Dales 1955; Michel et al. 1984; Chapter IV, this volume) suggest that mechanisms for intra-gut sorting and bypass are likely to be as important in digestive processes of deposit-feeding ampharetid, terebellid and trichobranchid polychaetes

as they are in deposit-feeding bivalves (e.g., Reid and Reid 1969; Hughes 1977). Structures that may indicate intra-gut sorting and bypass capabilities are found in representatives of these groups in environments that range from the intertidal and shallow, subtidal to the deep sea (Dales 1955; Allen and Sanders 1966; Self and Jumars 1978; Chapter IV, this volume). These distribution patterns suggest that there is no necessary relationship between bulk sediment parameters (e.g., mean particle size, percent organic carbon) and internal sorting. They suggest, instead, that the suites of particles available to these deposit feeders are heterogeneous enough, even in the deep sea, for these deposit feeders to benefit from digestive strategies that include mechanisms for internal particle sorting. Attempts to explain distributions of deposit feeders with respect to bulk sediment characteristics or to describe their food resources based on bulk sediment analyses may be limited by an inability to identify the biologically-important sedimentary parameters and to resolve their effects.

The experiments with Amphicteis scaphobranchiata yield the interesting and unexpected observation that fecal pellet volume increases with increasing throughput rate (volume $time^{-1}$). There is no relationship between pellet volume and pellet egestion rate (#pellets $time^{-1}$). These results have interesting biological implications for A. scaphobranchiata and important practical implications for research on deposit feeders. A. scaphobranchiata flings its fecal pellets from its feeding area (Nowell et al. 1984). There is some expenditure of energy and degree of risk associated with fecal pellet removal. A worm will benefit if it can minimize the number of pellets produced per unit of time as its throughput rate (= ingestion rate) increases. In other words, a worm will benefit if it increases pellet volume as its throughput rate increases. The implications for researchers are also clear. The rates at which deposit feeders process sediment are best quantified on a volumetric basis. If pellet size increases with processing rate (volume $time^{-1}$), counts of numbers of pellets egested per unit of time may not reflect actual processing rates. Sensitivity to detect differences among experimental treatments, for example, may

be lost.

First-generation models for deposit feeders' guts were ideal engineering constructs with potential biological applications. These tests of those initial models confirm their utility as frameworks for studies of digestive processes. They reveal necessary modifications of those ideal models and result in formulation of second-generation models that are not only more realistic biologically, but that provide additional insight into digestive processes and constraints in deposit feeders.

The modified plug-flow model for a deposit feeder's gut is characterized by the absence of both axial and radial mixing, and the initial condition that enzymes are perfectly mixed radially in material that is entering gut has been added based on the observations of sediment movement through the gut of Parastichopus californicus. I have assumed conservatively that the absence of radial mixing of particles implies absence of radial mixing in the liquid phase as well. If muscular contractions of the gut act to move and mix the liquid phase (i.e, phase containing digestive products) through the interstices of the sediment plug, movement of digestive products to the gut wall will only be enhanced. Further speculation will not serve to identify rate-limiting steps in the processes of foraging and digestion in deposit feeders with plug-flow guts. Experimental investigations of these processes should now go beyond simple measurements of ingestion rates and assimilation efficiencies and begin to attempt measurements of reaction rates, diffusion rates, absorption rates and assimilation rates.

The abilities of some deposit feeders to sort and selectively retain particles in their guts necessitate substantial modifications of the plug-flow model, -- e.g., incorporation of a specific mixing component and a bypass stream. Potential directions for investigation of foraging and digestive strategies in these deposit feeders are numerous; tests of gut-reactor models still seem to raise more questions than they answer. Investigations must continue with

much-needed descriptions (i.e., What are the patterns and mechanics of particle sorting in various types of guts? What is the function of the internal gut tongue found in some ampharetids?) and kinematic studies (i.e., Do degrees of mixing and sorting vary with ingestion and throughput rates?). Foraging and gut-reactor theory and models can provide the framework for integration of the results of such studies to yield a better understanding of processes of energy and nutrient acquisition in deposit feeders.

The resolution of the data collected in these experiments and the conclusions that can be drawn are limited directly by the lack of reproducible and nutritionally adequate food resources (not due to lack of effort) and the resulting inability to control throughput rates. Known, well-quantified, reproducible food resources must be used in order to control and manipulate ingestion and throughput rates if digestive processes in deposit feeders are to be quantified and the factors affecting these processes are to be identified.

Chapter IV. Relationships among gut architecture, gut kinematics and digestive constraints in deposit-feeding and carnivorous polychaetes.

INTRODUCTION

Optimal digestion theory (Penry and Jumars 1986, 1987; Sibly 1981) provides a basis for inference of digestive kinematics and feeding ecology from static descriptions of gut morphology. The theory identifies the important variables that describe the process of digestion and the mathematical relationships among them. The extent to which ingested food is digested and converted to usable products is a function of digestive reaction kinetics, concentration of some limiting or important food component (i.e., energy or some nutrient) and its throughput time, the ratio of gut volume to throughput rate. The actual mathematical relationships among these variables are determined completely by gut kinematics i.e., patterns of material flow through and within the gut. Gut kinematics find static expression in morphological features of guts.

We (Penry and Jumars 1986, 1987) have modeled gut kinematics in terms of three ideal chemical reactors, the batch reactor (characterized by discrete periods of operation and complete mixing of contents and two continuous-flow reactors), the plug-flow reactor (PFR, no mixing of material along the flow path) and the continuous-flow, stirred-tank reactor (CSTR, complete mixing of material). Given two basic models for digestive reaction kinetics, the Michaelis-Menten model for enzymatic reactions and an autocatalytic model for microbially-mediated digestive fermentation, we have shown that, in general, when enzymatic digestion is the most important component of an animal's digestive strategy its gut should function as a PFR. When, in addition to enzymatic digestion, microbially-mediated fermentation is an important component of a digestive strategy, and throughput time is not long, an animal's gut should function as a CSTR/PFR series (foregut fermentation) or a PFR/CSTR series (hindgut fermentation). The first general digestive strategy is expressed in terms of gut morphology as a more or less simple, tubular gut. Large gut chambers are important morphological features of the guts of many animals using fermentation because such expanded chambers allow both mixing and extend mean particle residence

times.

General descriptions of gut morphologies thus can be used to infer some aspects of basic gut kinematics. Given some understanding of gut kinematics (based either on actual observations or on inferences from gut morphologies), comparative descriptions of gut morphologies can be used to draw inferences about animals' feeding ecologies and digestive constraints. Necessary and very basic information on gut morphologies (e.g., gut volumes) is grossly lacking for marine deposit feeders. In this study we therefore analyze and group deposit-feeding polychaetes on the basis of similarities in gut morphologies and use these groups to infer gut kinematics and potential constraints on foraging and digestion. We choose one major class of animals to avoid issues of between-phylum variability.

We also examine implicit relationships between gut morphology and food quality (i.e., energetic and nutritional composition of food, susceptibility to digestive reactions). Sibly (1981) predicted that animals eating poorer quality food should have larger gut volumes than similarly-sized animals eating higher quality food. This prediction is borne out in herbivorous mammals and birds (Sibly 1981; Hume 1982). If deposit-feeding polychaetes follow a similar pattern, they should have larger gut volumes than similarly-sized carnivorous polychaetes. Among the deposit feeders deep-sea species (i.e., species from an environment that is relatively food poor) should have proportionally more gut than nearshore and shelf species (i.e., species from relatively food-rich environments). If increased relative gut volume as a function of food quality is expressed anatomically in deposit-feeding polychaetes as it is in some birds (Savory and Gentle 1976; Al Joborae 1980), deep-sea deposit feeders should have relatively longer guts than nearshore species and shelf species. A trend of increasing gut length with increasing depth of habitat (i.e., neasrshore to deep sea) has been observed among six species of deposit-feeding tellinid bivalves (cf. Allen and Sanders 1964).

Metabolic requirements generally scale as body mass or volume to

the 0.7 power. Ingestion rate (mass time^{-1}) appears to scale as do metabolic requirements, i.e., it also scales as body mass or volume to the 0.7 power (Calder 1984; Cammen 1980; Forbes and Lopez 1987). If throughput time remains constant as animals increase in size, gut volume should scale as body volume to the 0.7 power. If throughput time decreases as animals increase in size, gut volume should scale as body volume to some power less than 0.7, and if throughput time increases as animals increase in size, gut volume should scale as body volume to some power greater than 0.7. If, among polychaetes, gut volume scales as a function of body volume to a power different from 0.7, ontogenetic changes in digestive kinematics must occur and may indicate ontogenetic changes in diet.

Diet quality has been observed to decrease as body size increases in herbivorous mammals, presumably because larger animals are unable to obtain sufficient quantities of higher-quality, but relatively rare, food items (Parra 1978; Sibly 1981). Gut volume in herbivorous mammals generally scales as body mass or volume to a power of one or greater (Calder 1984). The resulting increase in throughput time with increasing body size may be one digestive adaptation to a lower-quality diet. If ontogenetic changes in diet quality occur among polychaetes we predict that changes will be in the same directions as those observed for herbivorous mammals: Diet quality should decrease as body volume increases, and gut volume should scale as body volume to a power greater than 0.7. In the extreme, switches from carnivory or herbivory to deposit feeding would be expected as juveniles grow into adults. A similar pattern has been observed among reptiles: Small species of lizards tend to be insectivorous while larger species tend to be herbivorous. Hatchlings of herbivorous species tend to be insectivorous until they reach some critical body mass (Pough 1973).

Diffusion limitations (cf. Penry and Jumars 1987) may be another important digestive constraint in deposit feeders. If digestion is diffusion limited we expect such limitation to be more important in individuals with greater gut diameters and in species ingesting

relatively less permeable sediments. We should observe ontogenetic changes in gut morphology with larger individuals having relatively longer, narrower guts, and species ingesting relatively less permeable sediments should be more likely to show such changes.

In this comparative study we take an "engineering" approach to description of polychaete guts. Our goal is to model guts in terms of reactor components and infer general characteristics of digestive processes. We thus describe guts in terms of their anatomically-distinct (not necessarily histologically-distinct or embryologically-distinct) compartments. We quantify differences in entire guts and their compartments among individuals and among species in basic engineering terms, e.g., ratios of body volume to gut volume and relative volumes of gut compartments, total gut aspect ratios (total gut length to mean diameter) and compartmental aspect ratios (compartment lengths to mean diameters). Such descriptions can serve as the first step for integration of histology and enzymology to yield better understanding of the digestive kinematics and feeding ecologies of polychaetes.

METHODS

Species of polychaetes known to be deposit feeders or carnivores were selected for analyses of gut morphology. They were chosen to include representatives of as many different families and, among the deposit feeders, as many different feeding guilds (Fauchald and Jumars 1979) as possible. The species used were selected from three environments: intertidal and shallow subtidal areas of Puget Sound, Washington, the continental shelf of North Carolina, and bathyal basins of southern California (Santa Catalina Basin and San Diego Trough).

The specimens from Puget Sound, Washington, were collected specifically for this study; specimens from the North Carolina shelf and the basins of southern California were obtained from the archived collections of two earlier studies (Jumars 1974; Weston 1983, 1988).

All animals were fixed in formalin and then preserved in alcohol until dissected. No relaxants were used because polychaetes continue to move material through their guts while in the relaxant bath (Jumars, personal observation), and thus the use of a relaxant before fixation would result in exchange of one potential set of artifacts for another.

Only whole individuals were used in these analyses. Each individual was rehydrated in deionized water before dissection. If the worm was large enough (i.e., greater than about 30 mm^3 body volume) its body volume was measured by displacement (3 or 5 independent trials for each individual). Tentacles, large branchiae (e.g., the tentacles and branchiae present in the family Terebellidae), and everted pharynges were removed before measurement. A container was filled to a scribed line with deionized water and weighed to the nearest 0.05 mg. The worm was immersed in the container, and the water displaced above the scribed line was pipetted off. The worm was removed, and the container and remaining water were re-weighed. Displacement volume was determined as the difference between initial and final weight times the density of water (ρ= 1 g cm^{-3}). For very large worms displacement volumes were determined by weighing the displaced water directly rather than by difference. For small worms that could not be measured by displacement a longitudinal cross-section of the body (dorsal view) was drawn using a dissecting microscope with a camera lucida attachment and used to calculate body volume.

For each worm a longitudinal cross-section of the gut (dorsal view) was drawn and used to calculate gut volume, gut length and mean radius. Gross anatomical characteristics were used to distinguish sections of the gut (e.g., anterior, middle and posterior sections, gut caeca), and each section was drawn and analyzed separately. Pharynges of carnivorous polychaetes were not considered to be digestive structures and were not included in measurements of gut volumes.

To calculate body volumes, gut volumes, gut lengths and radii from the longitudinal, cross-sectional outlines a video system (Motion Analysis Corporation, Santa Rosa, CA) was used to digitize each outline and describe it as a series of x and y coordinates of pixels, the smallest units of resolution of the digitized outline. A radius ($r_i = 0.5[y_{i1} - y_{i2} + 1]$) was calculated from the coordinates of pairs of pixels ($[x_i, y_{i1}]$, $[x_i, y_{i2}]$) at each point, x_i, along the body or gut axis (i = 1 to n, where n is the total number of pixel pairs along the body or gut axis and represents the number of transverse cross-sections into which any given longitudinal outline was divided) (Figure 1). Mean radius was calculated as the sum of all radii, r_i, (i = 1 to n) divided by n. Body or gut length was calculated as ($x_n - x_1 + 1$). The volume, v_i, of each transverse cross-section was estimated as the volume of a cylinder of radius r_i (in pixels) and height h (parallel to body or gut axis) of one pixel; the sum of all volumes, v_i, for i = 1 to n, yielded total body or gut volume ($pixel^3$). Measurements in pixels were converted to mm using conversion factors ($mm\ pixel^{-1}$) determined by digitizing reference scales and counting the pixels.

The two assumptions central to this method for obtaining body and gut volumes are (1) the body or gut is cylindrical in transverse cross-section, and (2) the body or gut axis is perfectly parallel to the x-axis of the video system when the longitudinal outlines are digitized. The sensitivity of results to violations of these assumptions was tested by comparing displacement volumes with calculated (video) volumes for solid glass cylinders and for individual Abarenicola pacifica (Arenicolidae). The displacement volumes of solid glass cylinders of various volumes and aspect ratios (length/diameter) were measured (five independent trials for each cylinder). The longitudinal, cross-sectional outlines of the cylinders then were drawn (five independent trials for each cylinder) and digitized, and their volumes were calculated. The axis of each of the five drawings of each cylinder was oriented parallel to the axis of the video system (0^o) and at 10^o, 20^o and 30^o to the x-axis of the video system.

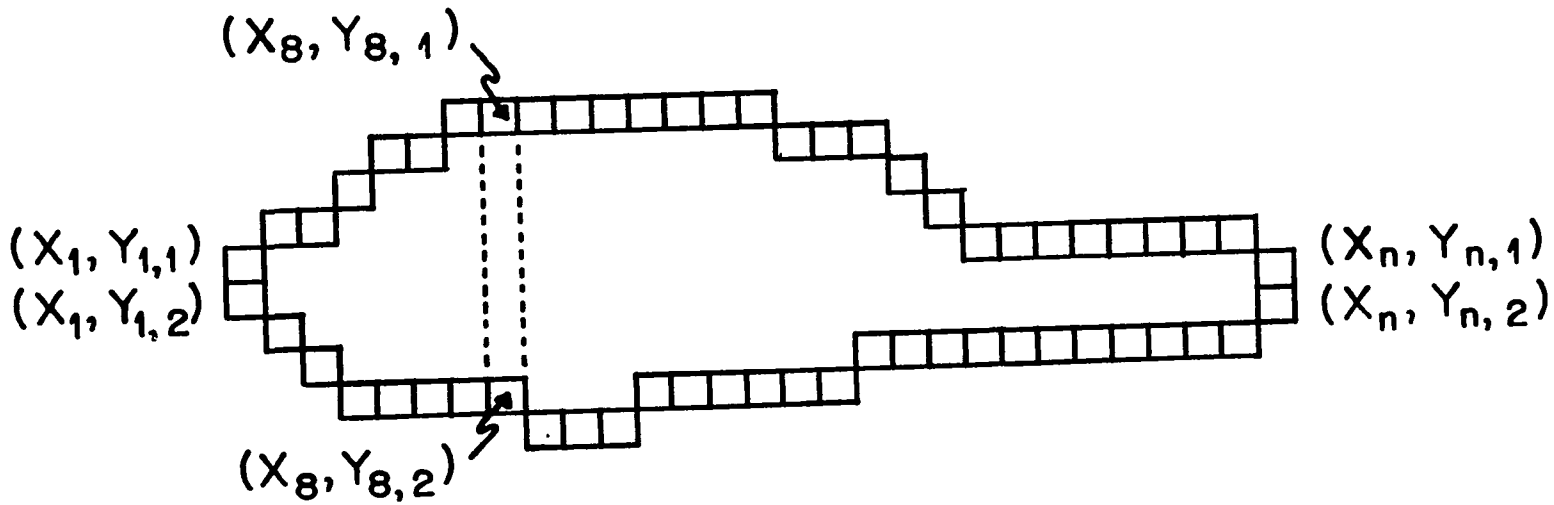

diameter of cross-section = $(Y_{8,1} - Y_{8,2} + 1)$ pixel

height of cross-section = 1 pixel

volume assuming cylindrical cross-section:

$$v_8 = \frac{\pi}{2}(Y_{8,1} - Y_{8,2} + 1)^2 \ (1) \text{ pixel}^3$$

$$\text{Total volume of worm} = \sum_{i=1}^{n} v_n \text{ pixel}^3$$

Figure IV-1. A schematic representation of a digitized outline of a longitudinal cross-section of a body or gut showing the method used for calculating volume.

Body volumes of 20 individuals of Abarenicola pacifica were determined by displacement (five independent trials for each worm). A. pacifica was chosen because (1) its body is more or less cylindrical, (2) its external structures (e.g., branchiae, setae) are relatively small, and therefore the excess water these structures may trap is unlikely to cause significant errors, and (3) its body volume is large enough (> 30 mm^3; > 30 mg of water displaced) to be measured by displacement. Longitudinal cross-sections of the bodies then were drawn (five independent trials for each worm: 2 dorsal views, 1 right lateral view, 1 left lateral view, and 1 ventral view) and digitized, and body volumes were calculated.

A total of 429 individuals of 42 species (Nephtys spp. includes 16 individuals of N. caecoides and 2 individuals of N. caeca) was dissected (Table 1). Body volume, volume, length and mean radius of the entire gut volume, length and mean radius of each section of the gut were determined for each individual. Gut sections were defined as the regions of the gut that could distinguished reliably in all individuals of a species on the basis of gross anatomical characteristics. Our use of terms such as foregut, midgut and hindgut do not necessarily have any histological or embryological connotations. If individuals of a species were obviously not cylindrical or nearly cylindrical in cross-section (e.g., Pseudopolydora kempi japonica), mean radii from dorsal and lateral views were used to estimate major and minor axes of elliptical cross-sections for use in volume calculations. Locations and volumes of sediment in guts were recorded, and sediment composition was described qualitatively (e.g., sand, muddy sand, sandy mud, mud).

Classification analysis (Wishart 1975) and discriminant analysis (Nie et al. 1975) were used to identify and analyze groupings of individuals based on these parameters. Two classification methods, (1) dissimilarity measure = squared Euclidean distance, Ward's method of sorting ("Euclidean" analysis), and (2) dissimilarity = Canberra metric coefficient, average linkage method of sorting ("Canberra" analysis),

Table IV-1. List of species and collection locations.

Species	n	Collection location
Ampharetidae		
Amphicteis scaphobranchiata	16	Puget Sound, WA
Ampharete acutifrons	10	North Carolina shelf off Cape Hatteras
A. americana	10	North Carolina shelf off Cape Hatteras
Anobothrus sp. A	9	San Diego Trough, CA
Ecamphicteis elongata	6	San Diego Trough, CA
Arenicolidae		
Abarenicola pacifica	23	Puget Sound, WA
A. vagabunda	14	Puget Sound, WA
Capitellidae		
Capitella cf. *capitata*	10	Puget Sound, WA
Cirratulidae		
Cirratulus cirratus	10	Puget Sound, WA
Tharyx multifilis	10	Puget Sound, WA
T. luticastellus	9	San Diego Trough, CA
Chaetozone cf. *setosa*	11	Santa Catalina Basin, CA
Fauveliopsidae		
Fauveliopsis glabra	10	San Diego Trough, CA
Glyceridae		
Glycera americana	7	North Carolina shelf off Cape Hatteras
G. dibranchiata	4	North Carolina shelf off Cape Hatteras
Hesionidae		
Ophiodromus pugettensis	10	Puget Sound, WA
Maldanidae		
Euclymene reticulata	20	Santa Catalina Basin, CA
Nephtyidae		
Nephtys spp.		
N. caeca	2	Puget Sound, WA
N. caecoides	16	Puget Sound, WA
Nephtys picta	10	North Carolina shelf off Cape Hatteras
Aglaophamus paucilamellata	6	San Diego Trough, CA

Table IV-1 - continued

Species	n	Collection location
Nereidae		
Ceratocephale pacifica	10	San Diego Trough, CA
Opheliidae		
Ophelina acuminata	6	Puget Sound, WA
Armandia agilis	9	North Carolina shelf off Cape Hatteras
A. maculata	10	North Carolina shelf off Cape Hatteras
Travisia foetida	12	Abyssal plain off Baja, CA
Paraonidae		
Levinsenia oculata	10	Santa Catalina Basin, CA
Polynoidae		
Harmothoe extenuata	10	North Carolina shelf off Cape Hatteras
Scalibregmatidae		
Scalibregma inflatum	23	Puget Sound, WA
S. inflatum	10	North Carolina shelf off Cape Hatteras
Spionidae		
Pseudopolydora kempi japonica	10	Puget Sound, WA
Paraprionospio pinnata	10	North Carolina shelf of Cape Hatteras
Spiophanes cf. *bombyx*	10	San Diego Trough, CA
Sternapidae		
Sternaspis scutata	13	Puget Sound, WA
S. fossor	6	Santa Catalina Basin, CA
Terebellidae		
Eupolymnia heterobranchia	12	Puget Sound, WA
Neoamphitrite robusta	6	Puget Sound, WA
Thelepus crispus	9	Puget Sound, WA
Polycirrus eximius	10	North Carolina shelf off Cape Hatteras
Artacamella hancocki	8	San Diego Trough, CA
Trichobranchidae		
Terebellides stroemi	12	North Carolina shelf off Cape Hatteras
Terebellides cf. *stroemi*	10	San Diego Trough, CA

were used in parallel to attempt to identify analytical artifacts. Two methods of discriminant analysis, direct and stepwise, were also applied. Direct analysis, in which all variables enter the analysis at the same time, was used when the number of variables was small (m = 4). Stepwise analysis (method = minimization of Wilks lamba; F-test probability for inclusion or removal of a variable = 0.2) was used when the number of variables was large (m = 16) to more easily identify a small set of variables with discriminating power.

GUT DESCRIPTIONS

Ampharetidae

Five species of ampharetids were dissected, Amphicteis scaphobranchiata, Ampharete acutifrons, Ampharete americana, Anobothrus sp. A, and Ecamphicteis elongata. The guts of all five species are characterized by three anatomically-distinct regions -- a foregut, midgut and hindgut. In each species the midgut projects anteriorly to some degree and envelopes the posterior portion of the foregut. A ventral gutter is present along the entire length of the midgut and hindgut in A. scaphobranchiata, A. acutifrons and A. americana. No ventral gutter was observed in Anobothrus sp. A or E. elongata, but the individuals examined were very small, and the gutter, thus, may have been difficult to distinguish. More detailed examinations (e.g., gut thin-sections and histology) may reveal the presence of ventral gutters in the guts of these two species as well. The midgut of Amphicteis scaphobranchiata is characterized by an internal midgut "tongue" ("internal caecum" in Fauvel 1897) that attaches to the anterior ventral margin of the midgut immediately below the opening of the foregut into the midgut and projects freely into the lumen of the midgut for about one-half its length. We have suggested that this "tongue" may function in intragut particle sorting (see Chapter III). The midgut "tongue" seems to be a feature of the genus Amphicteis (and the closely-related genus Hobsonia, P. Jumars and D. Penry, personal observations); no similar structure was observed in the guts of any of the other species examined.

Arenicolidae

Two species, Abarenicola pacifica and Abarenicola vagabunda, were dissected. The guts of both species are characterized by anatomically-distinct fore-, mid- and hindguts. In both species the gut forms a single loop where the midgut joins the hindgut. These species also have one pair of large, thin-walled, digestive caeca and numerous small, thicker-walled, accessory caeca. In A. vagabunda the internal structure of some of the larger accessory caeca seems to be characterized by numerous longitudinal folds or lamellae. These caeca do not normally contain sediment, and may have a secretory function or may function to increase surface area for absorption. (In two of the fourteen individuals of A. vagabunda we examined one of the two large caeca contained sediment, but we consider these occurrences to be anomalies). Differences in the number of accessory caeca are used to distinguish these two species taxonomically (Healy and Wells 1959). In A. pacifica the two large caeca and three to six accessory caeca all insert where a narrow, tube-like foregut joins a lobular midgut. In A. vagabunda, however, the two large caeca and 11 to 18 accessory caeca insert along a fourth anatomically-distinct region of the gut (which we called "anterior midgut", but which also could be called "posterior foregut"). This fourth gut section in A. vagabunda is a thin-walled, expanded sac in contrast to the narrow, tube-like foregut anterior to it and the lobular midgut posterior to it.

Capitellidae

One species, Capitella cf. capitata, was examined. Two anatomically-distinct gut sections were distinguished. The anterior section is a narrow, tightly-coiled (i.e., spring-like) tube that generally occupies the thoracic region. The posterior section is a tube that is wider than the anterior section, and it snakes back and forth in the body cavity. The entire gut is very distensible, and the posterior section collapses when empty. Gut volumes, thus, may have been underestimated in individuals without full guts, and ratios of body volume to gut volume may have been overestimated in these cases. Sediment in the gut is pelletized. Pellets are ovoid and seem to be formed before sediment moves into the posterior section. In one

individual several pellets were seen in the anterior-most region of the anterior gut section -- these pellets were either formed immediately after the sediment was ingested or were ingested as pellets. When the posterior gut section is full of pellets they generally are arranged in pairs, two pellets side by side across the gut with their long axes oriented dorso-ventrally.

Cirratulidae

Four species, Cirratulus cirratus, Chaetozone cf. setosa, Tharyx multifilis, and Tharyx luticastellus, were dissected. No anatomically-distinct sections can be identified reliably in the gut of C. cirratus. Regions that can be distinguished on the basis of changes in gut diameter in contracted individuals only parallel changes in body diameter and can not be distinguished in extended individuals. The posterior portion of the gut of C. cirratus may coil in the body cavitiy. C. setosa and T. multifilis both have short, straight, narrow anterior gut sections that widen into segmented posterior gut sections (one gut segment per body segment). T. luticastellus, a deep-sea cirratulid that constructs and lives doubled over and coiled inside a mud-ball concretion (Jumars 1975), is essentially all gut. A narrow, tubular, anterior gut section in the worm's thoracic region widens into a much-inflated and pouchy, but tubular, posterior section that snakes back and forth and occupies the entire body cavity. Each individual examined had a narrow constriction in the body at the point where it was doubled over to coil the posterior portion back along the anterior portion. In the four largest worms of the eight examined this body constriction was reflected in a gut constriction as well -- a short region in which the gut is a narrow, segmented tube that divides the posterior gut section approximately in half.

Fauveliopsidae

One species, Fauveliopsis glabra, was examined. Two anatomically-distinct gut sections were distinguished. The anterior gut section is a straight, narrow, segmented tube. The gut widens into the posterior section, a thin-walled, unsegmented tube of larger mean diameter than the anterior section. The posterior section loops once

or snakes back and forth in the body cavity. The anterior section was empty in all the individuals examined; the posterior section was usually filled with sediment.

Maldanidae

One species, Euclymene reticulata, was examined. Two anatomically-distinct gut sections were distinguished. The anterior gut section is a narrow, tightly-coiled (i.e., spring-like) tube. The gut widens into the posterior section, a thin-walled tube of larger mean diameter than the anterior section. The posterior section coils numerous times or snakes back and forth in the body cavity. Its thin walls make it difficult to stretch the gut to its full length, and thus the ratios of total gut length to mean gut diameter and posterior section length to mean posterior section diameter are probably underestimated.

Opheliidae

Four species of opheliids, Armandia maculata, Armandia agilis, Ophelina acuminata and Travisia foetida, were dissected. Two anatomically-distinct gut sections were identified in Armandia spp., three gut sections were identified in O. acuminata, and four gut sections were identified in T. foetida. All four species have a pair of caeca that insert in anterior regions of their guts. These gut caeca may be found in many, possibly all, opheliids: their presence has been noted by previous investigators (MacConnaughey and Fox 1949; Hartmann-Schroder 1958).

In Armandia maculata these gut caeca insert at the location of the dorsal blood sinus, and we used the point of caecal insertion to distinguish the anterior and posterior gut sections. The anterior gut section is a tube that is only slightly narrower in diameter than the posterior section, and the two sections probably could not be distinguished if it were not for the presence of the caeca. Sand grains in the gut of A. maculata were arranged more or less in single file.

In Armandia agilis a constriction separates the anterior and posterior gut sections that we distinguished, and the caeca insert about midway along the axis of the anterior section. As in A. maculata, the anterior section is generally smaller in diameter than the posterior section. The distinctions between anterior and posterior gut sections in A. maculata and A. agilis are based on very qualitative differences in the appearances of the guts. The important observation is that the guts in these two species are more or less simple tubes -- distinct, specialized regions, except for the small, thin-walled, anterior caeca, are not apparent.

Three sections were identified in the gut of Ophelina acuminata. The point of caecal attachment and the start of a dorso-ventral gut partition separate the anterior gut section from the middle and posterior gut sections. The caeca in O. acuminata are thin-walled, elongated and relatively larger than in Armandia spp. The dorso-ventral gut partition begins where the anterior section joins the middle section and extends posteriorly for the rest of the length of the gut. This partition or "typhlosole" is attached to the ventral gut wall along its entire length, and extends across the gut lumen to the dorsal gut wall. We could not determine if it is also attached to the dorsal gut wall, but if it is, the points of attachment are easily broken. Hartmann-Schroder (1958) describes a ventral, longitudinal midgut fold as the point of insertion for the caeca in O. acuminata; we could not determine if caecal insertion was related to the typhlosole in the individuals we examined. The posterior gut section, the posterior one-fourth of the gut, is separated from the middle section by a constriction.

Four sections were identified in the gut of Travisia foetida: two distinct sections (termed foregut and anterior midgut) anterior to the point of caecal attachment and two distinct sections (termed posterior midgut and hindgut) posterior to the point of caecal attachment. Hartmann-Schroder (1958) distinguishes only a single midgut region in Travisia -- the region posterior to the point of caecal insertion. The foregut is elaborated into a number of thick-walled, involuted sacs

with external blood sinuses. The foregut above the ventral mouth resembles externally a cauliflower on a stalk. A narrow tube leads posteriorly from the elaborate foregut, through several strong body septa, into the anterior midgut. The anterior midgut is a thin-walled sac with a thick, interior lining of easily-dislodged, spongy tissue. Two large, flattened, lima-bean-shaped caeca attach between the anterior and posterior midgut sections. The posterior midgut is a large, sacculated chamber. The hindgut fills most of the body cavity. It is thin-walled with obvious longitudinal muscle fibers. Dorsal and ventral bands of connective tissue or muscle run the length of the hindgut and draw the hindgut into a series of loops that resemble lateral sacs projecting from both sides of the midline.

Paraonidae

One species, Levinsenia oculata, was dissected. The gut of this species appears to be a simple tube with no anatomically-distinct sections. When full of sediment the gut fills the entire body cavity; when empty, it collaspes to a narrow tube that snakes back and forth (the posterior half may coil) in the body cavity. The total gut aspect ratio for this species must be considered a minimum estimate -- it is very difficult to straighten the body coils let alone straighten the gut coils within the body coils.

Scalibregmatidae

Individuals from two populations of one taxonomic species, Scalibregma inflatum, were examined. Three gut sections were identified in individuals of both populations. The relative volumes of the gut sections are similar in the two populations, but the aspect ratios of the sections differ. Gut sections are relatively longer and narrower in S. inflatum (NC), collected from a sandy environment on the continental shelf off North Carolina, than in S. inflatum (PS), collected from a muddy environment, Puget Sound, WA. The guts in both populations are very expandable, and the guts of individuals in the NC population were less full of sediment -- a factor that could contribute to, but not explain completely, the observed differences among the two populations. In both groups the anterior gut section or foregut is a

small, thin-walled sac. It widens into the middle gut section or midgut, a thin-walled section with dorsal and ventral bands of connective tissue or muscle that run the length of the section and draw the midgut into a series of loops that resemble lateral sacs on either side of the midline. When empty the midgut collapses into a ribbon-like section. In S. inflatum (NC) the midgut may form one large loop in the body cavity in addition to the numerous small loops that form sacs along the axis of the midgut. The posterior gut section or hindgut is a relatively straight, thin-walled tube in both groups. The junction between midgut and hindgut is more easily distinguished in S. inflatum (PS).

Spionidae

Three species, Pseudopolydora kempi japonica, Paraprionospio pinnata, and Spiophanes cf. bombyx, were dissected. In all three species the gut is essentially a straight, simple tube with no major, anatomically-distinct sections. In P. pinnata and S. bombyx there is a small, muscular bulb (less than ten percent of total gut volume) located about one-fourth of the way along the gut from the anterior end.

Sternaspidae

Two species, Sternaspis scutata and S. fossor, were examined. Three gut sections were identified in each species. The anterior section or foregut is a very narrow, extensible tube -- it is more or less straight in extended individuals and coiled in contracted individuals. The foregut widens into a middle gut section, the midgut. The midgut is separated from the posterior gut section, the hindgut, by a short, constricted tube that is much narrower than the midgut and somewhat narrower than the rest of the hindgut. The midgut and hindgut together are very long relative to body length and are highly coiled even in extended individuals. The hindgut is folded in half lengthwise. Its two halves lie side-by-side and together loop back on a coiled midgut to form one coiled mass of gut. The midgut loops tend to be towards the inside of the coiled mass. The side-by-side hindgut loops follow the midgut loops and tend to lie along the outsides of the

midgut loops and the coiled gut mass. The midgut is easily distinguished from the hindgut even when the two are coiled together because the diameter of midgut is 1.5 to 2 times greater than the diameter of the hindgut.

Terebellidae

Five species, Neoamphitrite robusta, Eupolymnia heterobranchia, Thelepus crispus, Polycirrus eximius, and Artacamella hancocki, were dissected. Five gut sections can be identified in N. robusta and E. heterobranchia. Their guts are similar to the gut of Amphitrite johnstoni which is described in great detail by Dales (1955). He calls the five sections of the gut of A. johnstoni the esophagus, fore-stomach, hind-stomach, fore-intestine and hind-intestine. We use Dales' criteria to distinguish sections of the guts of N. robusta and E. heterobranchia, but we prefer for internal consistency to use the terms foregut, anterior midgut, posterior midgut, anterior hindgut and posterior hindgut.

Four gut sections can be identified in T. crispus and P. eximius: foregut, anterior midgut, posterior midgut and hindgut. Two hindgut sections cannot be distinguished on the basis of gross anatomical characteristics as they can in N. robusta, E. heterobranchia, and A. johnstoni. In N. robusta, E. heterobranchia, T. crispus and P. eximius as in A. johnstoni the posterior midgut is a muscular section that may serve as a mixing chamber. Patterns of distribution of sediment in the gut provide circumstantial evidence to support this suggestion: The posterior midgut usually contains some sediment even when the rest of the gut is empty -- the expected pattern if the posterior midgut were a mixing chamber.

Three sections can be identified in the gut of Artacamella hancocki: foregut, (anterior) midgut and hindgut. There is no muscular posterior midgut, and there is only one distinct hindgut section. The hindgut is more or less straight; its anterior region does not form a single loop as it does (to varying degrees) in A. johnstoni (Dales 1955), N. robusta, E. heterobranchia, T. crispus and P. eximius. All

species of terebellids we examined have a ventral gutter that extends the length of the hindgut (the length of the anterior and posterior hindgut in species where two hindgut sections were identified).

Trichobranchidae

Two potentially different species, Terebellides cf. stroemi (SDT) from a muddy environment in the San Diego Trough off southern California and Terebellides stroemi (NC) from a muddy sand environment on the North Carolina continental shelf were examined. The gut of T. stroemi (SDT) is similar to that described for individuals from yet another population of Terebellides stroemi (FCC) from the Catalan Coast of France (Michel et al. 1984). Michel et al. (1984) describe five gut sections in T. stroemi (FCC): a ciliated, tubular esophagus, a ciliated fore stomach surrounded by a "digestive gland", a large, muscular hind stomach, a thick-walled fore intestine and a thin-walled hind intestine with a single loop in the region where it joins the fore intestine. We were able to distinguish anatomically only four gut sections in T. stroemi (SDT): an anterior, tubular section (foregut), a middle, muscular section (termed posterior midgut to correspond with the muscular, posterior midgut of terebellids), and two posterior sections, a thick-walled, anterior section (anterior hindgut) and a thin-walled, posterior section (posterior hindgut). The posterior region of the "foregut" in T. stroemi (SDT) is surrounded by a "digestive gland" similar to the one described by Michel et al. for T. stroemi (FCC). The posterior foregut region in T. stroemi (SDT) probably corresponds to the ciliated, fore stomach in T. stroemi (FCC), but it cannot be distinguished anatomically as a separate section in T. stroemi (SDT) as it appears the fore stomach can be in T. stroemi (FCC) (Figures 1B,C in Michel et al. 1984). As in T. stroemi (FCC) (Figure 1B Michel et al. 1984) there is a single loop in the posterior hindgut of T. stroemi (SDT) where it joins the anterior hindgut.

We identified three gut sections in T. stroemi (NC): an anterior, tubular section (foregut), a muscular, middle section (termed posterior midgut to correspond with the muscular, posterior midgut of terebellids), and a single posterior section (hindgut). The posterior

region of the foregut in T. stroemi (NC) is surrounded by a "digestive gland" (Michel et al. 1984) and probably corresponds to the fore stomach of T. stroemi (FCC), but, as in T. stroemi (SDT), a "fore stomach" region cannot be distinguished anatomically in T. stroemi (NC). The hindgut in T. stroemi (NC) cannot be divided anatomically into distinct anterior and posterior hindgut sections (or "fore intestine" and "hind intestine"). The hindgut in T. stroemi (NC) is a straight, more or less anatomically-undifferentiated tube. There is no hindgut loop as there is in T. stroemi (SDT) and T. stroemi (FCC). We were unable to identify clearly a ventral gutter in the hindgut of either T. stroemi (SDT) or T. stroemi (NC), but, since it is present in T. stroemi (FCC) (Michel et al. 1984), we assume it is present in both populations we examined. A ventral gutter appears to be one of the conservative features of gut anatomy among terebellids and presumably among the closely-related trichobranchids.

Carnivores

Nine species of carnivores were dissected: Glycera americana and G. dibranchiata (Glyceridae), Ophiodromus pugettensis (Hesionidae), Nephtys caeca and N. caecoides (combined in analyses as Nephtys spp.), Nephtys picta, and Aglaophamus paucilamellata (Nephtyidae), Ceratocephale pacifica (Nereidae) and Harmothoe extenuata (Polynoidae). In general all of these carnivorous species have straight, tubular guts with no easily or reliably distinguished, anatomically-distinct gut sections. An anterior, muscular section, however, can be identified in the guts of the two glycerids. This muscular section represents about 25% of the gut volume, but only 15% of the gut length. It is immediately posterior to the pharyngeal sheath (i.e., it is not necessarily part of the capturing apparatus) and may act to macerate newly ingested prey.

RESULTS

Tests of the video method for determining volumes

Comparisons of volumes calculated for glass cylinders oriented parallel to the video x-axis (i.e., at 0^{o}) and volumes measured by

displacement show that mean calculated volume at 0^{o} tends to be less than mean displacement volume for the smallest glass cylinders (< 50 mm^3), approximately equal to mean displacement volume for medium-sized cylinders (50 - 350 mm^3), and greater than mean displacement volume for the largest cylinders (> 700 mm^3) (Table 2). Calculated volumes probably represent more accurate estimates of actual volumes for the smallest cylinders than do displacement volumes because the volumes displaced are close to the limits of the measurement technique.

Departures of cylinder axes from orientations parallel to the video axis (i.e., cylinder axes oriented at 10^{o}, 20^{o} or 30^{o} with respect to the video axis) result in increases in calculated volumes. Calculated volumes at 10^{o} and calculated volumes at 20^{o} are not significantly different from calculated volumes at 0^{o} (Tables 3,4). For the smallest cylinder (cylinder E) calculated volumes at 30^{o} are also not significantly different from calculated volumes at 0^{o}. Overall, calculated volumes at 0^{o}, 10^{o} and 20^{o} differ from displacement volumes by a mean of 8% (|(calcualted - displacement)/displacement| x 100); calculated volumes at 30^{o} differ from displacement volumes by a mean of 13%.

Body volumes of 20 individuals of Abarenicola pacifica measured by the displacement method and calculated by the video method were compared using regression analysis (Nie et al. 1975). Since body volumes ranged over three orders of magnitude natural log transformations of body volumes were used in the analysis. If calculated volume is a perfect predictor of displacement volume the regression should have a slope equal to one. The result of this analysis is a regression (r^2 = 0.997; overall F = 6009, $p << 0.001$) with a slope close to, but significantly different from, the expected slope of one (m = 1.06; 95% C.L. = 1.03 to 1.09). Calculated body volumes are always greater than displacement volumes, and departures from the expected line (m = 1) increase as body volume increases (Figure 2). Variances of calculated body volumes (means of volumes calculated from the five outlines drawn for each worm: 2 dorsal views, 1 right lateral, 1 left lateral, and 1 ventral) increase with body

Table IV-2. Displacement volumes and calculated volumes for solid glass cylinders. Volumes were calculated with the axis of each cylinder oriented parallel (0^{o}) and at 10^{o}, 20^{o}, and 30^{o} to the axis of the video system. Values represent means of five trials. Standard deviations are in parentheses. All meaurements are in mm^{3}.

Cylinder	Aspect Ratio	Displacement Volume	Calculated volume 0^{o}	10^{o}	20^{o}	30^{o}
E	4.8	46 (9)	37 (1)	36 (1)	38 (1)	40 (1)
D	7.1	55 (3)	52 (3)	53 (3)	55 (3)	59 (3)
C	11.7	85 (7)	92 (4)	93 (4)	97 (4)	107 (5)
B	1.8	164 (8)	170 (5)	171 (4)	173 (5)	181 (4)
A	3.7	337 (12)	332 (6)	335 (7)	343 (8)	366 (6)
H	7.3	702 (12)	798 (14)	---	---	---
F	9.2	912 (9)	985 (12)	---	---	---
G	13.6	1397 (12)	1474 (26)	---	---	---

Table IV-3. Comparisons of mean displacement volumes and mean calculated volumes (oriented parallel to video axis) for solid glass cylinders using a t-test (variances equal) or a modified t-test (variances unequal).

H_0: $u_1 = u_2$ H_a: $u_1 \neq u_2$
(individual $\alpha = 0.01$; overall $\alpha = 0.08$)

Cylinder	t_s or t'_s	p	
A	0.266	$p > 0.50$	
B	0.460	$p > 0.50$	
C	0.600	$p > 0.50$	
D	1.625	$p > 0.10$	
E	0.747	$p > 0.40$	
F	3.374	$0.02 < p < 0.05$	
G	2.689	$0.05 < p < 0.10$	
H	5.206	$0.001 < p < 0.01$	**

Table IV-4. Comparisons of pairs of mean calculated volumes (mm^3) for solid glass cylinders oriented parallel (v_0), at 10^o (v_{10}), at 20^o (v_{20}), and at 30^o (v_{30}) to the video axis. Test is the least significant difference method for planned comparisons among means (LSD). ** = significant at p = 0.05.

Cylinder		y_1 = v_0	v_{10}	v_{20}	v_{30}	LSD 0.05[20]
A	v_0	0				10.655
	v_{10}	3	0			
y_2 =	v_{20}	11**	8	0		
	v_{30}	34**	31**	23**	0	
B	v_0	0				6.984
	v_{10}	1	0			
y_2 =	v_{20}	3	2	0		
	v_{30}	11**	10**	8**	0	
C	v_0	0				6.447
	v_{10}	1	0			
y_2 =	v_{20}	5	4	0		
	v_{30}	15**	14**	10**	0	
D	v_0	0				4.435
	v_{10}	1	0			
y_2 =	v_{20}	3	2	0		
	v_{30}	7**	6**	4	0	
E	v_0	0				5.378
	v_{10}	1	0			
y_2 =	v_{20}	1	2	0		
	v_{30}	3	4	2	0	

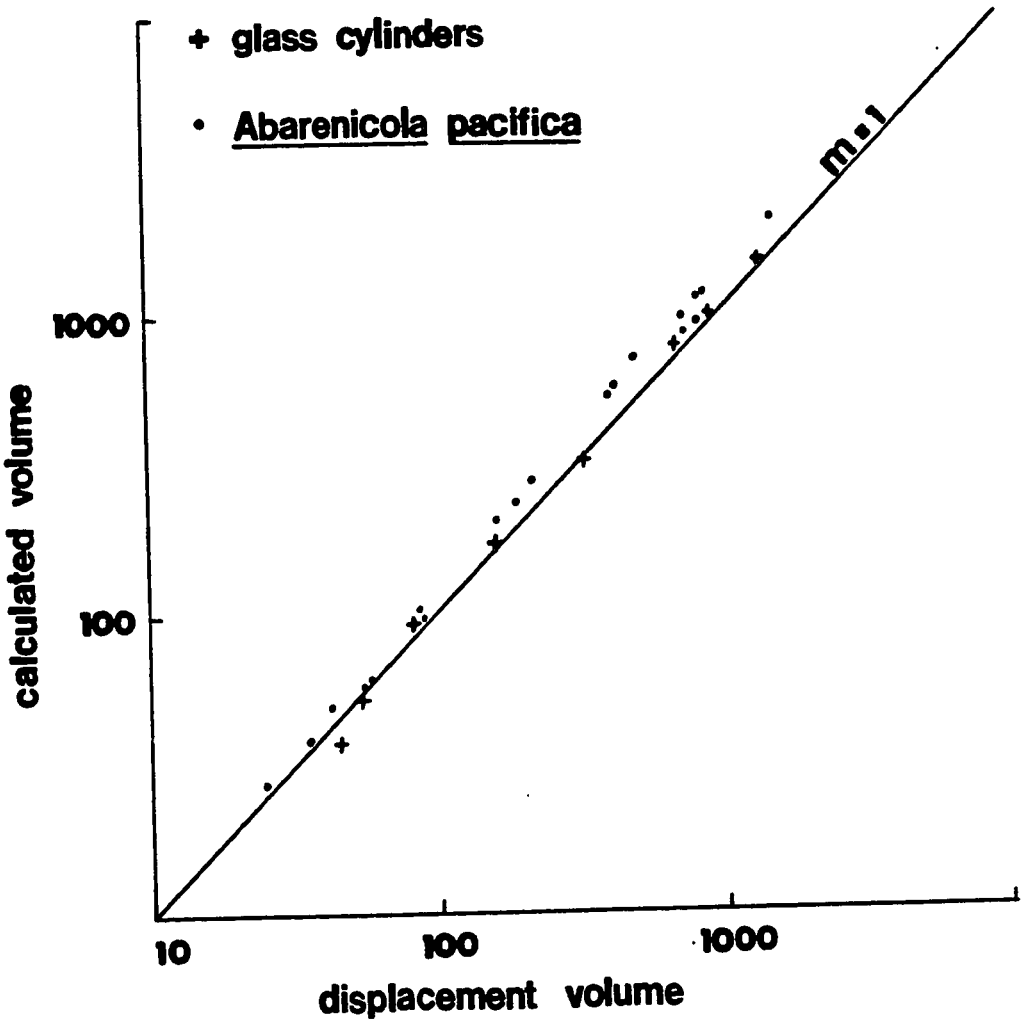

Figure IV-2. Volumes calculated from digitized, longitudinal cross-sections versus volumes measured by displacement for solid glass cylinders and Abarenicola pacifica (body volumes). Axes of cross-sections were oriented parallel to the axis of the video system. These data and their associated standard deviations are listed in Tables 2 (cylinders) and 5 (Abarenicola pacifica). All measurements are in mm^3.

volume suggesting that violations of the cylindrical assumption are more important in larger worms (Table 5). Larger worms are observed to be more dorso-ventrally flattened than smaller worms.

Body volumes are used in calculations of ratios of body volume to gut volume (B/G). Ratios of body volume to gut volume for Abarenicola pacifica range from two to six (median = 4) when determined as calculated body volume to gut volume; they range from two to five (median = 3) when determined as displacement body volume to gut volume. The medians are not significantly different (Wilcoxon two- sample test, $0.10 < p < 0.20$).

Multivariate analyses: A priori species groups

We expected deposit feeders and carnivores to differ in terms of general body and gut parameters (e.g., ratio of body volume to gut volume, ratio of gut length to diameter). Two a priori groups, deposit feeders (n = 354) and carnivores (n = 75), thus were identified and analyzed using discriminant analysis (direct method). Each individual dissected was treated as a separate case described by four measures, body volume (B), gut volume (G), gut length (L), and mean gut radius (R). Since body volumes and gut volumes ranged over five orders of magnitude, natural log transformations of B and G were used in this and all subsequent multivariate analyses. The ratio of B/G, body volume to gut volume, distinguishes deposit feeders from carnivores (Table 6). Median B/G for deposit feeders is 3 (95% C.L. = 3 to 4; range = 1 to 10), and median B/G for carnivores is 7.5 (95% C.L. = 5 to 11; range = 4 to 21).

Among the deposit feeders some of the intraspecific variation in B/G can be attributed to variations in degrees of gut fullness. The nonparametric trends test, Kendall's Tau, was used to examine correlations between percent gut fullness and B/G for eleven deposit-feeding species that exhibited the greatest intraspecific variations in B/G (i.e., range in B/G $\leq$ 4 units) (Table 7). In six of the eleven species tested there is a significant trend in increasing B/G with decreasing percent fullness ($p < 0.05$); the combination of

Table IV-5. Mean displacement volumes and mean calculated volumes for 20 individuals of Abarenicola pacifica. Each value represents the mean of five trials; standard deviations are given in parentheses. All measurements are in mm^3.

Worm #	Displacement volume	Calculated volume
33	25 (7)	28 (1)
24	36 (7)	42 (4)
32	43 (5)	49 (4)
25	56 (10)	56 (2)
03	60 (8)	63 (8)
62	92 (13)	97 (9)
44	89 (12)	195 (21)
05	167 (14)	209 (31)
42	195 (11)	234 (11)
18	221 (6)	280 (24)
35	408 (7)	543 (37)
02	429 (9)	578 (91)
46	506 (31)	714 (87)
12	762 (15)	864 (113)
39	852 (18)	932 (82)
48	754 (11)	980 (37)
08	752 (11)	984 (108)
60	846 (13)	1141 (232)
23	894 (25)	1196 (207)
04	1553 (11)	2054 (286)

Table IV-6. Results of discriminant analyses for a priori groups. Variables used in these analyses were body volume, gut volume, gut length and mean gut radius. The two volume measurements were transformed using natural logarithms. Each of the 429 individuals of the 41 species examined was treated as a separate case.

	Deposit feeders vs carnivores	Surface deposit feeders vs subsurface deposit feeders
A. Discriminating power of variables before generation of discriminant function		
Wilks lambda	0.48	0.94
Chi-square test (d.f. = 4)	315 ($p < 0.0001$)	23.20 ($p = 0.0001$)
B. Discriminant function		
Coefficients		
ln(body volume)	-8.22	-4.07
ln(gut volume)	7.86	3.35
gut length	0.08	0.74
gut radius	0.36	0.82
Eigenvalue	1.10	0.07
Percent of cases classified correctly	91	59

Table IV-7. Summary of results of tests for correlations between percent gut fullness and ratio of body volume to gut volume. Correlations were tested within each species using Kendall's Tau.

H_0: B/G is not correlated with percent gut fullness or B/G decreases as percent fullness increases.

H_A: B/G increases as percent fullness decreases.

Species	n	Range in fullness	%Range in B/G	z	p
Abarencola pacifica	23	8 - 100	2 - 5	4.67	0.00003
Amphicteis scaphobranchiata	16	32 - 95	2 - 5	1.18	0.12
Armandia maculata	10	0 - 90	2 - 6	3.15	0.0008
Capitella cf. capitata	10	0 - 53	3 - 7	1.85	0.03
Chaetozone cf. setosa	11	0 - 43	3 - 6	0.09	0.46
Cirratulus cirratus	10	0 - 55	2 - 5	0	0.50
Paraprionospio pinnata	10	63 - 95	3 - 7	2.05	0.02
Pseudopolydora kempi japonica	10	42 - 96	2 - 5	1.17	0.12
Scalibregma inflatum (NC)	10	0 - 99	3 - 10	1.90	0.03
Spiophanes cf. bombyx	10	0 - 91	3 - 9	0.95	0.17
Terebellides cf. stroemi (SDT)	10	26 - 99	2 - 6	2.63	0.004

Fisher's method for combining independent probabilities:

chi-square = 75.164, d.f. = 22, $p < 0.001$

probabilities for all eleven tests (Fisher's method for combining independent probabilities) is also significant ($p = 0.001$).

Twenty-four of the 354 individuals identified *a priori* as deposit feeders were grouped with the carnivores on the basis of their discriminant scores. No striking patterns emerge from examination of these "misclassified" deposit feeders; they are scattered among 13 species. The species with the highest number of misclassified individuals is *Scalibregma inflatum* (North Carolina) (misclassified = 4, n = 10). The dissected individuals of this species tended to have relatively empty guts. Fourteen of the 75 individuals identified *a priori* as carnivores were grouped with the deposit feeders on the basis of their discriminant scores. Twelve of these "misclassified" carnivores belong to two deep-sea species of carnivores, *Ceratocephale pacifica* (misclassified = 8, n = 10) and *Aglaophamus paucilamellata* (misclassified = 4, n = 6). These species also grouped consistently with deposit feeders in subsequent classification analyses.

Deposit feeders can be assigned to any number of groups based on any number of single criteria or combinations of criteria (e.g., functional guilds -- surface or subsurface feeders, motile or sedentary; sediment in guts -- sand, muddy sand, sandy mud, mud; environments -- intertidal, shallow subtidal, continental shelf, deep sea). Two *a priori* groups of deposit feeders, surface (n = 204) and subsurface (n = 150) deposit feeders, were examined using discriminant analysis (direct method; variables = lnB, lnG, L, R) (Table 6). These two groups can not be distinguished reliably using these general body and gut parameters. Since it was not obvious if or how these two groups should be subdivided further, classification analyses were used to identify species groups for subsequent discriminant analyses.

Multivariate analyses: Use of classification analyses to identify species groups

Computation time made it necessary to reduce the number of cases considered in these analyses. In earlier analyses each individual was treated as a separate case (n = 429); in these analyses each species, described by median values of gut parameters, was treated as a separate case (n = 41). The set of variables was expanded to include ratios of body volume to gut volume, (B/G), gut length to gut diameter (i.e., total aspect ratio, TAR), individual gut-section aspect ratios (length/diameter) and the volumes of individual gut sections expressed as percentages of total gut volume. These standardized variables were used because the initial classification results showed that species tended to cluster mostly on the basis of gut volume and body volume.

As few as one and as many as five anatomically-distinct gut sections were identified in the various species examined (Figure 3). A matrix of 41 species by 16 gut parameters was generated. Each species was described by B/G and TAR and some subset of the remaining 14 gut section parameters, Avol, AAR, Mvol, MAR, M_1vol, M_1AR, M_2vol, M_2AR, Pvol, PAR, P_1vol, P_1AR, P_2vol, and P_2AR (see Figure 3 for definitions). If, for example, two gut sections, an anterior section and a posterior section, were identified in a species (e.g., Fauveliopsis glabra, Figure 3) its gut was described in the matrix by the parameters B/G, TAR, Avol, AAR, Pvol and PAR, and zeroes were entered in the matrix for all other parameters. If no distinct gut sections were identified in a species (e.g., Pseudopolydora kempi japonica, Figure 3) its gut was described in the matrix by the parameters B/G, TAR, Pvol, and PAR, where Pvol = total gut volume and PAR = TAR; zeroes were entered for all other parameters.

The groupings identified in each of the two parallel classification analyses, "Euclidean" analysis and "Canberra" analysis, were examined pairwise using stepwise discriminant analysis to identify which of the 16 gut parameters were most important in distinguishing groups at each branching point. We began these analyses with the most dissimilar groups and worked towards the most

Figure IV-3. Representative gut schematics with sections identified on the basis of gross anatomical characteristics. (a) One gut section; example = Pseudopolydora kempi japonica. (b) Two gut sections; example = Fauveliopsis glabra. (c) Three gut sections; example = Abarenicola pacifica; (d) Five gut sections; example = Eupolymnia heterobranchia. The anterior-most section in species with $\geq$ 2 anatomically-distinct sections is coded "anterior section" and is described by the parameters Avol, anterior section volume relative to total gut volume, and AAR, anterior section aspect ratio. The middle section in species with three gut sections is coded "middle section" and described by parameters Mvol, relative section volume, and MAR, section aspect ratio. When the middle section can be subdivided into 2 distinct subsections and when the posterior-most of the middle subsections is a thick-walled, muscular chamber (e.g., terebellids and trichobranchids), the 2 middle subsections are coded "anterior middle section" (parameters M_1vol and M_1AR) and "posterior middle section" (parameters M_2vol and M_2AR). When the middle section can be divided into 2 subsections, but the posterior-most of these subsections is not a muscular chamber (e.g., Abarenicola vagabunda, Travisia foetida), the 2 subsections are coded "anterior middle section" (parameters M_1vol and M_1AR) and "middle section" (parameters Mvol and MAR). This combination of codes indicates that the posterior middle gut subsection is not a muscular chamber but resembles instead the middle gut section seen in species with three gut sections. The entire gut in species with no anatomically-distinct gut sections and the posterior-most section in species with 2 or 3 gut sections are all coded "posterior section" (parameters Pvol and PAR). When the posterior gut can be divided into 2 anatomically-distinct subsections the subsections are coded "anterior posterior section" (P_1vol and P_1AR) and "posterior posterior section" (P_2vol and P_2AR).

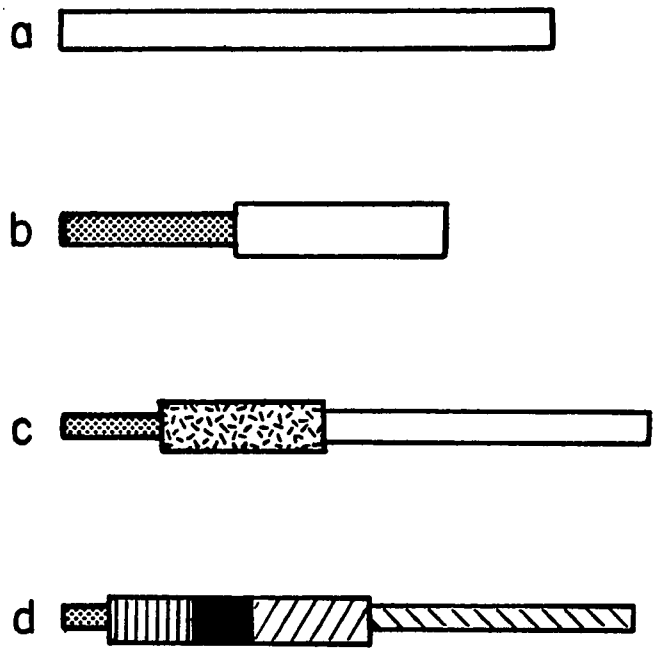

Parameters	Gut Sections
Avol, AAR	anterior
Mvol, MAR	middle
M_1vol, M_1AR	middle (anterior subsection)
M_2vol, M_2AR	middle (posterior subsection)
Pvol, PAR	posterior
P_1vol, P_1AR	posterior (anterior subsection)
P_2 vol, P_2AR	posterior (posterior subsection)

similar groups (i.e, increasing number of groups, decreasing group sizes) until the results of discriminant analysis indicated that groups could not be reliably distinguished on the basis of the variables provided. Seven groups can be distinguished in the Euclidean analysis, and six groups can be distinguished in the Canberra analysis, but biological interpretations of the distinctions among these groups are not strikingly clear or consistent across both analyses (Figure 4 and Table 8, Figure 5 and Table 9).

We identified groups of species that clustered together consistently using both classification methods (Tables 8 and 9). A subset of 26 species falling into four groups was thus selected and examined using stepwise discriminant analysis (Table 10). The biological interpretation of the results of this discriminant analysis is quite clear: These 26 species are grouped on the basis of general feeding strategy (i.e., carnivores vs deposit feeders) and gut structure (i.e., numbers and types of individual gut sections identified using gross anatomical characteristics). The four groups can be described in general terms as (1) carnivores (Figure 6), (2) deposit feeders with more or less simple tubular guts, i.e., species with guts characterized by only one or two anatomically-distinct sections (Figure 7), (3) deposit feeders with three anatomically-distinct gut sections, i.e., species with guts characterized by anatomically-distinct fore, mid, and hindguts (Figure 8), and (4) deposit feeders with four or five anatomically-distinct gut sections, i.e., species in which the midgut and/or hindgut can be further subdivided into anatomically-distinct subsections (Figure 9).

We changed the group assignments of three of the 26 species when the results of the discriminant analysis suggested they were misclassified initially. Abarenicola pacifica was reassigned to group 3; Armandia agilis and Fauveliopsis glabra were both reassigned to group 2. We then assigned the remaining 15 species to the four groups on the basis of their affinities in the classification analyses that were used to select the initial subset of 26 species. These final four groups (n = 41 species) (Table 11) were examined using stepwise

Figure IV-4. Groups generated by classification analysis (Euclidean method) and analyzed by discriminant analyses (stepwise Wilks method). Dissimilarity measure is squared Euclidean distance. Results of discrminant analysis (eigenvalue of discriminant function, percent of cases classified correctly by the discriminant function, and important differences between groups are given for each branching point. Species in Groups A - G are listed in Table 8. B/G = ratio of body volume to gut volume. Avol = volume of anterior gut section. Pvol = volume of posterior gut section. TAR = total gut aspect ratio. MAR = aspect ratio of middle gut section. PAR = aspect ratio of posterior gut section. See Figure 3 for definitions of gut sections.

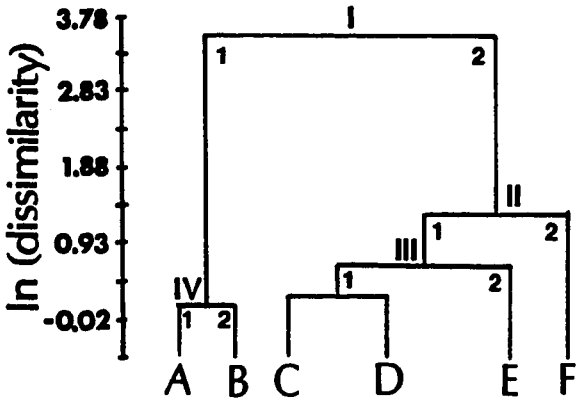

Results of discriminant analyses

I. Discriminant function: eigenvalue = 0.353; 78% classified correctly.
   1. Species with 1 posterior gut section and larger Avol IV
   2. Species with 2 posterior sections and smaller Avol II

II. Discriminant function: eigenvalue = 1.017; 86% classified correctly.
   1. Smaller MAR, Mvol, PAR III
   2. Larger MAR, Mvol, PAR . . . . . .Group F

III. Discrminant function: eigenvalue = 748; 100% classified correctly.
   1. Species with 4 or 5 gut sections . . . . . Groups C and D
   2. Species with $\leq$ 3 gut sections . . . . . .Group E

IV. Discriminant function: eigenvalue = 0.479; 74% classified correctly.
   1. Smaller B/G, MAR, Mvol . . . . . .Group A
   2. Larger B/G, MAR, Mvol . . . . . .Group B

Table IV-8. Species groups identified using classification analysis (Euclidean method). Relationships among groups indicated in Figure 4. Superscripts 1, 2, 3, 4 indicate species that grouped together in both classification analyses (Euclidean and Canberra methods) and identify the species subset and groups used in subsequent analyses.

GROUP A

[2]*Armandia maculata*
[2]*Levinsenia oculata*
[2]*Pseudopolydora kempi japonica*
Paraprionospio pinnata
[2]*Tharyx multifilis*
Cirratulus cirratus
[2]*Capitella* cf. *capitata*
[2]*Ceratocephale pacifica*
[2]*Aglaophamus paucilamellata*
[2]*Ophiodromus pugettensis*
[2]*Abarenicola pacifica*
[2]*Sternaspis fossor*

GROUP B

[1]*Nephtys* spp.
[1]*Nephtys picta*
[1]*Glycera dibranchiata*
Glycera americana
Euclymene reticulata
Harmothoe extenuata

GROUP C

Thelepus crispus
Polycirrus eximius
Spiophanes cf. *bombyx*
Terebellides stroemi (NC)

GROUP D

Tharyx luticastellus
Chaetozone cf. *setosa*

GROUP E

Abarenicola vagabunda
Travisia foetida

GROUP F

[3]*Armandia agilis*
Ophelina acuminata
[3]*Fauveliopsis glabra*
[3]*Scalibregma inflatum* (PS)
[3]*Scalibregma inflatum* (NC)
Sternaspis scutata
[3]*Artacamella hancocki*
[3]*Anobothrus* sp. A
[3]*Ecamphicteis elongata*
[3]*Ampharete acutifrons*
[3]*Ampharete americana*
[3]*Amphicteis scaphobranchiata*

GROUP G

[4]*Neoamphitrite robusta*
[4]*Terebellides* cf. *stroemi* (SDT)
[4]*Eupolymnia heterobranchia*

Figure IV-5. Groups generated by classification analysis (Canberra method) and analyzed by discriminant analyses (stepwise Wliks method). Dissimilarity measure is the Canberra metric coefficient (natural logs of coefficients used for purposes of figure). Results of discriminant analysis (eigenvalue of the discriminant function, percent of cases classified correctly by the function, and important differences between groups) are given for each branching point. The branching point for groups C and D was not analyzed because there is only one species in group C -- groups C and D can be considered essentially one group. Species in groups A - F are listed in Table 9. B/G = ratio of body volume to gut volume. Avol = volume of anterior gut section. Mvol = volume of middle gut section. MAR = aspect ratio of middle gut section. PAR = aspect ratio ot posterior gut section. See Figure 3 for definitions of gut sections

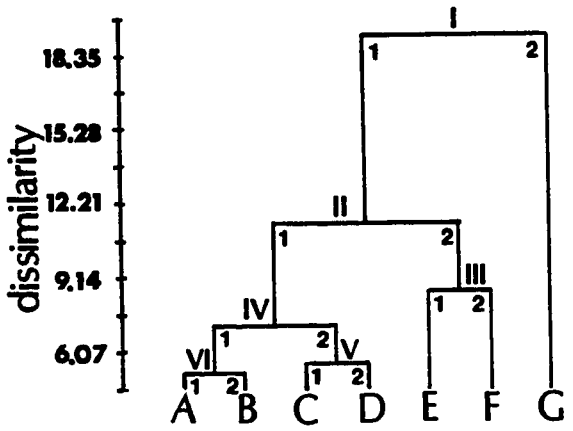

Results of discriminant analyses

I. Discriminant function: eigenvalue = 30,368; 100% classified correctly
   1. One posterior gut section II
   2. Two posterior gut sections . . . . . Group G

II. Discriminant function: eigenvalue = 3.545; 95% classified correctly.
   1. One or two gut sections; larger PAR and Avol IV
   2. Three or four gut sections; smaller PAR and Avol III

III. Discriminant function: eigenvalue = 7.179; 100% classified correctly
   1. Smaller TAR, MAR, PAR . . . . . .Group E
   2. Larger TAR, MAR, PAR . . . . . .Group F

IV. Discriminant function: eigenvalue = 1.020; 88% classified correctly.
   1. Species without 2 middle gut sections VI
   2. Most species with 2 middle gut section V

V. Discriminant function: eigenvalue = 1165; 100% classified correctly.
   1. Larger Avol; smaller Pvol . . . . . .Group C
   2. No middle gut section distinguished;
      smaller Avol; larger Pvol . . . . . .Group D

VI. Discriminant function: eigenvalue = 1.443; 88% classified correctly.
   1. Smaller B/G, TAR . . . . . .Group A
   2. Larger B/G, TAR . . . . . .Group B

Table IV-9. Species groups identified using classification analyses (Canberra method). Relationships among groups indicated in Figure 5. Superscripts 1, 2, 3, 4 indicate species that grouped together in both classification analyses (Euclidean and Canberra) and identify the species subset and groups used in subsequent analyses.

GROUP A

[2]Armandia maculata
[2]Levinsenia oculata
[2]Pseudopolydora kempi japonica
[2]Tharyx multifilis
Chaetozone cf. setosa
[2]Capitella cf. capitata
[2]Ceratocephale pacifica
[2]Aglaophamus paucilamellata
[2]Ophiodromus pugettensis
[2]Abarenicola pacifica
[2]Sternaspis fossor
Sternaspis scutata
Travisia foetida
Terebellides stroemi (NC)
Polycirrus eximius
Glycera americana

GROUP B

[1]Nephtys spp.
[1]Glycera dibranchiata
[1]Nephtys picta
[3]Anobothrus sp. A
[3]Ecamphicteis elongata
[3]Artacamella hancocki
[3]Amphicteis scaphobranchiata
[3]Armandia agilis
[3]Scalibregma inflatum (NC)
[3]Scalibregma inflatum (PS)
Paraprionospio pinnata

GROUP C

Abarenicola vagabunda

GROUP D

[4]Neoamphitrite robusta
[4]Eupolymnia heterobranchia
[4]Terebellides cf. stroemi (SDT)

GROUP E

[3]Fauveliopsis glabra
[3]Ampharete acutifrons
[3]Ampharete americana
Spiophanes cf. bombyx
Tharyx luticastellus
Harmothoe extenuata

GROUP F

Thelepus crispus
Ophelina acuminata
Euclymene reticulata

Table IV-10. Discriminant analysis: Subset of 26 species divided into four groups based on classification analyses. Species in this subset and group assignments in Tables 8 and 9. See Figure 3 for definitions of variable name abbreviations.

	Discriminant function		
	I	II	III
A. Discriminating power of variables before function generated			
Wilks lambda	0.00003	0.071	0.463
Chi-square	196	50	14.62
probability	<< 0.0001	<< 0.0001	0.023
B. Discriminant functions			
Eigenvalue	2181	5.51	1.16
Discriminating variables and coefficients			
B/G	-0.09	0.69	-0.60
TAR	-0.46	0.95	-0.06
AAR	0.86	-0.64	0.68
P_2AR	-1.64	0.24	0.10
Mvol	5.95	-0.52	2.26
M_2vol	-2.12	-0.40	0.15
P_1vol	1.38	0.53	0.21
Pvol	5.91	0.05	3.04

C. Percent species classified correctly (i.e., assigned to a priori groups) by these discriminant functions = 88%

Table IV-10. - continued

D. Group means

	Group			
	1	2	3	4
Discriminating variables				
B/G	8.3	4.0	3.5	3.5
TAR	83.7	49.1	28.1	45.7
AAR	0	5.2	6.2	8.7
P_2AR	0	0	0	21.5
Mvol	0	9.5	50.5	13.3
M_2vol	0	0	0	14.3
P_1vol	8.8	0	0	42.7
Pvol	91.2	86.6	39.7	0

Figure IV-6. Gut schematics: carnivores. To facilitate visual comparisons of gut architectures and relative gut dimensions gut lengths and diameters are drawn with respect to a standard volume. One standard volume was used to generate all gut schematics (Figures 6 - 9). Actual gut volumes (median value for each species in mm^3) are given in parentheses. (a) Glycera spp. (G. americana and G. dibranchiata). m = thick-walled, muscular section immediately posterior to the pharyngeal sheath. This gut section is unique to Glycera spp. among the 42 species examined. (b) Ophiodromus pugettensis; (c) Harmothoe extenuata; (d) Nephtys spp. (N. caeca and N. caecoides); (e) Nephtys picta; (f) Aglaophamus paucilamellata; (g) Ceratocephale pacifica.

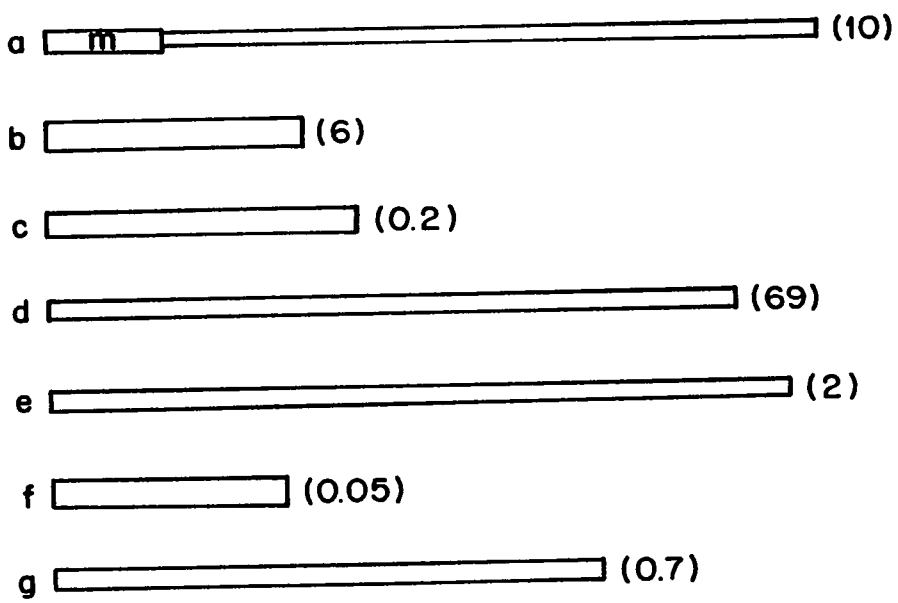
a
m
(10)
b
(6)
c
(0.2)
d
(69)
e
(2)
f
(0.05)
g
(0.7)

Figure IV-7. Gut schematics: deposit feeders with simple, tubular guts (1 or 2 anatomically-distinct sections). To facilitate visual comparisons gut lengths and diameters are drawn with respect to a standard volume. One standard volume was used to generate all gut schematics (Figures 6 - 9). Actual gut volumes (species medians in mm^3) are given in parentheses. (a) Armandia maculata; (b) Armandia agilis; (c) Cirratulus cirratus; (d) Tharyx multifilis; (e) Tharyx luticastellus; (f) Chaetozone cf. setosa; (g) Fauveliopsis glabra; (h) Capitella cf. capitata; (i) Pseudopolydora kempi japonica; (j) Paraprionospio pinnata, b = muscular gut bulb observed in P. pinnata and Spiophanes cf. bombyx, 2 of 3 spionids examined; (k) Spiophanes cf. bombyx, b = muscular gut bulb; (l) Euclymene reticulata; (m) Levinsenia oculata.

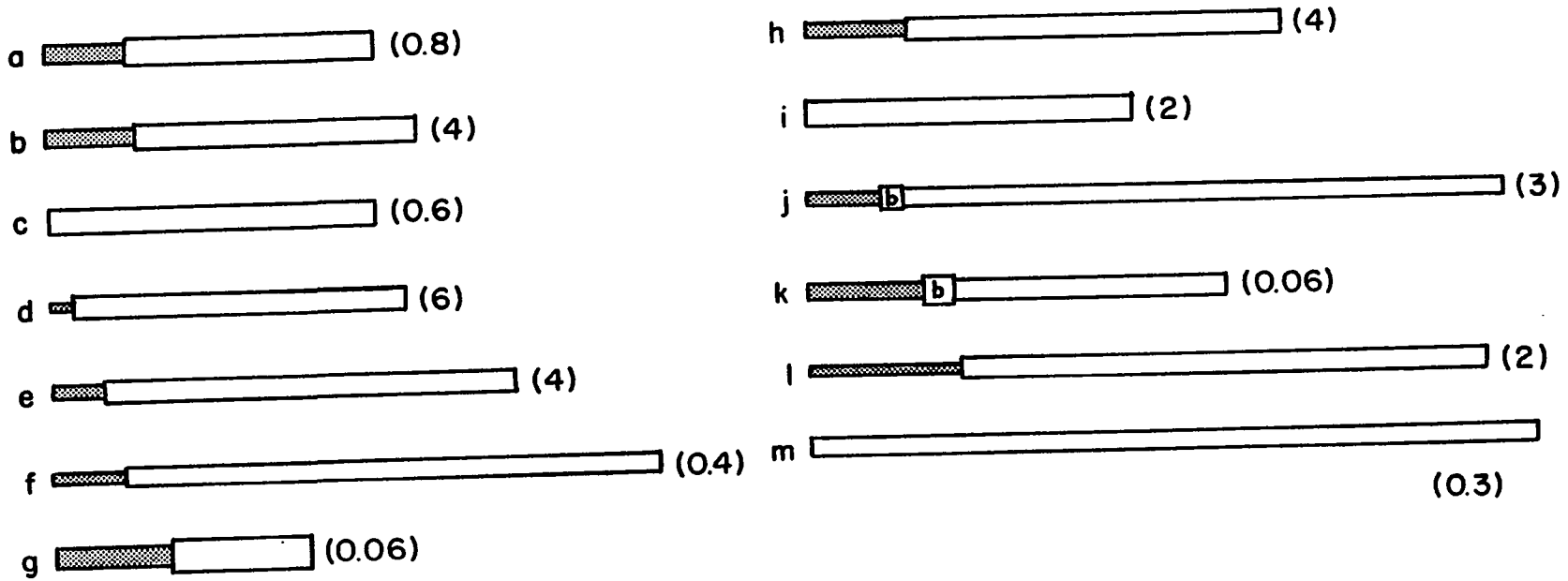
a
(0.8)
b
(4)
c
(0.6)
d
(6)
e
(4)
f
(0.4)
g
(0.06)
h
(4)
i
(2)
j
b
(3)
k
b
(0.06)
l
(2)
m
(0.3)

Figure IV-8. Gut schematics: deposit feeders with three antomically-distinct gut compartments. To facilitate visual comparisons gut lengths and diameters are drawn with respect to a standard volume. One standard volume was used to generate all gut schematics (Figures 6 - 9). Actual gut volumes (species medians in mm^3) are given in parentheses.
(a) Abarenicola pacifica; (b) Ophelina acuminata; (c) Scalibregma inflatum (PS); (d) Scalibregma inflatum (NC); (e) Sternaspis scutata; (f) Sternaspis fossor; (g) Amphicteis scaphobranchiata; (h) Ampharete acutifrons; (i) Ampharete americana; (j) Anobothrus sp. A; (k) Ecamphicteis elongata; (l) Artacamella hancocki.

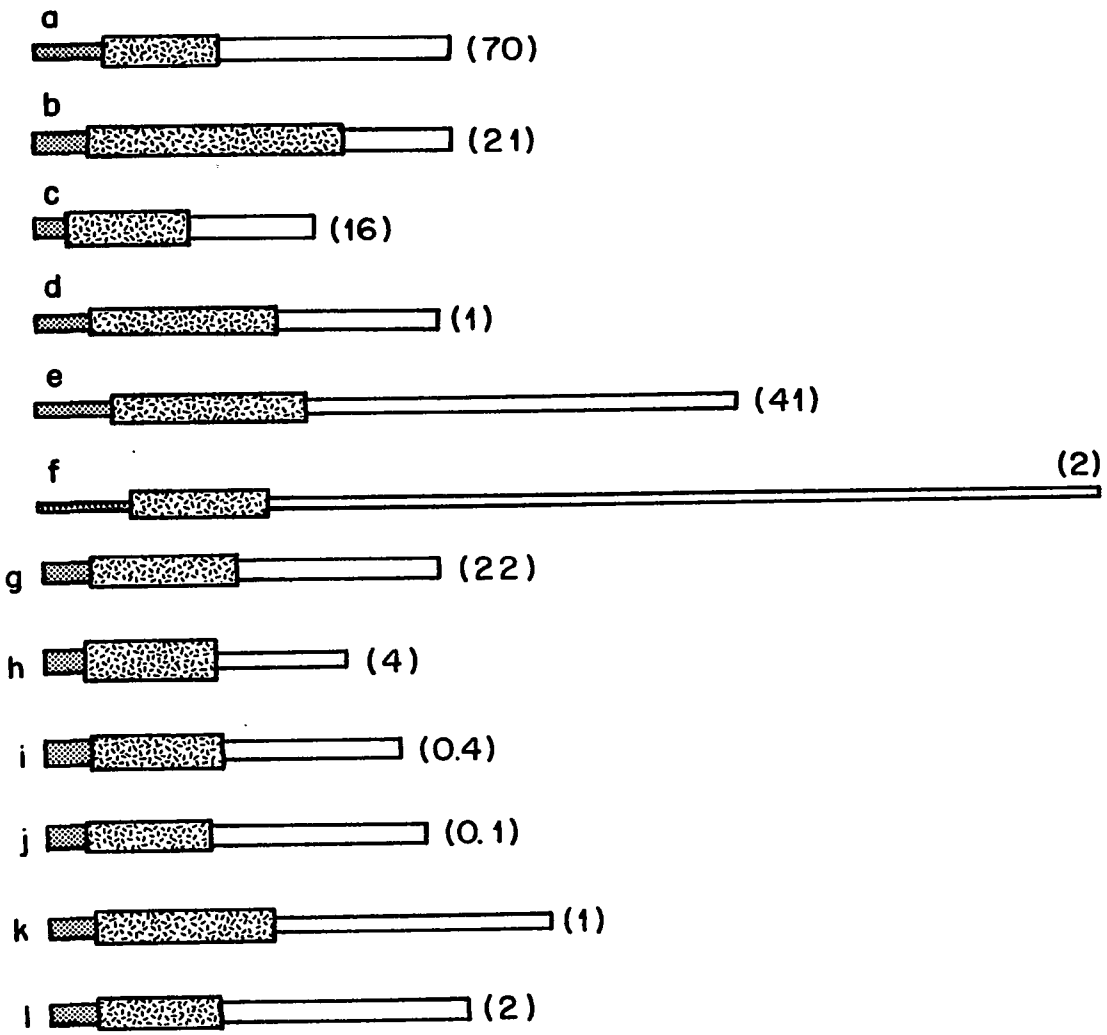
a
(70)
b
(21)
c
(16)
d
(1)
e
(41)
f
(2)
g
(22)
h
(4)
i
(0.4)
j
(0.1)
k
(1)
l
(2)

Figure IV-9. Gut schematics: deposit feeders with four or five anatomically-distinct gut sections. To facilitate visual comparisons gut lengths and diameters are drawn with respect to a standard volume. One standard volume was used to generate all gut schematics (Figures 6 - 9). Actual gut volumes (species medians in mm^3) are given in parentheses. (a) Polycirrus eximius; (b) Thelepus crispus; (c) Eupolymnia heterobranchia; (d) Neoamphitrite robusta; (e) Terebellides stroemi (NC). Only 3 anatomically-distinct gut sections were identified in T. stroemi (NC), but it is included in this group based on the results of the classification analyses and the anatomical similarities of its gut to T. stroemi (SDT) and the terebellids. (f) Terebellides cf. stroemi (SDT); (g) Travisia foetida; (h) Abarenicola vagabunda.

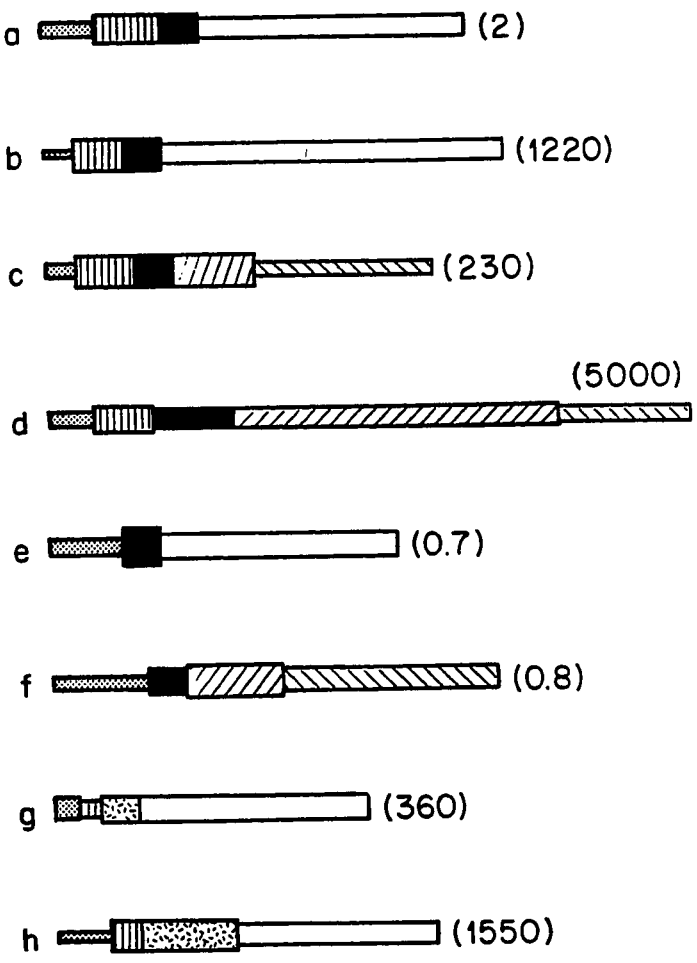
a
(2)
b
(1220)
c
(230)
(5000)
d
e
(0.7)
f
(0.8)
g
(360)
h
(1550)

Table IV-11. Species grouped by gut architecture. In cases where our predicted group assignments differ from assignments determined using classification analyses the classification assignments are given in parentheses. Bvol = body volume. Gvol = median gut volume. All volumes are measured in mm^3. B/G = median ratio of body volume to gut volume. TAR = median total gut aspect ratio. Environment (E): N = intertidal and shallow subtidal; H = continental shelf; D = deep sea. Qualitative description of sediment in gut (S): S = sand; MS = muddy sand; SM = sandy mud; M = mud.

Species	E	S	Bvol range	Gvol	B/G	TAR
GROUP 1: Carnivores						
Nephtys spp.	N	-	450 - 21000	69	11.7	84
Glycera dibranchiata	H	-	10 - 170	10	6.5	82
G. americana	H	-	40 - 200	10	9.8	99
Ophiodromus pugettensis (2)	N	-	25 - 95	6	6.5	16
Nephtys picta	H	-	4 - 50	2	6.6	85
Harmothoe extenuata	H	-	0.3 - 10	0.2	12.9	21
Ceratocephale pacifica (2)	D	-	0.2 - 9	0.7	4.7	57
Aglaophamus paucilamellata (2)	D	-	0.2 - 2	0.05	6.4	15
GROUP 2: Deposit feeders with simple, tubular guts						
Capitella cf. capitata	N	M	2 - 300	4	5.5	48
Euclymene reticulata	D	M	2 - 40	2	3.8	76
Armandia agilis	H	S	0.1 - 40	4	2.7	36
Armandia maculata	H	S	0.1 - 30	0.8	2.9	26
Tharyx multifilis	N	M	4 - 25	6	2.5	32
Paraprionospio pinnata	H	M	8 - 20	3	4.3	87
Cirratulus cirratus	N	M	1 - 14	0.6	1.9	18
Pseudopolydora kempi japonica	N	S	2 - 8	2	2.4	29
Tharyx luticastellus	D	M	3 - 8	4	1.2	40
Chaetozone cf. setosa	D	M	0.1 - 3	0.4	4.0	65
Fauveliopsis glabra	D	M	1 - 3	0.06	5.1	23
Spiophanes cf. bombyx (3)	D	M	0.2 - 2	0.06	4.0	31
Levinsenia oculata	D	M	0.3 - 1	0.3	2.4	83

Table IV-11. - continued

Species	E	S	Bvol range	Gvol	B/G	TAR
GROUP 3: Deposit feeders with three gut compartments						
Abarenicola pacifica	N	S	10 - 1550	70	2.8	43
Sternaspis scutata	N	M	15 - 280	41	2.7	72
Amphicteis scaphobranchiata	N	M	10 - 250	22	3.8	30
Ophelina acuminata	N	M	50 - 170	21	3.2	37
Artacamella hancocki	D	M	1 - 100	2	2.0	30
Scalibregma inflatum (PS)	D	M	20 - 70	16	1.9	19
Ampharete acutifrons	H	M	0.4 - 40	4	3.9	24
Ampharete americana	H	M	1 - 20	0.4	4.3	24
Scalibregma inflatum (NC)	H	S	2 - 16	1	4.4	26
Sternaspis fossor (2)	D	M	4 - 12	2	3.8	142
Ecamphicteis elongata	D	M	1 - 6	1	3.2	45
Anobothrus sp. A	D	M	0.1 - 1	0.1	3.6	24
GROUP 4: Deposit feeders with four or five gut compartments						
Neoamphitrite robusta	N	M	15000-24000	5000	4.4	65
Abarenicola vagabunda	N	S	2000-20000	1550	3.1	35
Thelepus crispus	N	SM	3500-5600	1220	3.9	40
Travisia foetida	D	M	4-4000	360	2.4	23
Eupolymnia heterobranchia	N	S	100-680	230	3.3	28
Terebellides cf. stroemi (SDT)	D	M	0.3-70	0.8	2.8	44
Polycirrus eximius	H	MS	1-38	2	3.0	32
Terebellides stroemi (NC)	H	MS	1-12	0.7	3.7	31

discriminant analysis (Table 12).

Interspecific patterns in body and gut parameters

Based on the individuals that were examined, the 41 species in this study can be partitioned into five general body size categories: (1) species with maximum observed body volumes $\leq$ 10 mm^3, (2) 10 to 100 mm^3, (3) 100 to 1000 mm^3, (4) 1000 to 10,000 mm^3 and (5) > 10,000 mm^3. There appears to be an upper limit on body size for depost feeders with simple, tubular, uncompartmentalized guts (Table 13). There is, however, no lower limit on body size for deposit feeders with compartmentalized guts. Carnivores come in all sizes.

We expected that deep-sea deposit feeders would have longer and narrower guts, i.e., greater total gut aspect ratios and/or greater standardized gut lengths, than deposit feeders from nearshore or shelf regions. Tests of this hypothesis must be limited to comparisons of closely-related taxa within groups defined on the basis of similarities in gut architecture. Comparisons thus are possible among the cirratulids, the spionids, the sternaspids, the trichobranchids, and the ampharetids and terebellids in group 3, but not, for example, among the opheliids. The four species of opheliids examined fall into three different gut-architecture groups. Median values of total gut aspect ratio (i.e., gut length divided by mean gut diameter) and standardized gut length (i.e., a relative measure of gut length adjusted for differences in body size) were used for each species (Table 14). These comparisons suggest that deep-sea species tend to have longer guts than nearshore and shelf species, but the results are not striking.

Intraspecfic patterns in body and gut parameters

Morphometric relationships between gut volume and body volume and between mean gut diameter and total gut length were examined for each species using parametric regression analyses (Nie et al. 1975). Regressions of gut volume versus body volume are significant in all cases: gut volume increases with body volume (overall F for regression: $p \leq 0.01$ for 37 species; $p \leq 0.05$ for 3 species; $p = 0.07$

Table IV-12. Discriminant analyses: Forty-one species assigned to four groups. Species names and group assignments listed in Table 11. In a few cases group assignments for species determined using classification analyses differ from our predicted assignments. We performed discriminant analyses twice, once with classification assignmemts and once with predicted assignments, and the results were almost identical; one additional discriminating variable was added to the list when predicted assignments were used (indicated with *). The results of the analysis using predicted assignments are given here. In both analyses 100% of the species were classified correctly by the discriminant functions.

	Discriminant function		
	I	II	III
A. Discriminating power of variables before function generated			
Wilks lambda	0.0008	0.020	0.261
Chi-square	237	129	44
probability	<< 0.0001	<< 0.0001	<< 0.0001
B. Discriminant functions			
Eigenvalue	25	12	2.8
Discriminating variables and coefficients			
B/G	-0.29	-0.07	0.87
TAR	0.26	-0.45	0.25
AAR	0.13	0.42	-0.62
M_1AR	0.85	1.32	0.24
M_2AR	-0.21	0.70	-0.30
Avol	0.04	-0.68	-0.34
Mvol	1.32	-0.12	0.22
M_1vol^*	-0.58	0.47	0.02
M_2vol	0.85	1.23	0.40
P_2vol	0.44	0.43	0.35

Table IV-12. - continued

C. Group means

	Group			
	1	2	3	4
Discriminating variables				
B/G	8.1	3.3	3.3	3.3
TAR	57.4	45.7	43.0	37.2
AAR	0	9.0	6.8	7.8
M_1AR	0	0	0	0.6
M_2AR	0	0.3	0	2.8
Avol	0	8.2	7.6	4.5
Mvol	0	0	61.2	16.8
M_1vol	0	0	0	2.5
M_2vol	0	1.0	0	12.0
P_2vol	0	0	0	9.5

Table IV-13. Matrix of species grouped by characteristics of gut architecture and maximum body volume observed among the individuals used in this study.

	Maximum body volume (mm^3)				
Species group	< 10	$10 - 10^2$	$10^2 - 10^3$	$10^3 - 10^4$	$>10^4$
Deposit feeders with simple, tubular guts	6	7	1		
Deposit feeders with 3 gut compartments	2	5	3	1	
Deposit feeders with 4 or 5 gut compartments	---	3	1	2	2
Carnivores	2	3	2	---	1

Table IV-14. Comparisons of median total gut aspect ratios (TAR) and median standardized gut lengths (SL): nearshore and shelf species versus deep-sea species. The numbers of species are too small in most cases to allow statistical comparisons.

Species	TAR	SL
Cirratulidae		
Nearshore		
Cirratulus cirratus	18	45
Tharyx multifilis	32	49
Deep sea		
Tharyx luticastellus	40	64
Chaetozone cf. *setosa*	65	84
Sternaspidae		
Nearshore		
Sternaspis scutata	72	91
Deep sea		
Sternaspis fossor	142	149
Trichobranchidae		
Shelf		
Terebellides stroemi (NC)	31	47
Deep sea		
Terebellides cf. *stroemi*	44	60
Spionidae		
Nearshore and shelf		
Pseudopolydora kempi japonica	29	45
Paraprionospio pinnata	87	97
Deep sea		
Spiophanes cf. *bombyx*	31	58

Table IV-14. - continued

Species	TAR	SL
Ampharetidae and Terebellidae (Group 3)		
Nearshore and shelf		
Amphicteis scaphobranchiata	30	51
Ampharete acutifrons	24	39
Ampharete americana	24	46
Deep sea		
Ecamphicteis elongata	45	65
Anobothrus sp A.	24	49
Artacamella hancocki	30	54

Results of Wilcoxon two-sample tests for nearshore and shelf versus deep-sea ampharetids and terebellids:

I. H_0: Median TAR for nearshore and shelf species is equal to or greater than median TAR for deep-sea species.

H_A: Median TAR for nearshore and shelf species is less than median TAR for deep-sea species.

Results: probability > 0.10

II. H_0: Median SL for nearshore and shelf species is equal to or greater than median SL for deep-sea species.

H_A: Median SL for nearshore and shelf species is less than median SL for deep-sea species.

Results: probability = 0.10

for 1 species). Slopes and intercepts are significantly different from zero in only five cases (F-tests for slope and intercept: individual probabilities $\leq$ 0.10 and sum of probabilities $\leq$ 0.10; Table 15). These regression results indicate that the ratio of body volume to gut volume remains constant as body volume increases in most of the species examined. It tends to increase as body volume increases in three species, Terebellides stroemi (NC), Ampharete americana, and Spiophanes cf. bombyx. It tends to decrease as body volume increases in two species, Euclymene reticulata and Aglaophamus paucilamellata. These patterns must be interpreted with caution. Given an alpha level of 0.10, five of 41 cases would be expected to be significant merely on the basis of chance (z-approximation for binomial test, $p = 0.32$).

Regressions of mean gut diameter versus gut length are significant in 33 cases: mean gut diameter increases with gut length (overall F for regression: $p \leq 0.01$ for 26 species; $p \leq 0.05$ for 3 species; $p \leq 0.10$ for 5 species). Slopes and intercepts are significantly different from zero in 18 of these 33 species (F-tests for slope and intercept: individual probabilities < 0.10 and sum of probabilities ≤ 0.10; Table 15). These regression results indicate that the ratio of gut length to mean diameter (TAR, total aspect gut ratio) tends to increase as gut length increases in each of the 18 species. These 18 species include four of the eight carnivores and seven of the eleven deep-sea deposit feeders examined. Of the seven nearshore or shelf deposit feeders included among the 18 species, five species live in muddy environments.

DISCUSSION

Evaluation of the video method for determining volumes

Reasonable estimates of body and gut volumes are obtained from computations using digitized, longitudinal cross-sectional outlines with the assumption that bodies or guts are cylindrical in tranverse cross-sections. Deviations of the body or gut axis from orientations parallel to the video axis are a lesser source of error in the volume estimates than are deviations from the assumption that the body or gut

Table IV-15. Results of within-species regression analyses: Gut volume versus body volume and mean gut diameter versus gut length. Regression coefficient (slope) = m; regression constant (y-intercept) = b. F-test probability for slope = p_m; F-test probability for intercept = p_b.

(1) H_0: slope = 0; H_A: slope $\neq$ 0.

(2) H_0: y-intercept = 0; H_A: y-intercept $\neq$ 0.

Species	n	m	p_m	b	p_b
A. Gut volume versus body volume					
Ampharete americana	10	0.151	< 0.001	0.113	0.001
Terebellides stroemi (NC)	12	0.219	< 0.001	0.142	0.089
Spiophanes cf. bombyx	10	0.122	< 0.001	0.024	0.018
Euclymene reticulata	10	0.413	< 0.001	-0.686	0.002
Aglaophamus paucilamellata	6	0.179	< 0.001	-0.007	0.100
B. Mean gut diameter versus gut length					
Capitella cf. captitata	10	0.007	0.094	0.389	0.016
Euclymene reticulata	10	0.010	< 0.001	0.714	0.004
Cirratulus cirratus	10	0.014	0.073	0.256	0.005
Chaetozone cf. setosa	11	0.009	0.008	0.076	0.062
Anobothrus sp. A	9	0.011	0.002	0.133	< 0.001
Eupolymnia heterobranchia	12	0.018	0.001	0.914	0.007
Artacamella hancocki	8	0.019	< 0.001	0.114	0.073
Scalibregma inflatum (PS)	23	0.027	0.006	0.512	0.005
Scalibregma inflatum (NC)	10	0.012	0.049	0.206	0.009
Sternaspis scutata	13	0.008	< 0.001	0.352	< 0.001
Sternaspis fossor	6	0.004	0.009	0.094	0.044
Paraprionospio pinnata	10	0.006	0.077	0.189	0.065
Spiophanes cf. bombyx	10	0.012	0.005	0.073	0.002
Fauveliopsis glabra	10	0.029	< 0.001	0.078	0.010
Ceratocephale pacifica	10	0.013	< 0.001	0.065	0.001
Harmothoe extenuata	10	0.034	< 0.001	0.042	0.007
Nephtys picta	10	0.005	0.003	0.175	< 0.001
Ophiodromus pugettensis	10	0.027	0.001	0.385	0.001

is cylindrical in cross-section. This second source of error is most important in computations of body volume. It can be mitigated by assuming an elliptical, transverse cross-section with the major axis of the ellipse defined by the mean radius of a dorsal, longitudinal cross-section and the minor axis of the ellipse defined by the mean radius of a lateral longitudinal cross-section.

The displacement method could be used only for measuring body volumes of individuals greater than about 30 mm^3 body volume. The video method is more accurate for body volumes of smaller individuals, and is suitable for measuring gut volumes of both large and small individuals. It is also the convenient for obtaining estimates of mean gut radii and volumes of gut compartments.

Among- and within-species patterns in gut parameters

Ratios of body volume to gut volume (B/G) are larger in carnivorous polychaetes than in deposit-feeding polychaetes. The differences in B/G between carnivores and deposit feeders can be attributed directly to differences in diet composition. Diets of carnivorous polychaetes obviously contain greater proportions of high quality food materials (i.e., higher in protein, lower ratios of carbon to nitrogen, probably more rapid digestive kinetics) than do diets of deposit feeders.

The between-group differences in ratios of body volume to gut volume for carnivorous and deposit-feeding polychaetes fit the general pattern of decreasing relative gut volume with increasing diet quality observed among other groups of animals. For example, empirical relationships for mammalian carnivores and herbivores show that gut masses in carnivores tend to be less than gut masses in similarly-sized ruminants. Gut mass (kg) (without contents) scales as a power function of body mass with an exponent of 1.01 for Carnivora and 1.16 for ruminants (Calder 1984). Among ruminant herbivores the weight of the reticulo-rumen and its contents (together representing about 80% of the weight of the total gut and contents) decreases relative to body weight as diet quality increases (Hoppe 1977).

To carry this prediction of the relationship between relative gut volume and food quality one step further among the polychaetes we might expect that nearshore and shelf deposit feeders should have proportionally less gut (i.e., larger B/Gs) than deep-sea deposit feeders. Median values of B/G range from about 1 to 6 among species in each group, however, and group medians are not different (Wilcoxon two-sample test, $p > 0.10$). Food quality is on average lower in the deep sea, but deep-sea deposit feeders might not be constrained by average food quality. They may key in on pulses of relatively higher quality organic matter (e.g., Gooday 1988; Jumars et al. 1988; Khripounoff and Sibuet 1980; Lochte and Turley 1988; Smith and Baldwin 1984) and function more like batch reactors (cf. hypotheses about foraging and digestive strategies of deposit-feeding ophiuroids, Penry and Jumars 1987). Digestive fermentation or carnivory (e.g., Euclymene reticulata) may be very important. Even at this relatively general level of comparison (i.e., nearshore and shelf species vs deep-sea species) the needs to quantify food resources and digestive kinematics are important limitations in our analyses.

We can identify four groups of polychaetes distinguished by basic feeding strategy and degree of compartmentalization of the gut: (1) carnivores with simple, tubular guts, (2) deposit feeders with simple, tubular guts, (3) deposit feeders with three gut compartments (not counting gut caeca), i.e., anatomical fore, mid, and hindguts, and (4) deposit feeders with four or five gut compartments (not counting gut caeca), i.e., mid or hindguts can be subdivided into anatomically distinct regions. All of the carnivores we examined have very simple guts while many of the deposit feeders have more anatomically-elaborate, compartmentalized guts. A similar pattern in gut architecture is seen in comparisons of mammalian carnivores (simple guts) and herbivores (more elaborate guts) (Hume 1982 and line drawings of guts therein). We predict, based on the patterns we have observed, that a polychaete with a simple, tubular gut and relatively large ratio of body volume to gut volume (i.e., $B/G > 7$) is more likely to be a carnivore than a deposit feeder.

Simple, tubular guts are also common among deposit feeders. We can predict based on digestion theory that the guts of species with simple, tubular guts operate as plug-flow reactors (no axial or radial mixing of sediment within the gut; Penry and Jumars 1986, 1987; Chapter III). Reasonable foraging and digestive constraints thus can be proposed for this group of deposit feeders. Among mammals simpler guts indicate relatively high quality diets and short throughput times (Hume 1982). Advantages of a simple gut for a deposit feeder are that it may be relatively inexpensive to construct and maintain. We expect that rapid growth and reproduction may be characteristic of many of these deposit feeders (e.g., Armandia spp., Woodin 1974; Capitella capitata, Grassle and Grassle 1974; Streblospio benedicti (Spionidae), Levin et al. 1987). A simple, tubular gut may allow relatively rapid ingestion rates and short throughput times (i.e., allow individuals to process rapidly large amounts of material), but this digestive strategy may limit these species to exploiting relatively higher quality food resources (e.g., to feeding on surface flocs or inhabiting areas of organic enrichment; to having feeding strategies that incorporate important degrees of carnivory or herbivory).

A number of the species with simple, tubular guts that we examined are characteristic of areas of organic enrichment or have been shown respond rapidly to organic enrichment (e.g., Capitella cf. capitata, Tharyx multifilis, Cirratulus cirratus, Paraprionospio pinnata, Chaetozone cf. setosa, Levinsenia oculata) (Pearson and Rosenberg 1978; Smith 1986; Weston, in prep.). Many "opportunistic" deposit feeders belong to three families of polychaetes, Capitellidae, Cirratulidae and Spionidae (Pearson and Rosenberg 1978), characterized by simple, tubular guts. There is evidence that the feeding strategies of at least two of the deep-sea species we examined, Levinsenia oculata and Euclymene reticulata, may incorporate important degrees of carnivory (Fauchald and Jumars 1979; this paper). We suggest that the opheliids, Armandia spp., probably burrow just beneath the sediment surface and thus are functionally surface deposit feeders. Next to nothing is known about the ecology of the two sessile deep-sea deposit feeders

with simple, tubular guts, Fauveliopsis glabra and Tharyx luticastellus. F. glabra is probably a surface deposit feeder; T. luticastellus is certainly a surface deposit feeder. T. luticastellus lives inside a mud concretion that it bulits on the sediment surface (Jumars 1975). Bacterial standing stocks are enhanced around mudballs when they are occupied by T. luticastellus (D. Thistle, personal communication).

The potential limitations imposed by relatively short throughput times and the need to ingest relatively high-quality food resources are not necessarily the only constraints, or even the most important constraints, on foraging and digestion in all deposit feeders with simple, tubular guts. Our results suggest that there may be an upper limit on body size of these deposit feeders. If there is such a limit it may reflect general, evolutionary body size constraints resulting from selection for relatively rapid growth and reproduction, or it may indicate additional digestive constraints. As we have noted (Penry and Jumars 1987) small deposit feeders with simple, tubular, plug-flow guts dominate areas of organic enrichment and the relatively food-poor deep sea, two environments characterized by sediments of low permeability. Our hypothesis that digestion may be diffusion limited (i.e., limited by the permeability of ingested sediments or by adsorption of enzymes and digestive products to mineral grains or their organic coatings) deserves continued consideration.

It is much more difficult to suggest general constraints for deposit feeders with compartmentalized guts. Similarities among these deposit feeders in gut architecture do not necessitate similarities in digestive processes. We know, for example, that axial mixing is important in the guts of at least two ampharetids, Amphicteis scaphobranchiata and Hobsonia florida (Self and Jumars 1978; Chapter III), and presumably in the guts of other terebellimorphs (Terebellidae and Trichobranchidae) (Dales 1955; Penry and Jumars 1987). Terebellimorphs have compartmentalized guts that can be modeled as continuous-flow, stirred-tank reactor series (Penry and Jumars 1987). Abarenicola pacifica and A. vagabunda (Arenicolidae), however, have

compartmentalized guts that operate as plug-flow reactors (Penry and Jumars 1987; Plante et al., in review). Travisia foetida (Opheliidae), one of the "outsiders" in Group 4 has an elaborate and unusual gut, and we suspect that microbial fermentation may be an important component of is digestive strategy -- an hypothesis also suggested by the characteristic smell of the species that is reflected in its name. Experimental descriptions of digestive kinematics (i.e., patterns and rates of sediment movement through the gut) (e.g., Chapter III) are necessary prerequisites to identification of foraging and digestive constraints among deposit feeders, especially those with compartmentalized guts.

In most of the polychaete species we examined gut volume remains a constant proportion of body volume as individuals increase in size. Gut volume is a linear function of body volume among both carnivores and deposit feeders rather than a power function of body volume with an exponent less than one as suggested by Forbes and Lopez (1987). Their conclusion is limited by the fact that they inferred trends in gut volume from patterns of gut fullness instead of measuring gut volume directly. Gut fullness directly affects gut volume estimates since polychaete guts are very extensible, but worms with relatively less full guts do not necessarily have relatively less gut volume as Forbes and Lopez (1987) assume.

Ontogenetic changes in foraging and digestive strategies among most polychaetes are more likely to be reflected in changes in food selection and digestive kinematics. Such a pattern has been demonstrated in a herbivorous reptile. Hatchling and juvenile iguanas (Iguana iguana) have the same digestive capacity (i.e., the same B/G) as adults, but meet their higher weight-specific metabolic requirements by selecting diets higher in protein. Their mean gut residence time is also about one-half that of adults (Troyer 1984).

In two of the 41 species we examined proportion of gut volume increases with body volume; in three species it decreases with body volume. Interpretation of these results must be viewed with caution

since we can expect this number of significant regressions to occur merely by chance in a group of 41 regressions with and alpha level of 0.10. Aglaophamus paucilmellata (Nephtyidae), a deep-sea carnivore, and Euclymene reticulata (Maldanidae), a deep-sea deposit feeder, exhibit a pattern of increasing proportion of body volume with increasing body volume suggesting that individuals of these species may switch from higher-quality diets to lower-quality diets, (e.g., from carnivory to deposit feeding) as they grow. We suspect that carnivory may be an important component of the foraging strategy of E. reticulata -- we did in fact observe a partially-digested, ovigerous harpacticoid copepod in the gut of one individual.

The proportion of gut volume decreases with body volume in Ampharete americana (Ampharetidae), Terebellides stroemi (NC) (Trichobranchidae) and Spiophanes cf. bombyx (Spionidae). If these results reflect actual patterns and not mere chance, it is unlikely that the converse of the above interpretation is true, i.e., that these species switch from lower-quality to higher-quality diets (e.g., from deposit feeding to carnivory) as they grow. These species are among the smallest deposit feeders we examined, and these changes may reflect a need for smaller individuals to process more sediment in order to meet higher weight-specific metabolic requirements. Processing more sediment by increasing ingestion rate may not be an option -- they might not be able to process enough sediment to compensate for decreased digestive conversions with decreased throughput times.

We predicted that relative gut proportions among deep-sea species would differ from nearshore and shelf species. Sedimentary organics in the deep sea may be more refractory and harder to digest than sedimentary organics in nearshore or shelf environments, and we thus predicted that deep-sea polychaete species should have longer guts (i.e., larger gut volumes and higher throughput times) than nearshore and shelf species. Such a pattern in gut length has been reported by Allen and Sanders (1964) for several species of deposit-feeding tellinid bivalves. We restricted our comparisons to within-gut-architecture groups, within-taxa comparisons to try to make

it more likely that the species compared would have similar digestive kinematics. When carefully paired this way most deep-sea species do seem to have longer guts than closely-related nearshore and shelf species, but, except for one case (Sternaspis fossor (deep sea) vs S. scutata (nearshore)), the differences are small. Larger differences in gut architecture and descriptive parameters are seen between widely-separated populations of single taxonomic species (e.g., Scalibregma inflatum (PS) vs S. inflatum (NC)) than are seen between some nearshore and deep-sea species (e.g., the ampharetid species we examined).

Within-species analyses of changes in gut parameters are more informative than across-species comparisons because they are less likely to be affected by our lack of knowledge of gut kinematics. Ontogenic changes in the relative proportions of the gut appear more common among polychaetes than changes in the total proportion of volume occupied by the gut. In fifteen of the 41 species we examined gut diameter is a constant proportion of gut length, but in 18 species guts become relatively longer and narrower as body size increases. These 18 species include seven of 11 deep-sea deposit feeders and five of eleven nearshore and shelf deposit feeders from muddy environments.

If digestion is diffusion-limited (Penry and Jumars 1987) we would expect larger individuals of species that feed on relatively less permeable sediments to have longer, narrower guts than smaller individuals (i.e., to minimize gut diameter while maintaining similar proportions of body volume to gut volume). The fact that a greater proportion of the deep-sea deposit feeders than the nearshore and shelf species we examined is in this group suggests that relative quality of food resources may also be an important factor. Diffusion limitations, if important, may be more important in species feeding on relatively poor quality food -- it may be necessary for individuals of these species to digest and absorb a greater proportion of the available organic matter in order to meet their metabolic requirements.

In general the scaling of throughput rate with body volume (or

mass) parallels the scaling of metabolic rate with body volume (or mass). Both rates scale as power functions of body volume with exponents less than one -- generally between two-thirds (0.67) and three-fourths (0.75) (Calder 1984). Forbes and Lopez (1987) found that egestion rate scales as body volume to the 0.70 power for Capitella sp I. In an among-species comparion of ingestion rates of deposit feeders Cammen (1980) found that ingestion rate scales as body mass to the 0.77 power when the fraction of organic matter in the food is removed as a covariable. (Note that ingestion rate, throughput rate and egestion rate are more or less equal in deposit feeders). Since gut volume scales as body volume to a power greater than 0.7 (i.e., scales as body volume to a power of one in most species examined) throughput time must increase as body size increases. Extent of digestion (digestive conversion) is completely determined by throughput time (Penry and Jumars 1987), and thus extent of digestion must increase with body size in deposit feeders (assuming food reasources and digestive kinetics do not change appreciably with body size).

These relationships suggest that digestive processing constraints may be more important in small individuals of deposit-feeding species with simple, tubular guts than they are in large individuals. Smaller individuals have higher weight-specific metabolic rates, relatively shorter throughput times and lower digestive conversions. We have suggested that digestive strategies of species with simple, tubular guts may in general limit them to exploiting relatively high quality food resources. We can suggest more specifically that availabilty of adequate food resources for juveniles of these species may be an important factor in determining their distributions.

Digestive conversion determines absolute amounts of digestive products available for absorption and assimilation; digestive reaction rates determine rates at which products become available for absorption and assimilation. Digestive reaction rates must decrease as digestive conversion increases, so the overall rate at which products become available for absorption and assimilation decreases. We can use these relationships to modify Sibly's prediction of increasing relative gut

volume with decreasing food quality as it applies to comparisons of similarly-sized animals. An increase in gut volume that results in an increase in throughput time should occur when food quantity becomes limiting, i.e. an animal should increase extent of digestion (Jumars and Penry 1988). An increase in gut volume with no corresponding increase in throughput time should occur when food quality is limiting, i.e., an animal should maximize production rate of digestive products. This latter response has been observed in laboratory experiments with birds (Savory and Gentle 1976; Al Joborae 1980).

Food quantity is unlikely to be limiting for deposit feeders. If food quality is limiting, and it is relatively poorer in the deep sea, and if (as predicted, but not conclusively demonstrated) deep-sea deposit feeders do have relatively larger gut volumes than nearshore and shelf species utilizing similar digestive strategies, we would predict that the deep-sea deposit feeders should feed at rates similar to the rates of the nearshore and shelf species. This prediction is in direct contrast to the prediction that results if Cammen's (1980) empirical relationship between feeding rate and sediment organic content is used to predict relative feeding rates for similarly-sized deposit feeders in nearshore and shelf environments and the deep sea. Although our prediction is sensitive to the fact that food qualities for and digestive kinematics of deposit feeders have yet to be quantified, this disparity in predictions should provide the impetus for deep-sea experimentation.

CONCLUSION

Digestion theory fills an inportant gap in existing ecological theory dealing with animals' strategies for acquiring energy and nutrients. It provides a general context for prediction, experimentation and inference, and promises to be as successful in stimulating studies of digestion as foraging theory has been in stimulating studies of foraging.

Experimental tests of gut-reactor models show that the models are more than ideal constructs. They describe patterns of sediment movement through the guts of the two deposit feeders examined and provide the basis for generalization of these results to other species with similar gut architectures. Modeling animal guts as chemical reactors is an iterative process -- tests of models lead to modifications of the models in order to better describe actual gut kinematics.

The ideal plug-flow model initially proposed for deposit feeders is modified to incorporate the absence of radial as well as axial mixing of gut contents. The modified plug-flow model can be characterized as an extreme case of segregated flow. Some limited mixing in the anterior-most portion of a "plug-flow" gut probably acts to mix digestive enzymes into ingested sediment, and thus may eliminate one potentially important constraint in an otherwise unmixed gut. This mixing can be incorporated in the modified plug-flow model as an initial condition: it can be assumed that enzymes are mixed throughout sediment as it is ingested and that digestive reactions occur homogeneously throughout any given cross-section.

The degree of mixing observed in the gut of Amphicteis scaphobranchiata is too great to be incorporated in a modified plug-flow model. Its gut and the guts of other terebellimorph polychaetes must be modeled as mixing reactor (CSTR) and plug-flow reactor series with the added component of a ventral bypass stream that

rapidly shunts particles from the mixing region of the gut through the plug-flow region of the gut for elimination in fecal pellets. Mixing and bypass may result in rapid elimination of relatively indigestible particles (i.e., larger, heavier particles) from the gut, increasing the proportion of the gut volume available for processing particles of relatively higher qualities.

This first round of tests and modifications of gut-reactor models for deposit feeders generates as many questions as are answered, and potential directions for experimentation are numerous. Digestive diffusion limitations (i.e., diffusion of enyzmes into ingested sediment and/or digestive products out of ingested sediment) are suggested as potentially important digestive constraints in deposit feeders, especially those species that ingest fine-grained, relatively less permeable sediments. Tests of this hypothesis must treat material in deposit feeders' guts as a two-phase system. I have assumed conservatively that the absence of radial mixing of particles in a plug-flow gut implies absence of radial mixing of fluids as well, but muscular contractions may enhance movement of fluids through the interstices of the sediment plug and to the gut wall. Tracer studies must be extended to include descriptions of movements of the fluid phase within deposit feeders' guts as well as the solid, particle phase.

The results of tests of gut-reactor models in a few species can be generalized, within the framework of digestion theory, to species not directly tested. Gut kinematics, thus, can be inferred from gut architecture. I suggest that deposit feeders with simple, tubular guts operate as plug-flow reactors and derive some reasonable constraints for this group of species. Plug-flow guts may allow relatively rapid ingestion rates and short throughput times. Distribution patterns of these deposit feeders -- they are common in both organic-rich and organic poor (e.g., deep sea) environments characterized by fine-grained sediments of relatively low permeability -- and their generally small body sizes suggest that digestive diffusion limitations may be important. The relative importance of diffusion limitations

within this group may be a function of food quality.

The central role of food quality in determining gut structure and function is demonstrated clearly in comparisons of gut architectures in carnivorous versus deposit-feeding polychaetes. Carnivores have much less gut volume per unit of body volume than do deposit feeders. This pattern does not extend across major taxa to comparisons of shallow-water versus deep-sea deposit feeders. Average food quality may be lower in the deep sea, but deep-sea deposit feeders may not be constrained by average food quality. They may key in on seasonal pulses of relatively higher quality organics -- their food may come in batches, and on long time scales, it may be necessary to model some deep-sea species as plug-flow reactors operating discontinuously.

Evaluation of these hypotheses requires that food "quality" be quantified. The development of gut-reactor models and the resulting rigorous framework for quantification of digestive processes indicates that qualitative characteristizations of food resources are now inadequate. Deposit feeders simplify tests of gut-reactor models because most of the material they ingest is inert mineral grains, and thus volume of material in the gut does not change during digestion. Deposit feeders complicate tests of gut-reactor models, however, because their food resources, "organic components of sediments", are variable and poorly characterized. These models now provide the impetus for investigations of sediment geochemistry with specific applications to deposit feeders and their food resources. They demonstrate the need for development of techinques (e.g., Mayer et al. 1986; Plante et al., in review) to measure or control food resources in laboratory and field experiments.

I have concentrated on application of digestion theory and gut-reactor models to deposit feeders because understanding, predicting, and quantifing their roles in sedimentary processes is of interest to oceanographers studying benthic environments. The generality of digestion theory, however, should not be overlooked: it can be applied to other marine animals and and their roles in

oceanographic processes (e.g., herbivorous copepods and their roles in particle transformations in the upper ocean) as well as to animals completely removed from the marine realm (e.g., mammalian herbivores and folivores).

BIBLIOGRAPHY

Al-Joborae, F. F. 1980. The influence of diet on the gut morphology of the starling (Sturnus vulgaris L. 1758). Ph.D. thesis, University of Oxford, Oxford, UK.

Allen, J. A. 1979. The adaptations and radiation of deep-sea bivalves. Sarsia 64:19-27.

Allen, J. A., and H. L. Sanders. 1966. Adaptations to abyssal life as shown by the bivalve Abra profundorum (Smith). Deep-sea Res. 13: 1175-1184.

Aller, R. C. 1980. Quantifying solute distributions in the bioturbated zone of marine sediments by defining an average microenvironment. Geochim. Cosmochim. Acta 44:1955-1965.

Aller, R. C. 1982. The effects of macrobenthos on chemical properties of marine sediment and overlying water. Pages 53-102 in P. L. McCall and M. J. S. Tevesz, eds. Animal-sediment relations. Plenum Press, New York.

American Geological Institute. 1976. Dictionary of geological terms. Anchor Press, Garden City, NY.

Aris, R. 1965. Introduction to the analysis of chemical reactors. Prentice-Hall, Englewood Cliffs, NJ.

Aris, R. 1982. The scope of R.T.D. theory. Pages 1-21 in A. Petho and R. D. Noble, eds. Residence time distribution theory in chemical engineering. Verlag Chemie, Deerfield Beach, FL.

Bailey, J. E., and D. F. Ollis. 1977. Biochemical engineering fundamentals. McGraw-Hill, New York.

Balch, C. C. 1950. Factors affecting the utilization of food by dairy cows. 1. The rate of passage of food through the digestive tract. Br. J. Nutr. 4:361-388.

Barnes, R. D. 1980. Invertebrate zoology, 4th ed. Saunders College, Philadelphia.

Bellman, R. 1957. Dynamic programming. Princeton University Press, Princeton, NJ.

Bischoff, K. B. 1966. Optimal continuous fermentation reactor design. Can. J. Chem. Eng. 44:281-284.

Brandt, C. S., and E. J. Thacker. 1958. A concept of rate of food passage through the gastro-intestinal tract. J. Anim. Sci. 17:218-223.

Briggs, G. E., and J. B. S. Haldane. 1925. A note on the kinetics of enzyme action. Biochem. J. 19:338-339.

Buchanan, J. B. 1964. A conparative study of some features of the biology of Amphiura filiformis and Amphiura chiajei (Ophiuroidea) considered in relation to their distribution. J. Mar. Biol. Assoc. U. K. 44:565-576.

Calder, W. A. 1984. Size, function, and life history. Harvard University Press, Cambridge, MA.

Calow, P. 1975. Defaecation strategies of two fresh-water gastropods, Ancylus fluviatilis Mull. and Planorbis contortus Linn. (Pulmonata) with a comparison of field and laboratory estimates of food absorption rate. Oecologia 20:51-63.

Cammen, L. M. 1980a. The significance of microbial carbon in the nutrition of the deposit-feeding polychaete Nereis succinea. Mar. Biol. 61:9-20.

Cammen, L. M. 1980b. Ingestion rate: An empirical model for aquatic deposit feeders and detritivores. Oecologia 44:303-310.

Carberry, J. J. 1976. Chemical and catalytic reaction engineering. McGraw-Hill, New York.

Cavanaugh, C. M., S. L. Gardiner, M. L. Jones, H. W. Jannasch, and J. B. Waterbury. 1981. Prokaryotic cells in the hydrothermal vent tubeworm Riftia pachyptila Jones: possible chemoautotrophic symbionts. Science 213:340-342.

Charnov, E. L. 1976. Optimal foraging, the marginal value theorem. Theoret. Pop. Biol. 9: 129-136.

Conover, R. J., R. Durvasula, S. Roy, and R. Wang. 1986. Probable loss of chlorophyll-derived pigments during passage through the gut of zooplanton, and some of the consequences. Limnol. Oceanogr. 31:878-887.

Costerton, J. W., T. J. Marrie, and K. J. Cheng. 1985. Phenomena of bacterial adhesion. Pages 3-43 in D. C. Savage and M. Fletcher, eds. Bacterial Adhesion. Plenum Press, New York.

Cowie, R. J. 1977. Optimal foraging in great tits (Parus major). Nature 268:137-139.

Dales, R. P. 1955. Feeding and digestion in terebellid polychaetes. J. Mar. Biol. Assoc. UK. 34:55-79.

Dales, R. P., and J. S. Pell. 1970. The nature of the peritrophic membrane in the gut of the terebellid polychaete Neoamphitrite figulus. Comp. Biochem. Physiol. 34:819-826.

Demment, M. W., and P. J. Van Soest. 1985. A nutritional explanation for body-size patterns of ruminant and nonruminant herbivores. Am. Nat. 125:641-672.

Ellis, W. C., J. H. Matis, and C. Lascano. 1979. Quantitating ruminal turnover. Federation Proc. 38: 2702-2706.

Fauchald, K., and P. A. Jumars. 1979. The diet of worms: a study of polychaete feeding guilds. Oceanogr. Mar. Biol. Ann. Rev. 17: 193-284.

Fauvel, P. 1897. Recherches sur les Ampharetiens. Theses presentees a la Faculte des Sciences de Paris. L. Danel, Lille.

Feral, J-P., and C. Massin. 1982. Digestive systems: Holothuroidea. Pages 191-212 in M. Jangoux and J. M. Lawrence, eds. Echinoderm nutrition. A. A. Balkema, Rotterdam, Netherlands.

Fisher, R. A. 1970. Statistical methods for research workers. Hafner Publishing Co., Darien, CT.

Forbes, T. L., and G. R. Lopez. 1987. The allometry of deposit feeding in Capitella species I (Polychaeta:Capitellidae): the role of temperature and pellet weight in the control of egestion. Biol. Bull. 172:187-201.

Froment, G. E., and K. B. Bischoff. 1979. Chemical reactor analysis and design. John Wiley, New York.

Gooday, A. J. 1988. A response by benthic Foraminifera to the deposition of phytodetritus in the deep sea. Nature 332:70-73.

Grassle, J. F., and J. P. Grassle. 1975. Opportunistic life-histories and genetic systems in marine benthic polychaetes. J. Mar. Res. 32:253-284.

Grovum, W. L., and V. J. Williams. 1977. Rate of passage of digesta in sheep. 6. The effect of level of food intake on mathematical predictions of the kinetics of digesta in the reticulorumen and intestines. Br. J. Nutr. 38:425-436.

Hartmann-Schroder, G. 1958. Zur Morphologie der Opheliiden (Polychaeta sedentaria). Zeitschrift fur wissenschaftliche Zoologie 161:84-143.

Healy, E. A., and G. P. Wells. 1959. Three new lugworms (Arenicolidae, Polychaeta) from the North Pacific area. Proc. Zool. Soc. Lond. 133:315-335.

Hershey, D. 1973. Transport analysis. Plenum Press, New York.

Herwig, R. P., J. T. Staley, M. K. Nerini, and H. W. Braham. 1984. Baleen whales: preliminary evidence for forestomach microbial fermentation. Appl. Environ. Microbiol. 47:421-423.

Hessler, R. R., and P. A. Jumars. 1974. Abyssal community analysis from replicate box cores in the central North Pacific. Deep-sea Res. 21:185-209.

Hoppe, P. P. 1977. Rumen fermentation an body weight in African ruminants. Pages 141-150 in Proceedings of XIIIth Congress of Game Biologists, Atlanta, GA.

Hornicke, H., and G. Bjornhag. 1980. Coprophagy and related strategies for digesta utilization. Pages 707-730 in Y. Ruckebusch and P. Thivend, eds. Digestive physiology and metabolism in ruminants. AVI Publishing Company, Westport, CT.

Hubbell, S. P., A. Sikora, and O. H. Paris. 1965. Radiotracer, gravimetric, and calorimetric studies of ingestion and assimilation rates of an isopod. Health Physics 11:1485-1501.

Hughes, R. N. 1980. Optimal foraging in the marine context. Oceanogr. Mar. Biol. Ann. Rev. 18:423-481.

Hughes, T. G. 1977. The processing of food material within the gut of Abra tenuis (Bivalvia:Tellinacea). J. moll. Stud. 43:162-180.

Hughes, T. H., and J. H. Matis. 1984. An irreversible two-compartment model with age-dependent turnover rates. Biometrics 40: 501-505.

Hume, I. D. 1982. Digestive physiology and nutrition of marsupials. Cambridge University Press, Cambridge.

Janis, C. 1976. The evolutionary strategy of the Equidae and the origins of rumen and caecal digestion. Evolution 30:757-774.

Jumars, P. A. 1974. Dispersion patterns and species diversity of macrobenthos in two bathyal communities. Ph.D. dissertation, University of California at San Diego, San Diego, CA.

Jumars, P. A. 1975. Target species for deep-sea studies in ecology, genetics, and physiology. Zool. J. Linn. Soc. 57:341-348.

Jumars, P. A., A. V. Altenbach, G. J. De Lange, S. R. Emerson, B. T. Hargrave, P. J. Muller, F. G. Prahl, C. E. Reimers, T. Steiger, and E. Suess. 1988. Transformation of seafloor-arriving fluxes into the sedimentary record. In W. H. Berger, V. S. Smetacek, and G. Wefer, eds. Productivity of the ocean: present and past. Dahlem Konferenzen. John Wiley and Sons, Chichester, U.K.

Jumars, P. A., and E. D. Gallagher. 1982. Deep-sea community structure: three plays on the benthic proscenium. Pages 217-255 in W. G. Ernst and J. G. Morin, eds. The environment of the deep sea. Prentice-Hall, New York.

Jumars, P. A., and D. L. Penry. 1988. Digestion theory applied to deposit feeding. In G. Lopez and G. Taghon, eds. Ecology of marine deposit feeders. Springer-Verlag, New York.

Jumars, P. A., and R. F. L. Self. 1986. Gut-marker and gut-fullness methods for estimating field and laboratory effects of sediment transport on ingestion rates of deposit feeders. J. Exp. Mar. Biol. Ecol. 98:293-310.

Juniper, S. K. 1986. Deposit feeding strategy of Amphibola crenata - feeding behaviour, selective feeding and digestion. Mauri Ora 13:103-115.

Karasov, W. H., and J. M. Diamond. 1985. Digestive adaptations for fueling the cost of endothermy. Science 228:202-204.

Khirpounoff, A. and M. Sibuet. 1980. La nutrition d'echinoderms abyssaux I. Alimentation des holothuries. Mar. Biol. 60:17-26.

Kiorboe, T., F. Mohlenberg, and K. Hamburger. 1985. Bioenergetics of the planktonic copepod Acartia tonsa: relation between feeding, egg production and respiration, and composition of specific dynamic action. Mar. Ecol. Prog. Ser. 26:85-97.

Larson, R. J. 1976. Cubomedusae: feeding-functional morphology, behavior and phylogenetic position. Pages 237-245 in G. O. Mackie, ed. Coelenterate ecology and behavior. Plenum Press, New York.

Lehninger, A. L. 1970. Biochemistry. Worth Publishers, New York.

Leopold, A. S. 1953. Intestinal morphology of gallinaceous birds in relation to food habits. J. Wildl. Mgmt. 17: 197-203.

Levenspiel, O. 1972. Chemical reaction engineering, 2nd ed. John Wiley, New York.

Levin, L. A., H. Caswell, K. D. DePatra, and E. L. Creed. 1987. Demographic consequences of larval development mode: planktotrophy vs. lecithotrohpy in Streblospio benedicti. Ecology 68:1877-1886.

Lochte, K., and T. M. Turley. 1988. Bacteria and cyanobacteria associated with phytodetritus in the deep sea. Nature 333:67-69.

Longbottom, M. R. 1970. The distribution of Arenicola marina (L.) with particular reference to the effects of particle size and organic matter of the sediments. J. Exp. Mar. Biol. Ecol. 5:138-157.

Lopez, G. R., and I-J. Cheng. 1983. Synoptic measurements of ingestion rate, ingestion selectivity, and absorption efficiency of natural foods in the deposit-feeding molluscs Nucula annulata (Bivalvia) and Hydrobia totteni (Gastropoda). Mar. Ecol. Prog. Ser. 11:55-62.

Macagno, E. O., and J. Christensen. 1980. Fluid mechanics of the duodenum. Ann. Rev. Fluid Mech. 12:139-158.

MacConnaughey, B. H., and D. L. Fox. 1949. The anatomy and biology of the marine polychaete Thoracophelia mucronata (Treadwell). Opheliidae. Univ. California Publications in Zoology 47:319-328.

Madsen, F. J. 1961. On the zoogeography and origin of the abyssal fauna in view of the knowledge of the Porcellanasteridae. Galathea Rept. 4:177-218.

Michel, C., M. Bhaud, P. Boumati, and S. Halpern. 1984. Physiology of the digestive tract of the sedentary polychaete Terebellides stroemi. Mar. Biol. 83:17-31.

Miller, D. C. 1984. Mechanical post-capture particle selection by suspension- and deposit-feeding Corophium. J. Exp. Mar. Biol. Ecol. 82:59-76.

Mills, E. L., R. C. Ready, M. Jahncke, C. R. Hanger, and C. Trowbridge. 1984. A gastric evacuation model for young yellow perch, Perca flavescens. Can. J. Fish. Aquat. Sci. 41:513-518.

Milton, K. 1981. Food choice and digestive strategies of two sympatric primate species. Am. Nat. 117:496-505.

Moss, R. 1974. Winter diets, gut lengths, and interspecific competition in Alaskan ptarmigan. The Auk 91:737-746.

Nie, N. H., C. H. Hull, J. G. Jenkins, K. Steinbrenner, and D. H. Bent. 1975. Statistical package for the social sciences, 2nd ed. McGraw-Hill, New York.

Nowell, A. R. M., P. A. Jumars, and K. Fauchald. 1984. The foraging strategy of a subtidal and deep-sea deposit feeder. Limnol. Oceanogr. 29:645-649.

Ockelmann, K. W., and O. Vahl. 1970. On the biology of the polychaete Glycera alba, especially its burrowing and feeding. Ophelia 8: 275-294.

Orians, G. H., and N. E. Pearson. 1979. On the theory of central place foraging. Pages 155-177 in D. J. Horn, G. R. Stairs, and R. D. Mitchell, eds. Analysis of Ecological Systems. Ohio State University Press, Columbus, OH.

Owen-Smith, N., and P. Novellie. 1982. What should a clever ungulate eat? Am. Nat. 119:151-178.

Parra, R. 1978. Comparison of foregut and hindgut fermentation in herbivores. Pages 205-229 in G. G. Montgomery, ed. The ecology of arboreal folivores. Smithsonian Institution, Washington, D. C.

Pearson, T. H., and R. Rosenberg. 1978. Macrobenthic succession in relation to organic enrichment and pollution of the marine environment. Oceanogr. Mar. Biol. Ann. Rev. 16:229-311.

Pehrson, A. 1983. Caecotrophy in caged Mountain hares (Lepus timidus). J. Zool., Lond. 199:563-574.

Penry, D. L., and P. A. Jumars. 1986. Chemical reactor analysis and optimal digestion theory. Bioscience 36:310-315.

Penry, D. L., and P. A. Jumars. 1987. Modeling animal guts as chemical reactors. Am. Nat. 129:69-96.

Petho, A., and R. D. Noble, eds. 1982. Residence time distribution theory in chemical engineering. Verlag Chemie, Deerfield Beach, FL.

Pickard, D. W., and C. E. Stevens. 1972. Digesta flow through the rabbit large intestine. Am. J. Physiol. 222:1161-1166.

Pough, F. H. 1973. Lizard energetics and diet. Ecology 54:837-844.

Pyke, G. H. 1984. Optimal foraging: a critical review. Ann. Rev. Ecol. Syst. 15:523-575.

Reid, R. G. B., and F. R. Bernard. 1980. Gutless bivalves. Science 208: 609-610.

Reid, R. G. B., and A. Reid. 1969. Feeding processes of members of the genus Macoma (Mollusca:Bivalvia). Can. J. Zool. 47:649-657.

Savory, C. J., and M. J. Gentle. 1976. Changes in food intake and gut size in Japanese quail in response to manipulation of dietary fibre content. Br. Poult. Sci. 17: 571-580.

Scheibling, R. E. 1981. Optimal foraging movements of Oreaster reticulatus (L.) (Echinodermata: Asteroidea). J. Exp. Mar. Biol. Ecol. 44:67-83.

Schoener, T. W. 1971. Theory of feeding strategies. Ann. Rev. Ecol. Syst. 2:369-404.

Self, R. F. L., and P. A. Jumars. 1978. New resource axes for deposit feeders? J. Mar. Res. 36:627-641.

Self, R. F. L, and P. A. Jumars. 1988. Cross-phyletic patterns of particle selection by deposit feeders. J. Mar. Res. 46:119-143.

Sheppard, C. W. 1962. Basic principles of the tracer method. John Wiley and Sons, New York.

Shick, J. M., K. C. Edwards, and J. H. Dearborn. 1981. Physiological ecology of the deposit-feeding sea star Ctenodiscus crispatus: ciliated surfaces and animal-sediment interactions. Mar. Ecol. Prog. Ser. 5:165-184.

Sibly, R. M. 1981. Strategies of digestion and defecation. Pages 109-139 in C. R. Townsend and P. Calow, eds. Physiological ecology: an evolutionary approach to resource use. Sinauer Associates, Sunderland, MA.

Smith, C. R. 1985. Food for the deep sea: utilization, dispersal and flux of nekton falls at the Santa Catalina Basin floor. Deep-sea Res. 32:417-442.

Smith, C. R. 1986. Nekton falls, low-intensity disturbance and community structure of infaunal benthos in the deep sea. J. Mar. Res. 44:567-600.

Smith, J. M. 1981. Chemical engineering kinetics, 3rd ed. McGraw-Hill, New York.

Smith, K. L., Jr., and J. R. Baldwin. 1984. Seasonal fluctuations in deep-sea community oxygen consumption: central and eastern North Pacific. Nature 307:624-626.

Southward, A. J., and E. C. Southward. 1968. Uptake and incorporation of labelled glycine by pogonophores. Nature (London) 218:875-876.

Stevens, C. E., R. A. Argenzio, and E. T. Clemens. 1980. Microbial digestion: rumen versus large intestine. Pages 685-705 in Y. Ruckebusch and P. Thivend, eds. Digestive physiology and metabolism in ruminants. AVI Publishing Company, Westport, CT.

Taghon, G. L. 1981. Beyond selection: optimal ingestion rate as a function of food value. Am. Nat. 118:202-214.

Taghon, G. L. 1982. Optimal foraging by deposit-feeding invertebrates: Roles of particle size and organic coating. Oecologia 52:295-304.

Taghon, G. L., and P. A. Jumars. 1984. Variable ingestion rate and its role in optimal foraging behavior of marine deposit feeders. Ecology 65:549-558.

Taghon, G. L., R. F. L. Self, and P. A. Jumars. 1978. Predicting particle selection by deposit-feeders: A model and predictions. Limnol. Oceanogr. 23:752-759.

Tendal, O. S. 1979. Aspects of the biology of Komokiacea and Xenophyophoria. Sarsia 64:13-17.

Townsend, C. R., and P. Calow, eds. 1981. Physiological Ecology: An Evolutionary Approach to Resource Use. Sinauer Associates, Sunderland, MA.

Townsend, C. R., and R. H. Hughes. 1981. Maximizing net energy returns from foraging. Pages 86-108 in C. R. Townsend and P. Calow, eds. Physiological ecology: an evolutionary approach to resource use. Sinauer Associates, Sunderland, MA.

Troyer, K. 1984. Diet selection and digestion in Iguana iguana: the importance of age and nutrient requirements. Oecologia 61: 201-207.

Tyler, P. A. 1980. Deep-sea ophiuroids. Oceanogr. Mar. Biol. Ann. Rev. 18:125-153.

Van Soest, P. J. 1982. The kinetics of digestion. Pages 211-229 in P. J. Van Soest, ed. Nutritional ecology of the ruminant. O & B Books, Corvallis, OR.

Westoby, M. 1974. An analysis of diet selection by large generalist herbivores. Am. Nat. 108:290-304.

Weston, D. P. 1983. Distribution of macrobenthic invertebrates on the North Carolina continental shelf with consideration of sediment, hydrography and biogeography. Ph.D. dissertation, College of William and Mary in Virginia, Williamsburg, VA.

Weston, D. P. 1988. Macrobenthos-sediment relationships on the continental shelf off Cape Hatteras, North Carolina. Continental Shelf Res. 8:267-286.

Whitlatch, R. B., and J. R. Weinberg. 1982. Factors influencing particle selection and feeding rate in the polychaete Pectinaria gouldii. Mar. Biol. 77:33-40.

Wieser, W. 1978. Consumer strategies of terrestrial gastropods and isopods. Oecologia 36:191-201.

Wishart, D. 1975. Clustan, release 1c. University College, London.

Woodin, S. A. 1974. Polychaete abuncance patterns in a marine soft-sediment environment: the importance of biological interactions. Ecol. Monogr. 44:171-187.

Appendix I. Data for Chapter III.

Section A: Records of water temperature in sea table during 9/87 and 10/87 runs of tracer experiments (Chapter III).

All measurements are in ^{o}C.

A. Sea Table Temperature Records

Time	Temperature 9/87	10/87
0430		12.1
0700		12.5
0900		12.7
1000	14.8	12.9
1200	15.2	12.6
1300	15.3	14.7
1400	15.3	14.9
1530	15.4	15.1
1630	15.5	15.1
1730	15.5	15.0
1830	15.6	14.7
1900	15.5	14.6
2000	15.5	14.5
2100	15.5	14.3
2200	15.5	14.0
2300	15.3	14.0

Time	Temperature 9/87	10/87
2400	15.1	14.0
0100	15.1	13.9
0200	14.5	14.0
0400	14.5	14.0
0500	14.5	14.1
0600	14.4	14.1
0700	14.2	14.2
0900	14.5	14.0
1000	14.7	14.0
1100		14.3
1200		14.4
1300		14.6
1400		14.8
1500		15.0
1630		15.0

Section B: Raw data for 9/87 and 10/87 tracer experiments:
Time series of pellet weights and tracer counts.

B. Amphicteis scaphobranchiata tracer experiments: Weights and tracer counts for individual pellets.

Individual pellets were aspirated onto filters that were subdivided into 12 equally-sized areas.
Seven of 12 areas on each filter were selected randomly, and all tracers within those areas were counted.
Pellet tracer concentration = (tracer count x 12/7) divided by pellet weight divided by 7.
"Start" = time of step up in tracer concentration. 10/87 run started at t=0430; 9/87 run started at 0945.
"Switch" = time up step up in tracer concentration.
In the 9/87 run, some pellets were divided in half, and halves were analyzed separately.
Anterior half designated (1/2); posterior half designated (2/2).
# indicates actual order in which pellets were produced was unknown.

Elapsed Time (min)	Pellet Number	Filter Number	Pellet Weight (mg)	Counts of fluorescent glass beads (number per 1/12 filter area)							Counts of fluorescent polystrene beads (number per 1/12 filter area)						
10/87 Worm 1S																	
0		-------start-------															
120	1	11	2.76	5	5	5	3	9	11	12	63	55	61	78	73	71	71
255	2	18	2.00	9	9	5	10	5	7	7	42	33	55	43	41	59	46
495	3	27	1.02	0	0	1	3	2	0	2	6	19	15	13	15	13	19
585	4	32	0.74	0	1	0	0	1	0	0	8	3	11	13	4	2	3
735	5	40	0.38	1	3	1	1	1	2	2	7	11	6	2	5	7	9
915	6	42	0.33	0	1	0	3	0	0	2	3	3	7	6	5	5	5
1140		-------switch-------															
1380	7	51	0.56	2	1	0	2	0	3	2	8	12	19	12	19	10	12
1950	8	67	0.86	0	1	0	0	0	0	0	1	2	1	2	2	1	0
2145	9	71	2.84	2	2	0	1	3	1	1	4	4	6	6	3	1	2
10/87 Worm 2S																	
0		-------start-------															
255	1	19	2.81	5	15	10	7	10	14	10	21	22	18	20	19	17	24
345	2	21	2.85	13	27	24	22	15	21	29	118	112	100	102	104	100	110
555	3	30	0.27	4	2	2	1	1	4	1	20	23	13	19	6	9	12
735	4	39	4.18	58	70	62	41	34	40	43	177	224	172	141	117	161	149
1020	5	45	0.57	3	9	6	9	5	8	3	54	46	52	55	53	46	47
1080	6	47	0.81	2	3	7	7	9	6	11	81	60	65	74	86	71	80
1140		-------switch-------															
1170	7	48	1.69	9	12	10	10	21	8	10	81	116	109	82	107	78	73
1350	8	50	0.95	2	2	7	4	1	2	2	19	25	31	18	21	18	20
1650	9	61	0.25	0	0	0	0	0	0	0	0	0	0	2	0	0	1
1710	10	63	0.80	0	1	0	1	0	2	2	8	6	6	13	8	23	36
2115	11	70	2.14	3	1	3	1	1	2	0	8	3	4	5	9	2	5
10/87 Worm 5S																	
0		-------start-------															
225	1	16	0.97	6	2	3	4	3	4	3	20	26	19	28	22	35	31
405	2	24	2.29	6	6	12	13	10	7	13	70	80	88	74	97	75	84
885	3	41	0.92	4	4	9	1	4	8	3	45	45	35	51	48	48	44
1500	4	55	2.26	21	10	5	11	18	19	13	98	140	124	146	132	115	139
1515		-------switch-------															
1950	5	68	2.59	12	17	17	13	25	13	19	111	119	114	141	121	95	131
2100	6	69	1.44	1	0	1	0	0	2	2	21	22	18	27	12	22	24

Elapsed Time (min)	Pellet Number	Filter Number	Pellet Weight (mg)	Counts of fluorescent glass beads (number per 1/12 filter area)							Counts of fluorescent polystrene beads (number per 1/12 filter area)						
10/87 Worm 4P																	
0		-------start-------															
360	1	22	1.51	6	2	5	5	7	4	5	27	19	19	24	23	17	18
480	2	26	0.88	0	2	1	0	1	2	2	10	6	5	5	6	7	11
570	3	31	0.63	1	4	5	4	8	1	1	20	18	24	21	21	28	21
600	4	34	0.73	3	1	2	2	2	0	1	22	14	14	14	17	13	21
660	5	36	0.49	0	1	1	0	1	4	1	12	9	13	10	11	12	10
720	6	38	0.51	2	2	0	3	3	1	1	12	22	17	16	22	18	24
1140		-------switch-------															
1410	7	52	2.89	5	9	9	5	2	5	2	51	57	58	53	60	72	68
1440	8	53	1.13	2	1	1	4	2	1	1	15	9	9	5	14	20	9
1470	9	54	1.48	0	0	0	0	0	0	0	1	2	2	1	5	0	0
1560	10	57	1.15	0	1	0	3	1	0	0	4	5	3	3	5	2	5
1620	11	58	0.74	0	0	0	0	0	0	0	2	6	3	1	2	2	2
1790	12	64	1.28	0	0	1	0	0	1	1	2	2	0	2	2	1	2
10/87 Worm 7P																	
0		-------start-------															
120	1	not collected															
225	2	15	2.41	11	10	10	13	12	12	19	62	94	67	71	91	66	69
330	3	20	1.12	6	6	5	3	2	4	2	9	12	10	9	9	7	9
375	4	23	0.51	0	2	1	1	0	0	0	5	11	10	11	7	8	4
510	5	33	2.18	4	5	7	7	6	2	2	20	11	14	16	16	9	11
585	6	34	1.28	3	2	2	2	2	1	2	18	19	20	19	17	17	17
660	7	37	1.35	4	6	5	8	4	2	7	42	26	26	26	29	23	22
1005	8	44	2.72	9	8	11	7	9	7	8	61	61	65	70	67	62	59
1140		-------switch-------															
1320	9	49	4.11	13	14	19	16	10	19	12	6	15	14	12	8	15	5
1560	10	56	1.70	1	4	5	6	6	7	4	29	23	25	29	32	33	31
1620	11	59	1.31	6	4	0	3	5	1	0	0	2	2	1	1	0	0
1680	12	62	0.36	0	0	0	0	0	0	0	0	1	0	0	0	0	2
1770	13	65	0.94	0	0	0	0	0	1	1	2	0	1	1	1	2	2
10/87 Worm 8P																	
0		-------start-------															
120	1	12	1.29	2	0	0	0	1	0	1	15	12	19	14	13	9	19
435	2	25	1.07	0	0	2	2	1	1	0	2	4	2	3	0	3	4
960	3	43	1.10	0	0	0	0	1	0	0	4	2	4	1	2	5	3
1515		-------switch-------															
1620	4	60	0.74	4	6	4	1	4	4	4	17	23	24	28	27	19	19
1920	5	66	0.16	3	3	1	1	3	2	2	22	14	17	12	24	16	28

Elapsed Time (min)	Pellet Number	Filter Number	Pellet Weight (mg)	Counts of fluorescent glass beads (number per 1/12 filter area)							Counts of fluorescent polystrene beads (number per 1/12 filter area)						
9/87 Worm 1S																	
0		-------start-------															
165	1	74	1.92	11	9	11	7	8	10	8	5	5	4	3	3	4	2
330	2	76	3.30	18	22	28	16	16	18	20	7	10	19	7	14	7	18
540	3	86	1.51	28	21	12	25	18	28	22	13	16	9	14	23	16	20
830	4	98	2.14	40	41	42	44	42	49	40	25	18	21	17	23	15	23
860	5	102	2.13	103	98	109	76	77	97	86	86	87	72	71	80	76	53
965	6	104	2.16	110	118	116	122	112	114	127	92	105	109	95	96	88	78
1085	7	118	3.37	161	150	143	142	137	151	136	140	141	136	116	86	131	119
1085		-------switch-------															
1155	8	119	3.98	140	141	133	128	123	132	151	120	100	103	126	106	106	108
1190	9(1/2)	122	1.15	56	52	48	47	60	52	50	72	74	86	94	87	67	81
1190	9(2/2)	123	0.75	31	31	28	36	31	25	34	70	58	53	68	59	41	52
1850	10	136	7.82	109	150	141	130	158	153	141	74	69	93	84	62	59	63
9/87 Worm 2S																	
0		-------start-------															
555	1	87	3.93	59	49	67	57	74	58	59	61	70	47	50	56	49	35
630	2	88	3.10	16	11	7	12	13	10	11	11	6	7	5	7	13	7
1025	3	111	1.76	91	88	92	93	83	82	88	91	104	82	88	87	91	84
1220	4	126	2.47	128	105	129	110	118	127	128	112	107	81	95	98	99	89
1265	5	127	3.60	120	117	129	154	132	143	123	114	86	91	84	85	108	104
1265		-------switch-------															
1370	6	130	2.18	97	113	103	122	76	94	105	78	104	65	69	56	69	68
18508	7	141	3.40	47	15	27	13	27	24	26	14	17	26	25	24	19	31
18508	8	144	2.54	27	36	25	38	31	31	33	16	23	21	30	25	18	20
1935	9	153	2.43	20	19	23	20	25	19	24	21	22	31	24	28	30	28
9/87 Worm 5S																	
0		-------start-------															
45	1	73	4.00	42	44	46	41	55	65	47	29	25	22	31	35	33	35
405	2	79	3.90	8	8	9	11	9	12	10	6	2	9	4	2	4	1
465	3	82	2.16	10	6	9	9	17	12	13	2	6	4	1	2	8	2
1025	4	114	4.23	264	226	218	258	272	226	214	94	136	146	88	116	124	122
1150	5	120	5.66	212	232	196	236	208	234	234	114	138	120	138	128	146	128
1160		-------switch-------															
1850	6	140	0.69	14	15	27	13	27	24	26	14	17	26	25	24	19	31
28658	7	157	2.37	17	22	18	18	23	26	22	14	16	11	15	9	15	17
28658	8	143	2.39	14	20	7	13	20	19	19	14	18	13	13	14	17	15
28658	9	151	7.04	33	40	35	27	32	35	38	33	27	27	16	25	26	23
28658	10	154	6.21	27	32	33	32	27	23	28	26	31	29	22	27	26	27

Elapsed Time (min)	Pellet Number	Filter Number	Pellet Weight (mg)	Counts of fluorescent glass beads (number per 1/12 filter area)							Counts of fluorescent polystrene beads (number per 1/12 filter area)						
9/87 Worm 3P																	
0		-------start-------															
15	1	72	1.52	12	2	9	3	5	5	6	6	2	4	1	7	7	6
495	2	83	1.42	6	3	2	2	4	2	4	1	2	2	0	3	1	3
800	3(1/2)	95	0.54	4	7	5	9	12	7	11	5	12	8	11	11	15	14
800	3(2/2)	96	1.17	17	17	17	18	12	13	12	14	20	12	25	19	21	14
830	4(1/2)	99	0.67	6	9	9	11	11	9	10	3	5	3	2	5	4	1
830	4(2/2)	100	0.76	3	6	5	7	6	5	4	3	2	2	2	3	1	3
9650	5	105	2.58	218	244	234	226	234	232	268	88	74	162	160	106	140	110
9650	6(1/2)	106	1.04	88	84	85	88	60	68	74	122	139	119	130	90	117	118
9650	6(2/2)	107	1.54	77	47	85	84	59	89	94	144	114	189	146	100	142	141
995	7(1/2)	108	0.98	50	54	60	46	50	66	66	100	140	147	94	100	136	120
995	7(2/2)	110	1.72	150	90	96	100	110	100	110	262	246	184	198	224	280	226
1010		-------switch-------															
1025	8(1/2)	112	1.35	85	72	72	70	52	63	66	140	134	140	129	155	162	132
1025	8(2/2)	113	1.36	39	35	31	37	38	46	34	104	89	100	76	94	113	93
1415	9(1/2)	131	0.93	57	63	61	60	46	49	43	118	131	148	126	99	138	135
1415	9(2/2)	132	1.65	91	92	89	71	61	47	66	182	172	151	155	201	149	169
18500	10	142	1.64	35	48	45	38	51	32	36	76	88	99	99	84	84	79
18500	11	137	0.91	28	37	29	26	31	27	36	41	51	36	49	41	42	33
18500	12	152	3.09	50	56	42	35	40	44	41	103	118	98	95	97	117	77
9/87 Worm 4P																	
0		-------start-------															
240	1	75	1.04	3	1	2	5	2	1	2	0	2	1	1	1	1	0
330	2	77	0.48	3	1	1	2	2	3	1	0	0	0	2	2	3	3
345	3	78	0.43	2	2	4	0	1	1	1	2	0	0	1	0	0	2
420	4(1/2)	80	0.20	1	0	1	3	2	2	0	2	1	2	3	2	5	0
420	4(2/2)	81	0.51	0	0	1	2	3	1	1	0	2	1	6	5	4	4
495	5(1/2)	84	0.49	8	7	8	8	12	8	7	3	4	3	6	1	4	6
495	5(2/2)	85	0.46	11	15	8	14	9	10	9	12	15	11	16	21	11	23
675	6(1/2)	90	0.30	38	29	36	38	31	48	32	61	56	44	35	39	54	46
675	6(2/2)	91	0.27	58	69	77	56	52	57	59	91	104	108	97	95	89	109
735	7	92	0.26	45	60	40	56	52	56	31	75	59	55	59	52	58	60
800	8	97	0.42	33	42	36	28	45	45	29	70	88	68	71	73	78	74
875	9	101	0.28	47	46	57	53	40	52	43	56	58	58	53	39	71	60
875		-------switch-------															
10550	10(1/2)	115	0.25	18	43	18	35	42	23	40	63	74	37	85	57	52	83
10550	10(2/2)	116	0.19	12	15	13	24	15	18	15	36	33	35	45	37	39	31
10550	11	117	0.95	42	47	61	51	56	49	54	161	155	130	124	166	163	132
1145	12	121	0.42	35	32	33	33	36	38	27	101	117	133	108	100	103	77
1415	13	133	0.49	25	29	27	34	40	23	28	138	121	125	138	142	100	120
18500	14	159	0.68	21	27	28	29	24	31	24	43	41	35	54	41	59	47
18500	15	147	0.38	13	17	12	19	14	12	10	31	28	24	30	20	26	33
18500	16	139	0.68	17	25	20	19	21	21	22	41	33	49	34	42	45	37
18500	17	150	0.56	10	12	11	10	15	11	9	16	22	15	20	31	15	14
18500	18	158	0.40	6	7	10	8	9	7	6	13	15	9	7	11	14	16
18500	19	155	0.67	10	10	6	11	7	7	12	19	8	15	19	21	15	23

Elapsed Time (min)	Pellet Number	Filter Number	Pellet Weight (mg)	Counts of fluorescent glass beads (number per 1/12 filter area)							Counts of fluorescent polystrene beads (number per 1/12 filter area)						
9/87 Worm 8P																	
0		-------start-------															
630	1	89	3.47	17	17	9	15	13	13	15	15	11	13	11	14	16	12
795	2(1/2)	93	1.51	36	46	31	36	30	43	40	12	11	11	11	8	11	7
795	2(2/2)	94	1.34	53	42	60	47	50	58	73	9	10	13	10	11	15	9
1160	3(1/2)	124	0.60	48	44	46	36	37	41	40	57	47	53	43	48	51	52
1160	3(2/2)	125	0.67	68	63	74	71	69	73	66	103	102	121	90	108	101	116
1295	4(1/2)	128	1.41	107	94	82	104	73	91	88	129	116	135	122	129	86	118
1295	4(2/2)	129	2.10	72	76	63	59	70	67	87	98	99	82	101	131	137	156
1295		-------switch-------															
1850@	5(1/2)	134	0.97	61	60	56	53	72	48	50	98	97	96	106	74	82	91
1850@	5(2/2)	135	0.93	51	47	53	66	66	55	47	120	134	113	119	102	97	97
1850@	6(1/2)	148	0.88	47	36	55	60	48	52	47	70	77	80	91	98	91	56
1850@	6(2/2)	149	0.63	39	40	48	41	45	38	36	69	74	67	69	79	83	76
1850@	7(1/2)	145	0.66	26	26	20	30	25	29	18	46	34	41	46	53	49	38
1850@	7(2/2)	146	1.10	33	51	39	54	49	55	50	46	79	73	90	92	75	79
1850@	8	138	3.02	70	101	100	116	111	117	129	84	93	82	109	102	84	80

Appendix II. Data for Chapter IV.

Section A. Collection locations for species used in gut architecture analyses.

Section A: List of collection locations for species used in analyses of gut architecture (Chapter IV).

Station	Latitude (N)	Longitude (W)
Puget Sound, WA		
Clam Bay	47° 34.5'	122° 32.6'
Eagle Harbor	47° 37.2'	122° 30.8'
Eagle Cove	48° 27.5'	123° 01.8'
Eastsound	47° 37.2'	122° 50.8'
English Camp	48° 35.2'	123° 09.0'
False Bay	48° 29.4	123° 04.1'
Friday Harbor	48° 32.3'	123° 01.0'
Lopez Sound	48° 31.0'	122° 51.2'
Massacre Bay	48° 38.9'	122° 58.5'
Mitchell Bay	48° 42.4'	123° 09.0'
North Carolina continental shelf		
E-2-77		
014-1	34° 34.9'	76° 07.9
080-1	35° 39.4'	75° 13.0'
080-3	35° 39.4'	75° 13.0'
136-1	35° 56.8'	75° 11.2'
142-1	35° 59.3'	75° 14.2'
149-1	36° 00.6'	75° 10.6'
211-2	35° 39.5'	75° 13.0'
223-3	35° 51.5'	75° 13.0'
224-1	35° 49.5'	75° 13.0'
226-1	35° 45.4'	75° 12.9'
226-2	35° 45.4'	75° 12.9'
228-2	35° 42.5'	75° 13.0'
237-1	35° 31.5'	75° 13.0'
269-1	35° 16.3'	75° 10.8'
279-1	35° 04.2'	75° 34.4'
283-1	35° 03.2'	75° 26.3'

Station	Latitude (N)	Longitude (W)
E-5-77		
015-1	34° 37.9'	76° 09.6'
149-2	35° 31.2'	75° 12.7'
258-1	35° 04.0'	75° 24.5'
332-2	35° 39.5'	75° 13.0'
E-8-77		
006-1	34° 38.0'	76° 05.8'
013-1	34° 37.5'	76° 09.4'
029-1	35° 08.1'	75° 16.6'
103-1	36° 03.0'	75° 13.0'
106-1	36° 00.5'	75° 15.1'
112-1	35° 49.5'	75° 13.0'
176-1	35° 02.4'	75° 32.2'
200-1	35° 08.7'	75° 16.9'
201-1	35° 16.7'	75° 13.5'
238-1	35° 39.5'	75° 13.0'
238-2	35° 39.5'	75° 13.0'
283-1	35° 39.5'	75° 13.0'
322-1	35° 23.5'	75° 13.0'
E-1-78		
026-1	35° 02.3'	75° 28.4'
028-1	35° 05.5'	75° 22.0'
151-1	35° 03.8'	75° 32.5'
157-1	35° 02.1'	75° 34.5'
229-1	35° 23.5'	75° 13.2'
Southern California bathyal basins and abyssal plain		
J9	32° 58.1'	118° 21.8'
J10	32° 57.7'	118° 22.2'
J11	32° 58.3'	118° 22.2'
J12	32° 58.3'	118° 22.3'
J13	32° 58.1'	118° 22.2'
J14	32° 28.2'	117° 29.8'
J15	32° 28.1'	117° 29.8'

Station	Latitude (N)	Longitude (W)
J22 (= J16)	32° 28.9′	117° 30.1′
J24 (= J17)	32° 27.3′	117° 27.2′
H22	32° 28.2′	117° 29.8′
Quagmire	32° 58.0′	118° 22.0′
SDT	32° 28.0′	117° 28.0′
MET133	32° 25.0′	120° 40.0′
MV67-11-22	37° 20.0′	123° 53.0′
MV70-3-1	31° 33.0′	120° 13.0′

Section B: Gut measurements for all individuals used in analyses of gut architecture (Chapter IV).

Key to abbreviations used in tables:

BV = body volume in mm^3
SV = volume of sediment in gut in mm^3
V = volume of gut subsection in mm^3
L = length of gut subsection in mm
R = radius of gut subsection in mm

See "Gut Descriptions" and Figure 3 in Chapter IV for definitions of gut subsections for each species.

Species: Aglaophamus paucilamellata
Collection location: Quagmire

	Entire Gut			
Worm	BV	V	L	R
ag01	0.30	0.05	2.62	0.08
ag02	0.19	0.03	1.64	0.08
ag03	0.34	0.06	2.52	0.08
ag04	0.25	0.03	1.92	0.07
ag05	1.8	0.31	4.16	0.15
ag06	0.34	0.05	2.50	0.08

Species: Nephtys spp. = N. caeca (np01,np02); N. caecoides (np03-np18)
Collection location: False Bay

	Entire Gut			
Worm	BV	V	L	R
np03	377	30.2	59.5	0.4
np04	763	68.8	86.8	0.5
np05	572	78.4	75.9	0.6
np06	559	50.0	77.4	0.4
np07	557	61.5	67.9	0.5
np08	817	69.5	95.9	0.5
np09	468	66.6	76.1	0.5
np10	604	48.8	69.3	0.5
np11	787	74.8	75.9	0.6
np12	628	30.1	56.8	0.4
np13	838	64.5	82.7	0.5
np14	939	46.3	84.9	0.4
np15	1159	303.3	109.2	0.9
np16	1487	161.6	104.9	0.7
np17	1467	122.5	107.9	0.6
np18	1868	173.7	83.9	0.8
np01	21000	2404	282.4	1.6
np02	4500	626	159.9	1.1

Species: Nephtys picta
Collection location: E-8-77: 112-1, 201-1, 238-3

	Entire Gut			
Worm	BV	V	L	R
ns01	29	2.4	30.0	0.16
ns02	33	4.2	34.1	0.20
ns03	10	0.7	18.0	0.11
ns04	20	1.9	29.4	0.14
ns05	7	0.9	15.9	0.13
ns06	8	1.0	18.2	0.12
ns07	4	0.8	13.6	0.13
ns08	14	1.9	25.6	0.15
ns09	10	1.7	22.0	0.16
ns10	50	5.2	44.2	0.19

Species: Ceratocephale pacifica
Collection location: J22, J24

		Entire Gut		
Worm	BV	V	L	R
cc01	9.4	2.3	21.7	0.18
cc02	3.8	0.8	13.6	0.13
cc04	6.5	1.0	16.6	0.13
cc05	4.4	0.9	14.4	0.13
cc07	4.0	0.7	13.9	0.13
cc09	3.0	0.7	15.5	0.12
cc06	0.2	0.02	3.8	0.04
cc08	0.4	0.1	5.0	0.07
cc10	0.4	0.09	5.4	0.07
cc03	1.5	0.3	8.5	0.09

Species: Glycera americana
Collection location: E-2-77: 279-1, 279-1, 237-1
E-8-77: 106-1, 176-1, 238-1, 283-1

		Anterior Gut			Posterior Gut		
Worm	BV	V	L	R	V	L	R
ga01	124	3.0	7.3	0.36	14.7	40.1	0.34
ga04	120	5.0	8.9	0.41	10.1	50.7	0.25
ga05	209	16.4	13.0	0.63	26.5	47.7	0.42
ga02	61	1.8	4.0	0.38	4.0	27.6	0.21
ga03	39	1.2	7.4	0.21	6.3	38.3	0.23
ga06	53	1.3	6.0	0.26	6.1	38.0	0.23
ga07	98	2.2	4.8	0.37	7.5	44.8	0.23

Species: Glycera dibranchiata
Collection location: E-2-77 080-1; E-8-77 029-1

		Anterior Gut			Posterior Gut		
Worm	BV	V	L	R	V	L	R
gd01	168	7.1	7.2	0.55	12.2	39.6	0.31
gd02	26	0.7	5.4	0.20	2.0	31.2	0.14
gd03	103	1.9	6.5	0.30	15.5	39.4	0.35
gd04	12	0.6	3.9	0.21	1.7	23.9	0.15

Species: Harmothoe extenuata
Collection location: E-2-77: 149-1, 211-2, 226-2, 228-2, 014-1, 226-1, 142-1

		Entire Gut		
Worm	BV	V	L	R
hr01	5.8	0.4	0.65	0.13
hr02	5.4	0.5	7.3	0.15
hr05	5.1	0.2	6.2	0.11
hr03	1.9	0.2	4.4	0.10
hr04	1.9	0.1	4.0	0.10
hr06	0.4	0.3	2.5	0.06
hr10	0.6	0.03	2.6	0.06
hr07	9.0	0.5	7.7	0.14
hr08	0.4	0.02	2.0	0.06
hr09	0.3	0.02	2.0	0.05

Species: Ophiodromus pugettensis
Collection location: Mitchell Bay

		Entire Gut		
Worm	BV	V	L	R
od01	92	12.8	18.3	0.5
od02	94	9.3	18.0	0.4
od03	60	7.9	15.4	0.4
od04	58	8.5	14.4	0.4
od05	46	6.7	12.8	0.4
od06	38	6.1	12.8	0.4
od07	32	3.9	10.3	0.3
od08	37	4.3	10.1	0.4
od09	32	2.8	9.2	0.3
od10	25	2.3	8.9	0.3

Species: Capitella cf. capitata
Collection location: Mitchell Bay

		Foregut			Hindgut			
Worm	BV	V	L	R	V	L	R	SV
ca01	2.2	0.06	2.51	0.09	0.27	7.22	0.10	0
ca02	2.3	0.08	2.20	0.10	0.41	7.87	0.12	0.1
ca03	2.1	0.06	2.42	0.08	0.27	6.54	0.10	0
ca04	14	0.39	4.37	0.16	3.32	16.2	0.24	1.1
ca05	15	0.32	5.59	0.13	3.20	14.0	0.25	1.4
ca06	43	0.89	7.53	0.19	11.9	22.7	0.41	3
ca07	24	0.69	5.75	0.19	5.76	24.0	0.28	1
ca08	24	0.55	5.67	0.17	5.36	24.6	0.26	1
ca09	105	0.85	5.28	0.21	32.7	45.9	0.48	18
ca10	296	1.54	8.48	0.22	43.4	72.2	0.44	3

Species: Cirratulus cirratus
Collection location: Clam Bay

		Entire Gut			
Worm	BV	V	L	R	SV
cr01	13.6	3.4	20.3	0.22	0.9
cr02	11.7	4.1	15.0	0.28	2.2
cr04	2.1	0.7	6.8	0.16	0
cr06	8.5	2.9	9.4	0.28	0.1
cr08	1.6	0.3	6.9	0.12	0
cr10	2.5	1.3	6.6	0.24	0.5
cr03	0.9	0.2	4.8	0.10	0.01
cr05	1.3	0.4	5.0	0.14	0.2
cr07	1.9	0.5	4.3	0.17	0.1
cr09	1.2	0.4	4.0	0.16	0.2

Species: Tharyx multifilis
Collection location: Eagle Harbor

		Foregut			Hindgut			
Worm	BV	V	L	R	V	L	R	SV
tx01	11.3	0.07	1.35	0.12	5.02	29.27	0.23	2.4
tx02	4.4	0.05	1.07	0.11	1.83	11.35	0.22	1.0
tx03	12.0	0.04	1.16	0.09	5.89	18.33	0.31	3.5
tx04	18.1	0.05	1.16	0.10	8.13	19.30	0.35	7.4
tx05	15.7	0.07	1.07	0.13	5.09	16.39	0.30	3.9
tx06	22.1	0.09	1.07	0.15	8.80	18.43	0.38	6.3
tx07	24.6	0.12	1.26	0.16	10.58	22.99	0.36	7.0
tx08	12.9	0.12	1.46	0.15	5.73	17.65	0.31	3.6
tx09	9.2	0.06	1.16	0.12	4.10	13.29	0.30	3.0
tx10	25.4	0.06	1.16	0.12	11.44	19.98	0.41	11.4

Species: Tharyx luticastellus
Collection Location: SDT

		Foregut			Hindgut			
Worm	BV	V	L	R	V	L	R	SV
tl01	4.7	0.13	1.97	0.14	3.60	15.70	0.26	3.7
tl02	3.7	0.10	2.26	0.11	2.22	16.92	0.20	1.8
tl03	6.7	0.22	2.44	0.16	3.93	20.59	0.24	3.9
tl04	7.3	0.14	2.16	0.14	4.93	20.40	0.26	5.1
tl05	7.5	0.21	2.35	0.16	4.12	20.02	0.24	4.2
tl06	4.5	0.13	1.88	0.14	2.30	11.37	0.24	2.0
tl07	8.4	0.22	2.35	0.17	4.41	19.36	0.26	5.0
tl08	4.5	0.13	2.54	0.12	2.67	17.20	0.21	2.4
tl09	3.4	0.10	2.53	0.11	1.82	11.94	0.21	1.8

Species: Chaetozone cf. setosa
Collection location: J11

		Foregut			Hindgut			
Worm	BV	V	L	R	V	L	R	SV
ch01	1.41	0.05	1.80	0.09	0.40	10.28	0.11	0.09
ch02	2.59	0.04	2.00	0.08	0.66	13.91	0.12	0.06
ch03	2.93	0.05	2.15	0.09	0.46	9.29	0.13	0.07
ch04	1.83	0.02	1.85	0.05	0.39	13.17	0.10	0.08
ch05	0.09	0.003	0.081	0.03	0.03	3.59	0.05	0
ch06	2.32	0.01	1.37	0.06	0.37	12.14	0.10	0.04
ch07	1.35	0.006	1.26	0.06	0.30	10.73	0.09	0.06
ch08	1.04	0.01	1.41	0.05	0.27	8.92	0.10	0.08
ch09	1.32	0.01	1.33	0.06	0.33	11.62	0.09	0.09
ch10	2.25	0.02	1.92	0.05	0.44	13.10	0.10	0.20
ch11	1.79	0.03	1.78	0.07	0.47	12.28	0.11	0.07

Species: Fauveliopsis glabra
Collection location: J14, J15

		Foregut			Hindgut			
Worm	BV	V	L	R	V	L	R	SV
fv05	0.06	0.002	0.66	0.03	0.11	0.62	0.07	0.01
fv06	0.10	0.004	0.67	0.04	0.03	1.00	0.09	0.03
fv07	0.13	0.005	0.93	0.04	0.03	0.92	0.10	0.03
fv10	0.14	0.005	1.05	0.04	0.03	1.14	0.09	0.03
fv12	0.09	0.005	0.88	0.04	0.02	0.94	0.07	0.02
fv03	0.29	0.02	1.31	0.06	0.05	1.70	0.09	0.05
fv04	0.83	0.03	2.51	0.06	0.16	2.32	0.14	0.16
fv02	3.35	0.13	3.79	0.13	0.85	5.21	0.21	0.85
fv09	1.35	0.04	2.52	0.07	0.20	2.45	0.16	0.20
fv11	1.13	0.07	2.47	0.09	0.23	3.19	0.15	0.23

Species: Euclymene reticulata
Collection location: J9, J11, J12

		Foregut			Hindgut			
Worm	BV	V	L	R	V	L	R	SV
er01	2.39	0.16	5.41	0.09	0.55	10.30	0.12	0.33
er03	7.47	0.22	4.09	0.13	1.99	24.02	0.16	1.21
er04	7.19	0.18	4.95	0.10	1.41	17.29	0.16	1.26
er05	3.00	0.17	4.22	0.11	0.44	11.29	0.10	0
er06	6.54	0.18	4.55	0.11	2.00	21.78	0.17	2.06
er07	3.44	0.18	5.21	0.10	0.60	14.45	0.11	0.66
er09	3.25	0.18	6.53	0.09	0.75	11.22	0.14	0.53
er10	8.65	0.25	6.40	0.11	2.53	20.20	0.20	1.98
er08	42.8	1.85	10.93	0.22	15.21	45.30	0.33	16.2
er11	15.5	0.60	6.25	0.17	5.27	31.24	0.22	5.27

Species: Armandia maculata
Collection location: E-2-77: 149-1,269-1; E-5-77: 258-1;
E-8-77: 006-1, 013-1, 103-1

		Foregut			Hindgut			
Worm	BV	V	L	R	V	L	R	SV
am09	0.11	0.004	0.61	0.05	0.02	1.91	0.05	0.004
am10	0.21	0.01	1.01	0.06	0.03	2.54	0.06	0.02
am03	3.27	0.09	1.72	0.12	0.65	7.70	0.16	0.36
am04	5.79	0.20	2.38	0.16	0.73	0.845	0.16	0
am05	2.09	0.07	1.58	0.12	0.42	5.63	0.15	0.33
am06	2.02	0.05	1.41	0.11	1.02	6.91	0.21	0.55
am07	1.45	0.06	1.63	0.10	0.26	5.54	0.12	0
am08	2.83	0.11	2.07	0.12	0.95	6.60	0.21	0.95
am01	17.89	1.00	5.40	0.24	3.77	8.55	0.36	3.77
am02	32.96	0.61	3.49	0.23	9.45	16.43	0.42	8.58

Species: Armandia agilis
Collection location: E-8-77: 200-1, 322-3; E-1-78: 028-1, 157-1, 229-1

		Foregut			Hindgut			
Worm	BV	V	L	R	V	L	R	SV
aa01	38.7	3.81	8.40	0.36	8.94	17.14	0.40	8.9
aa02	9.8	0.41	5.21	0.15	3.58	13.61	0.28	3.5
aa03	33.1	0.85	4.54	0.24	13.19	19.99	0.44	12.6
aa04	38.1	0.62	5.54	0.18	15.28	20.92	0.47	15.3
aa05	10.7	0.55	3.86	0.21	2.78	14.62	0.24	2.8
aa06	12.4	0.47	3.63	0.20	3.86	13.00	0.30	3.9
aa07	5.9	0.31	3.37	0.17	1.98	11.88	0.22	2.0
aa08	0.9	0.04	1.79	0.08	0.12	5.18	0.08	0.12
aa09	0.06	0.002	0.62	0.03	0.01	1.83	0.04	0.005

Species: Levinsenia oculata
Collection location: J10

		Entire Gut			
Worm	BV	V	L	R	SV
pg01	1.08	0.54	20.19	0.09	0.26
pg02	0.62	0.30	12.54	0.09	0.08
pg03	0.69	0.30	12.86	0.09	0.23
pg04	0.83	0.25	15.78	0.07	0.17
pg05	0.78	0.31	18.50	0.07	0.17
pg06	0.46	0.17	11.78	0.07	0.09
pg07	1.00	0.44	19.26	0.09	0.15
pg08	0.66	0.25	13.44	0.08	0.13
pg09	0.50	0.18	13.25	0.07	0.12
pg10	0.29	0.14	10.50	0.07	0.07

Species: Paraprionaspio pinnata
Collection location: E-2-77: 283-1; E-1-78: 026-1, 151-1

		Foregut			Bulb			Hindgut			
Worm	BV	V	L	R	V	L	R	V	L	R	SV
pp01	13.8	0.32	3.20	0.61	0.18	0.94	0.23	3.73	27.22	0.21	3.2
pp02	16.2	0.33	2.81	0.18	0.16	0.86	0.24	2.47	27.85	0.17	2.5
pp03	16.7	0.31	3.04	0.17	0.11	0.86	0.18	4.38	35.26	0.20	4.6
pp04	10.7	0.16	3.35	0.12	0.14	0.94	0.20	1.34	18.72	0.15	1.0
pp05	8.3	0.08	2.18	0.10	0.11	0.78	0.21	2.34	24.34	0.18	2.3
pp06	13.0	0.25	2.81	0.16	0.12	0.86	0.20	3.23	23.71	0.21	3.4
pp07	19.8	0.20	3.12	0.12	0.17	1.01	0.21	4.51	29.72	0.22	4.4
pp08	15.0	0.12	2.65	0.11	0.11	0.94	0.19	2.14	27.92	0.16	1.8
pp09	14.2	0.20	2.96	0.14	0.09	0.78	0.19	3.31	28.47	0.19	3.1
pp10	10.0	0.16	2.65	0.13	0.11	0.86	0.19	2.30	25.35	0.17	1.8

Species: Spiophanes cf. bombyx
Collection location: J14, H22

		Foregut			Bulb			Hindgut			
Worm	BV	V	L	R	V	L	R	V	L	R	SV
sb01	0.21	0.007	1.01	0.05	0.002	0.22	0.06	0.031	2.75	0.06	0
sb02	0.27	0.011	1.13	0.05	0.003	0.23	0.06	0.021	2.92	0.05	0
sb06	0.15	0.008	1.26	0.04	0.002	0.25	0.05	0.018	1.93	0.05	0
sb08	0.15	0.003	0.62	0.04	0.002	0.22	0.05	0.051	2.48	0.08	0.05
sb09	0.18	0.011	1.24	0.05	0.004	0.27	0.06	0.023	1.71	0.06	0.02
sb10	0.22	0.008	1.13	0.06	0.004	0.27	0.06	0.047	2.95	0.07	0.01
sb03	0.48	0.021	1.59	0.06	0.011	0.35	0.10	0.081	4.51	0.07	0
sb04	0.52	0.019	1.67	0.06	0.009	0.32	0.09	0.057	3.97	0.08	0
sb05	0.66	0.018	1.59	0.06	0.009	3.78	0.06	0.050	3.78	0.06	0.01
sb07	1.61	0.048	1.76	0.09	0.025	0.48	0.13	0.149	5.89	0.09	0

Species: Pseudopolydora kempi japonica
Collection location: False Bay

		Entire Gut			
Worm	BV	V	L	R	SV
ps03	2.45	0.95	6.66	0.20	0.91
ps04	1.60	0.55	7.74	0.14	0.50
ps05	4.98	2.36	11.12	0.25	2.10
ps06	5.86	1.25	12.01	0.18	0.53
ps07	3.27	1.60	9.95	0.21	1.53
ps09	3.99	1.41	9.85	0.20	1.16
ps02	7.68	3.47	14.39	0.27	3.23
ps08	4.20	2.68	14.45	0.23	2.54
ps10	5.19	2.51	15.97	0.18	1.30
ps01	4.78	2.1	12.53	0.21	1.71

Species: Scalibregma inflatum
Collection location: Eastsound

		Foregut			Midgut			Hindgut			
Worm	BV	V	L	R	V	L	R	V	L	R	SV
sc10	14	0.43	1.31	0.31	4.70	4.65	0.54	2.10	5.94	0.31	2
sc11	19	0.43	1.35	0.31	4.34	4.92	0.50	1.23	6.48	0.23	1
sc12	19	0.29	1.33	0.25	4.84	5.11	0.52	1.30	6.93	0.23	1
sc13	7	0.29	1.12	0.25	2.75	3.90	0.44	1.01	5.48	0.23	1
sc05	27	0.66	1.86	0.31	8.79	7.42	0.59	2.78	6.44	0.36	3
sc07	28	0.86	1.82	0.35	6.66	6.20	0.55	8.28	7.77	0.55	14
sc08	26	0.92	2.13	0.35	7.88	5.84	0.64	1.41	4.72	0.29	6
sc09	30	1.19	2.17	0.38	7.01	7.35	0.52	2.56	7.18	0.32	9
sc01	44	1.51	3.01	0.38	22.8	9.59	0.84	4.18	7.28	0.40	4
sc02	64	2.01	2.73	0.45	23.7	11.2	0.79	8.15	9.96	0.48	8
sc03	56	2.10	3.38	0.42	18.6	8.46	0.81	6.35	8.37	0.47	12
sc04	46	1.78	2.63	0.43	16.7	9.54	0.71	2.85	8.60	0.31	6
sc06	33	1.45	2.02	0.45	10.8	6.44	0.70	2.74	6.77	0.33	3
sc14	59	1.20	2.73	0.36	13.1	9.56	0.64	10.2	11.1	0.51	18
sc15	52	1.18	2.86	0.34	11.0	9.88	0.60	4.37	10.1	0.32	14
sc16	68	0.73	2.02	0.31	16.0	12.2	0.65	6.48	9.23	0.42	21
sc17	63	1.76	2.54	0.45	11.9	9.43	0.60	6.32	9.75	0.42	14
sc18	43	1.00	2.47	0.34	11.7	7.86	0.64	8.30	9.10	0.50	20
sc19	56	0.79	2.08	0.33	11.4	11.2	0.57	6.35	9.36	0.42	12
sc20	30	0.53	1.89	0.29	5.70	10.5	0.40	4.61	8.12	0.39	8
sc21	31	0.62	2.54	0.26	2.70	8.12	0.30	2.70	8.12	0.30	3
sc22	22	0.59	2.08	0.28	3.75	6.63	0.41	2.36	7.80	0.30	4
sc23	15	0.45	1.82	0.26	4.90	7.28	0.43	0.88	5.98	0.20	4

Species: Scalibregma inflatum
Collection location: E-2-77: 142-1, 149-1, 223-3, 224-1

		Foregut			Midgut			Hindgut			
Worm	BV	V	L	R	V	L	R	V	L	R	SV
se01	16	0.20	2.08	0.16	2.52	9.47	0.28	1.07	11.4	0.16	0.55
se02	2.9	0.05	1.48	0.10	0.11	2.89	0.10	0.14	4.75	0.09	0
se03	4.5	0.07	1.44	0.11	0.32	3.57	0.16	0.43	4.94	0.16	0.43
se04	4.6	0.05	1.18	0.11	0.71	3.99	0.23	0.24	4.63	0.12	0.79
se05	3.1	0.04	0.95	0.11	0.48	4.86	0.17	0.06	2.70	0.08	0.29
se06	1.8	0.04	1.18	0.09	0.14	3.46	0.11	0.07	2.66	0.09	0.09
se07	3.3	0.04	1.29	0.10	0.99	4.41	0.24	0.12	3.08	0.11	0.96
se08	6.2	0.09	1.29	0.14	0.77	5.66	0.20	0.38	5.00	0.14	0.92
se09	4.9	0.02	1.06	0.08	0.83	3.83	0.25	0.37	6.16	0.13	1.2
se10	5.9	0.03	1.14	0.09	0.73	4.41	0.22	0.24	3.69	0.14	0.97

Species: Sternaspis scutata
Collection location: Lopez Sound

		Foregut			Midgut			Hindgut			
Worm	BV	V	L	R	V	L	R	V	L	R	SV
st01	97	1.7	5.5	0.28	18.0	14.9	0.59	10.8	35.6	0.31	30
st04	206	3.5	5.9	0.40	43.5	26.4	0.72	22.7	48.3	0.39	70
st07	278	1.9	7.1	0.27	60.3	24.1	0.86	17.8	53.0	0.33	80
st10	98	1.4	6.2	0.25	16.6	17.9	0.52	9.5	36.2	0.29	28
st38	73	1.1	4.4	0.27	13.4	14.1	0.52	7.6	24.2	0.32	22
st39	168	2.6	9.7	0.28	29.1	18.2	0.68	16.6	42.5	0.35	48
st41	137	2.2	9.0	0.27	30.3	17.7	0.74	13.9	36.7	0.35	46
st43	237	2.6	9.9	0.27	39.5	23.0	0.74	22.9	45.11	0.40	65
st48	76	1.0	6.0	0.22	17.1	17.0	0.55	8.6	35.3	0.28	27
st49	142	3.2	11.8	0.28	35.1	20.9	0.66	13.6	36.7	0.34	52
st50	112	2.0	8.8	0.26	24.5	24.2	0.54	14.7	35.7	0.36	41
st29	15	0.07	2.1	0.10	2.7	8.5	0.31	1.3	12.4	0.18	4
st31	37	0.28	1.9	0.20	8.8	8.6	0.56	4.2	23.1	0.24	13

Species: Sternaspis fossor
Collection location: J9, J10, J11, J12, J13

		Foregut			Midgut			Hindgut			
Worm	BV	V	L	R	V	L	R	V	L	R	SV
sf01	12.1	0.07	2.11	0.09	0.76	3.35	0.25	0.81	29.9	0.09	1.6
sf02	12.4	0.09	3.82	0.08	1.46	5.89	0.27	1.40	34.0	0.11	2.9
sf03	6.4	0.08	2.85	0.08	0.88	5.07	0.23	0.71	27.4	0.09	1.6
sf04	5.6	0.10	2.30	0.10	0.75	4.45	0.22	0.66	26.0	0.09	1.4
sf05	4.6	0.09	4.50	0.08	0.45	3.35	0.20	0.54	22.6	0.09	1.0
sf06	4.3	0.04	2.11	0.07	0.53	3.35	0.22	0.47	19.8	0.09	1.0

Species: Amphicteis scaphobranchiata
Collection location: Massacre Bay, Eastsound, Lopez, Sound

		Foregut			Midgut			Hindgut			
Worm	BV	V	L	R	V	L	R	V	L	R	SV
as02	290	4.3	4.5	0.51	62.6	21.0	0.97	17.8	16.3	0.56	66
as03	313	4.1	5.9	0.45	60.2	20.8	0.94	18.4	20.6	0.52	79
as04	236	5.9	4.5	0.63	37.0	15.7	0.84	24.4	23.7	0.55	46
as05	305	5.5	4.3	0.63	43.8	17.9	0.87	34.2	21.6	0.69	64
as06	285	7.1	5.3	0.62	49.5	20.0	0.86	12.0	18.9	0.44	55
as07	321	6.5	4.3	0.68	49.4	18.7	0.90	30.1	25.3	0.59	45
as08	194	4.4	4.0	0.58	20.9	14.7	0.64	12.8	20.0	0.44	13
as01	9	0.3	1.6	0.22	2.2	5.6	0.35	1.1	5.7	0.24	3
as09	50	2.6	3.7	0.43	4.0	9.0	0.55	5.0	15.6	0.31	14
as10	44	1.6	3.5	0.37	9.1	10.2	0.52	6.5	12.2	0.40	15
as11	53	1.2	3.1	0.35	5.9	9.9	0.42	6.4	13.0	0.38	12
as12	90	1.4	3.0	0.38	15.3	11.4	0.63	11.1	16.8	0.44	26
as13	78	2.6	3.6	0.46	14.7	11.0	0.62	6.0	16.3	0.33	8
as14	56	1.0	2.6	0.33	7.2	9.4	0.48	3.8	13.1	0.28	11
as15	59	0.9	2.4	0.34	7.9	9.9	0.49	3.7	12.5	0.29	12
as16	49	1.6	2.9	0.39	8.1	8.9	0.52	4.8	12.3	0.34	13

Species: Ampharete acutifrons
Collection location: E-2-77: 136-1, 149-1

		Foregut			Midgut			Hindgut			
Worm	BV	V	L	R	V	L	R	V	L	R	SV
ap01	26	0.36	1.46	0.24	5.74	7.29	0.49	1.56	8.91	0.22	3
ap02	40	0.52	1.94	0.28	8.47	8.51	0.55	2.28	10.7	0.25	8
ap03	16	0.54	1.94	0.28	2.17	5.91	0.34	0.91	7.37	0.19	2
ap04	42	0.82	2.11	0.34	9.54	3.34	0.59	0.96	7.61	0.19	10
ap05	19	0.57	2.11	0.28	4.27	6.40	0.45	0.63	7.05	0.16	2
ap09	27	0.63	1.86	0.31	4.82	8.00	0.44	0.61	5.27	0.19	5
ap06	8.6	0.13	1.01	0.20	1.07	4.31	0.28	0.48	4.00	0.18	1
ap07	8.9	0.17	1.32	0.19	2.00	5.10	0.24	0.28	4.52	0.14	1
ap10	4.9	0.16	1.72	0.17	1.26	3.30	0.34	0.13	3.48	0.10	1
ap08	0.4	0.02	0.65	0.09	0.04	1.08	0.11	0.01	1.42	0.14	0.04

Species: Ampharete americana
Collection location: E-2-77: 224-1

		Foregut			Midgut			Hindgut			
Worm	BV	V	L	R	V	L	R	V	L	R	SV
an01	2.3	0.05	1.15	0.11	0.18	2.56	0.15	0.19	5.18	0.10	0
an02	1.1	0.06	1.04	0.13	0.16	1.76	0.17	0.06	3.17	0.08	0.03
an03	1.6	0.03	0.76	0.10	0.24	2.63	0.16	0.07	3.20	0.08	0.04
an04	1.6	0.04	0.68	0.14	0.29	2.59	0.18	0.06	3.24	0.08	0
an05	0.7	0.03	0.61	0.12	0.08	1.87	0.11	0.05	3.20	0.07	0.04
an07	4.0	0.09	1.08	0.16	0.51	2.66	0.24	0.20	4.93	0.11	0.07
an08	1.8	0.04	0.94	0.12	0.34	2.23	0.22	0.07	3.42	0.08	0
an09	0.7	0.02	0.61	0.09	0.09	2.27	0.11	0.04	2.66	0.07	0
an10	2.0	0.06	0.90	0.14	0.30	2.88	0.18	0.06	9.02	0.08	0
an06	22	0.53	2.37	0.26	2.11	5.18	0.35	0.74	3.29	0.18	0.7

Species: Ecamphicteis elongata
Collection location: J14, H22

		Foregut			Midgut			Hindgut			
Worm	BV	V	L	R	V	L	R	V	L	R	SV
ec02	5.7	0.12	1.97	0.14	1.13	4.80	0.26	0.64	10.3	0.14	1.0
ec03	5.6	0.13	1.34	0.17	0.87	5.63	0.22	0.34	8.32	0.10	0.1
ec04	5.1	0.06	0.96	0.14	1.16	6.78	0.23	0.41	6.85	0.13	0.3
ec01	2.8	0.04	0.107	0.10	0.51	4.03	0.20	0.19	9.33	0.08	0.3
ec05	2.6	0.06	1.17	0.12	0.54	4.74	0.19	0.48	6.89	0.13	0.7
ec06	0.9	0.04	1.07	0.11	0.15	3.06	0.12	0.17	3.67	0.12	0.3

Species: Anobothrus sp. A
Collection location: H22

		Foregut			Midgut			Hindgut			
Worm	BV	V	L	R	V	L	R	V	L	R	SV
au07	0.13	0.002	0.30	0.05	0.02	1.11	0.08	0.01	1.17	0.05	0
au08	0.10	0.002	0.26	0.05	0.02	0.84	0.08	0.01	0.92	0.05	0
au03	0.41	0.01	0.58	0.07	0.07	1.58	0.12	0.04	3.08	0.06	0.07
au04	0.15	0.01	0.48	0.08	0.03	0.66	0.08	0.02	2.14	0.05	0
au05	0.14	0.01	0.40	0.06	0.03	1.74	0.07	0.02	1.42	0.06	0
au09	0.39	0.01	0.42	0.08	0.05	1.14	0.11	0.05	2.74	0.08	0.04
au01	1.10	0.02	0.74	0.09	0.14	2.17	0.14	0.13	4.90	0.09	0.21
au02	1.08	0.04	0.88	0.11	0.14	2.20	0.14	0.12	6.30	0.08	0.21
au06	0.90	0.02	0.66	0.09	0.09	1.82	0.12	0.11	4.66	0.09	0

Species: Artacamella hancocki
Collection location: J14, J15, J16, H22

		Foregut			Midgut			Hindgut			
Worm	BV	V	L	R	V	L	R	V	L	R	SV
at06	0.50	0.02	0.80	0.08	0.08	1.47	0.12	0.04	3.04	0.06	0.1
at03	2.13	0.03	1.15	0.09	0.39	4.59	0.16	0.21	4.37	0.12	0.6
at04	0.93	0.02	0.76	0.10	0.13	1.82	0.15	0.07	3.33	0.08	0.2
at08	0.87	0.13	4.43	0.09	0.11	1.96	0.13	0.13	4.84	0.09	0.2
at01	6.18	0.54	2.03	0.28	1.60	3.48	0.37	1.25	9.16	0.20	2
at02	33	0.43	1.72	0.27	4.73	7.37	0.44	7.09	19.8	0.33	12
at05	96	0.44	2.32	0.23	7.6	9.8	0.48	6.6	24.4	0.28	14
at07	19	0.42	2.02	0.24	3.04	5.96	0.38	3.92	17.6	0.26	6

Species: Abarenicola pacifica
Collection location: False Bay

		Foregut			Midgut			Hindgut			
Worm	BV	V	L	R	V	L	R	V	L	R	SV
ab33	25	2.0	4.2	0.37	5.1	6.8	0.48	7.5	16.1	0.38	15
ab24	36	0.9	3.4	0.29	4.3	5.7	0.47	8.2	15.7	0.40	8
ab32	43	0.9	3.0	0.30	4.2	5.9	0.47	8.4	18.1	0.38	11
ab25	56	2.4	5.7	0.35	4.7	7.9	0.52	9.3	18.9	0.38	18
ab03	60	1.1	6.1	0.24	6.4	8.5	0.47	4.7	14.7	0.31	1
ab62	92	1.8	4.8	0.34	10.7	9.0	0.61	16.3	23.5	0.47	15
ab44	89	0.9	5.6	0.22	14.9	11.2	0.63	5.7	16.2	0.33	5
ab05	167	4.7	8.2	0.41	17.3	13.5	0.59	19.2	25.6	0.48	17
ab42	195	9.1	7.6	0.59	25.5	13.1	0.77	73.0	34.5	0.81	107
ab18	221	5.0	8.8	0.41	22.7	11.4	0.76	42.3	34.9	0.60	19
ab35	408	27.7	10.3	0.88	82.1	14.8	1.3	171	46.4	1.1	277
ab02	429	8.7	9.9	0.51	54.4	23.7	0.79	58.0	44.2	0.65	31
ab46	506	18.8	13.2	0.65	95.2	17.9	1.2	124	35.5	1.0	139
ab12	762	14.6	12.5	0.59	103	23.1	1.1	84.4	30.5	0.99	79
ab39	852	10.9	8.6	0.61	121	26.9	1.1	107	39.2	1.0	107
ab48	754	12.2	11.3	0.56	76.8	23.8	0.95	74.1	34.4	0.83	75
ab08	752	20.8	15.3	0.64	107	20.8	1.2	111	34.5	0.99	123
ab60	846	19.0	9.5	0.73	105	23.6	1.1	7.375	22.6	0.90	68
ab23	894	18.7	19.2	0.54	143	26.0	1.2	77.5	29.9	0.87	93
ab04	1553	108	15.7	1.4	364	44.8	1.6	193	34.6	1.3	666
ab70	14	0.6	4.0	0.21	2.7	5.9	0.37	2.1	11.4	0.24	5
ab71	11	1.2	4.2	0.29	2.5	4.7	0.40	2.4	11.2	0.26	6
ab72	11	0.7	3.2	0.25	2.2	5.7	0.34	1.7	9.5	0.23	4

Species: Ophelina acuminata
Collection location: Lopez Sound

		Foregut			Midgut			Hindgut			
Worm	BV	V	L	R	V	L	R	V	L	R	SV
op01	171	3.5	4.7	0.47	30.1	26.8	0.60	7.1	9.3	0.46	31
op02	126	3.1	4.7	0.43	18.8	20.6	0.53	5.0	10.6	0.37	24
op03	77	1.9	3.4	0.39	20.4	20.8	0.56	1.4	6.0	0.26	17
op04	55	1.6	3.4	0.37	13.4	19.2	0.47	2.6	5.6	0.36	13
op05	51	1.4	3.5	0.34	5.5	14.2	0.35	1.5	6.0	0.28	5
op06	51	1.3	3.6	0.32	8.2	17.0	0.39	3.0	6.7	0.35	9

Species: Abarenicola vagabunda
Collection location: Eagle Cove

		Foregut			Ant. Midgut			Post. Midgut			Hindgut			
Worm	BV	V	L	R	V	L	R	V	L	R	V	L	R	SV
av01	4838	61	22	0.9	220	13	2.2	567	29	2.3	548	61	1.7	548
av02	3395	69	19	1.0	245	13	2.3	257	34	1.4	770	64	1.8	164
av04	3402	42	23	0.7	251	10	2.6	430	27	2.2	507	59	1.6	257
av05	4827	86	23	1.0	312	12	2.8	672	36	2.4	812	69	1.9	399
av06	6441	82	25	1.0	404	19	2.5	768	34	2.5	1137	77	2.2	856
av08	5005	60	21	0.9	299	9	3.2	840	36	2.5	1159	68	2.1	950
av07	4991	47	16	0.9	116	9	2.0	780	41	1.4	760	70	1.8	471
av09	20259	256	26	1.7	820	13	4.2	2607	49	3.9	4673	134	3.3	4783
av10	15087	148	25	1.3	504	11	3.7	2021	46	3.6	3819	112	3.3	3819
av11	18546	199	32	1.4	497	10	3.7	1964	39	3.7	2431	120	2.5	2114

Species: Travisia foetida
Collection location: MV67-11-22, MET133, MV70-3-1

		Foregut			Ant. Midgut			Post. Midgut			Hindgut			
Worm	BV	V	L	R	V	L	R	V	L	R	V	L	R	SV
tv01	4128	123	8	2.0	84	10	1.5	228	11	2.4	1185	75	2.2	1413
tv02	3712	121	9	1.8	77	10	1.4	159	9	2.2	653	90	1.5	812
tv03	3863	90	8	1.7	76	12	1.3	190	12	2.1	1054	81	2.0	1245
tv04	1243	40	6	1.3	21	5	1.0	50	9	1.2	448	50	1.6	498
tv05	1354	26	5	1.2	21	5	1.0	50	6	1.5	505	55	1.7	555
tv06	493	11	3	0.97	14	9	0.7	25	7	1.0	109	31	1.0	148
tv07	75	1.5	2	0.49	1.4	2.7	0.4	1.4	2.7	0.4	24	11	0.7	24
tv08	78	2.7	2	0.65	0.8	1.9	0.3	---	--	---	18	23	0.5	18
tv09	4	0.1	0.9	0.13	0.1	0.9	0.2	---	--	---	0.9	8	0.2	0.9
tv10	6	0.1	0.9	0.18	0.05	0.8	0.1	---	--	---	1.5	10	0.2	1.7

Species: Polycirrus eximius
Collection location: E-2-77: 369-2, 142-1, 080-3; E-5-77: 332-2, 149-2;
E-8-77: 238-1, 238-2, 106-1

		Foregut			Ant Midgut			Post Midgut			Hindgut			
Worm	BV	V	L	R	V	L	R	V	L	R	V	L	R	SV
pc04	7.0	0.1	2.4	0.11	0.5	1.6	0.29	0.6	2.0	0.28	1.7	10.2	0.22	0.4
pc06	2.4	0.06	1.7	0.10	0.2	1.9	0.20	0.1	1.0	0.17	0.7	9.6	0.15	1.0
pc07	1.4	0.02	1.2	0.07	0.1	1.1	0.15	0.2	1.1	0.21	0.2	6.4	0.10	0
pc08	2.4	0.06	1.9	0.09	0.2	1.8	0.16	0.1	1.4	0.18	0.5	6.9	0.14	0.7
pc09	7.4	0.05	1.5	0.10	0.2	1.8	0.18	0.2	1.2	0.24	1.5	10.8	0.20	1.9
pc10	2.7	0.07	1.8	0.10	0.2	1.8	0.16	0.1	1.4	0.15	0.5	6.3	0.16	0.2
pc01	26	0.4	2.9	0.21	1.9	4.1	0.38	1.2	2.2	0.40	4.8	11.1	0.36	7.9
pc03	11	0.3	2.6	0.18	0.5	2.7	0.23	0.4	1.6	0.26	3.7	9.8	0.33	2.8
pc02	38	0.4	2.7	0.21	6.8	6.4	0.57	1.4	2.8	0.39	5.0	12.1	0.35	8.2
pc05	37	0.2	2.4	0.14	0.8	3.1	0.27	0.8	2.2	0.33	15.5	27.7	0.40	7.0

Species: Terebellides cf. stroemi
Collection location: J14, J15, J22, J24

		Foregut			Post Midgut			Ant Hindgut			Post Hindgut			
Worm	BV	V	L	R	V	L	R	V	L	R	V	L	R	SV
tb07	0.3	0.01	1.0	0.06	0.01	0.5	0.08	0.02	0.9	0.08	0.01	1.4	0.04	0.03
tb08	0.4	0.01	1.3	0.04	0.01	0.6	0.08	0.02	1.1	0.08	0.05	2.6	0.07	0.08
tb05	1.8	0.06	2.5	0.08	0.08	0.8	0.17	0.21	1.6	0.20	0.22	5.9	0.10	0.5
tb06	2.9	0.07	2.5	0.09	0.10	0.9	0.18	0.51	3.2	0.22	0.36	7.5	0.12	1.0
tb09	1.3	0.04	2.0	0.08	0.06	0.8	0.15	0.18	2.5	0.15	0.22	4.3	0.12	0.5
tb10	1.8	0.05	2.4	0.08	0.11	1.0	0.18	0.13	1.4	0.16	0.33	5.7	0.13	0.6
tb01	47	0.7	6.0	0.18	0.9	1.8	0.38	3.8	7.4	0.40	3.4	25.8	0.20	2
tb02	70	2.1	5.2	0.35	5.5	2.9	0.74	17.0	8.5	0.76	10.1	13.4	0.46	34
tb03	20	1.3	5.0	0.28	0.9	1.9	0.38	2.6	3.3	0.48	7.0	15.0	0.37	11
tb04	11	0.2	3.8	0.14	0.4	1.5	0.28	1.7	5.6	0.30	2.3	11.8	0.24	4

Species: Terebellides stroemi
Collection location: E-5-77: 015-1

		Foregut			Post Midgut			Hindgut			
Worm	BV	V	L	R	V	L	R	V	L	R	SV
td01	12	0.2	2.3	0.15	0.5	1.6	0.32	1.8	10.1	0.24	2
td02	2	0.06	1.6	0.10	0.20	1.4	0.20	0.34	4.5	0.15	0.6
td03	1	0.02	1.2	0.08	0.09	0.8	0.18	0.15	3.5	0.11	0.2
td04	9	0.2	3.4	0.13	0.3	1.6	0.25	1.9	7.8	0.26	2
td05	1	0.02	1.6	0.06	0.12	0.8	0.22	0.28	4.1	0.14	0.4
td06	1	0.03	1.6	0.08	0.14	0.9	0.22	0.22	5.7	0.11	0.4
td10	2	0.05	1.8	0.09	0.20	0.9	0.25	0.34	5.4	0.13	0.6
td11	1	0.01	1.2	0.06	0.08	0.7	0.18	0.16	4.9	0.10	0.2
td07	4	0.08	1.9	0.11	0.27	1.3	0.25	0.88	8.0	0.18	1
td08	3	0.06	2.2	0.08	0.25	1.0	0.27	0.57	7.0	0.15	0.8
td09	3	0.07	2.0	0.10	0.26	1.1	0.26	0.48	7.6	0.14	0.7
td12	6	0.11	2.6	0.11	0.37	0.14	0.28	0.98	7.4	0.20	1

Species: Neoamphitrite robusta
Collection location: Friday Harbor

		Foregut			Ant Midgut			Post Midgut			Ant Hindgut			Post Hindgut			
Worm	BV	V	L	R	V	L	R	V	L	R	V	L	R	V	L	R	SV
ne01	15610	182	21	1.6	727	22	3.1	736	41	2.3	1476	129	1.9	792	76	1.8	1914
ne02	21750	147	24	1.4	987	30	3.2	681	33	2.6	2571	152	2.3	362	57	1.4	4561
ne03	14993	279	22	1.9	574	19	3.0	960	49	2.5	2124	159	2.1	603	61	1.8	4368
ne04	22122	389	21	2.4	696	32	2.5	679	48	2.1	3098	195	2.2	377	54	1.5	5153
ne05	22085	229	21	1.9	1116	24	3.8	1069	34	3.1	2934	185	2.2	712	68	1.8	5787
ne06	24230	220	21	1.8	817	28	3.0	812	39	2.5	2959	128	2.7	885	75	1.9	4900

Species: Eupolymnia heterobranchia
Collection location: False Bay

		Foregut			Ant Midgut			Post Midgut			Ant Hindgut			Post Hindgut			
Worm	BV	V	L	R	V	L	R	V	L	R	V	L	R	V	L	R	SV
eu01	437	3	5	0.4	23	10	0.8	20	5	1.0	61	12	1.2	42	27	0.7	145
eu02	479	3	6	0.4	32	9	1.0	18	6	1.0	53	10	1.2	55	25	0.8	113
eu03	414	3	5	0.4	33	8	1.1	29	6	1.2	60	15	1.1	24	25	0.5	88
eu04	642	3	5	0.4	44	10	1.2	25	6	1.1	89	10	1.6	51	21	0.8	49
eu05	381	1	4	0.3	30	10	1.0	21	8	0.9	29	8	1.1	14	18	0.5	29
eu06	763	3	6	0.4	60	11	1.3	33	7	1.2	121	12	1.8	38	26	0.7	46
eu10	875	6	6	0.5	90	12	1.5	36	6	1.4	128	16	1.5	69	38	0.7	203
eu07	803	6	5	0.6	57	10	1.3	28	7	1.1	70	12	1.3	24	33	1.3	28
eu08	967	7	6	0.6	106	14	1.5	57	7	1.6	120	15	1.6	66	35	0.8	106
eu09	873	5	6	0.5	105	12	1.6	59	7	1.5	89	9	1.6	125	40	1.0	180
eu11	1546	5	6	0.5	107	13	1.6	62	9	1.4	154	19	1.6	173	49	1.0	118
eu12	2195	5	6	0.5	147	16	1.7	95	11	1.6	324	29	1.8	105	43	0.9	460

Species: Thelepus crispus
Collection location: English Camp

		Foregut			Ant Midgut			Post Midgut			Hindgut			
Worm	BV	V	L	R	V	L	R	V	L	R	V	L	R	SV
tc01	4896	10	5	0.8	348	16	2.5	67	7	1.7	533	93	1 ?	67
tc02	3736	11	8	0.6	229	15	2.2	113	10	1.8	676	99	1.5	467
tc03	3448	16	9	0.7	229	14	2.2	91	10	1.6	490	99	1.2	448
tc04	3935	17	8	0.8	330	17	2.3	163	13	1.9	716	92	1.6	832
tc05	5328	7	6	0.6	228	13	2.3	107	8	1.9	1150	103	1.9	834
tc06	5607	6	7	0.5	248	20	1.9	149	13	1.8	927	117	1.6	944
tc07	5415	6	5	0.5	373	17	2.6	171	11	2.2	818	123	1.5	544
tc08	4769	9	6	0.7	289	18	2.1	110	11	1.6	853	98	1.7	213
tc09	3577	5	6	0.5	239	16	2.1	75	8	1.6	479	105	1.2	315

VITA

Deborah Lynn Penry

Born: 28 February 1957, Fort Dix, NJ

Parents: Edward B. and Joan B. Penry

Education: Henderson Senior High School, West Chester, PA

University of Delaware, Newark, DE
B.A.A.S in Biology, 1979

College of William and Mary in Virginia, Williamsburg, VA
M.A. in Marine Science, 1982

University of Washington, Seattle, WA
Ph.D. in Oceanography, 1988